



**TerC –
an essential protein for the integration of CP43
into the thylakoid membrane and its assembly
into photosystem II**

Dissertation
zur Erlangung des Doktorgrades der Fakultät für Biologie
der Ludwig-Maximilians-Universität München

Vorgelegt von
Henning Strissel
aus Kempten

29. Juni 2011

Erstgutachter: Prof. Dr. Dario Leister

Zweitgutachter: Prof. Dr. Peter Geigenberger

Tag der mündlichen Prüfung: 28.07.2011

“Science is organized knowledge. Wisdom is organized life.”

Immanuel Kant (1724 - 1804)

Summary

During evolution, most genes of the cyanobacterial ancestor of plastids were transferred to the nuclear genome of the host cell (endosymbiosis). Consequently, to maintain the physiological properties of plastids, new regulatory elements and protein import machineries have evolved. For proper assembly of the photosystem II complex, whose core proteins are still plastid encoded, several nuclear encoded assembly factors like LPA1, LPA2, LPA3, PAM68 and ALB3 are required.

In *Arabidopsis thaliana* an albinotic and hence seedling lethal mutant was described in previous publications. Thylakoids of *terc-1* were devoid of subunits of photosystem II and therefore a crucial role for TerC in the biogenesis of thylakoids was suggested. During this thesis, the function of TerC during the assembly of photosystem II was characterised in-depth. Downregulation of *AtTerC* transcripts induced by artificial micro RNA (*amiR-TerC* plants) leads predominantly to a reduction of the photosynthetic performance of photosystem II and to a decreased accumulation of respective proteins. Protein-protein interaction and co-localisation experiments reveal that TerC specifically interacts with subunits of photosystem II, as well as with photosystem II assembly factors. During the stepwise assembly of photosystem II, the insertion of CP43 (Chlorophyll binding protein of 43 kDa) into the CP43 free complex controls the PSII core monomerisation. The function of TerC is attributed to this step based on two dimensional gel analysis and *in vivo* labelling experiments of plastidic proteins. In both experiments a reduced amount of unassembled CP43 protein and a block before photosystem II core monomerisation is observed.

Taken together, a function of TerC in both, the integration of CP43 into the thylakoid membrane and the assembly of CP43 into the photosystem II, is proposed in a two step model: During the first step, TerC, LPA2 and LPA3 together with ALB3 integrate the unfolded form of the CP43 protein into the thylakoid membrane. In a second step, this complex consisting of TerC, LPA2, LPA3 and CP43 joins the CP43-free photosystem II complex and, mediated by interaction of TerC with photosystem II subunits, LPA1 and PAM68 the assembly of monomeric photosystem II is completed.

Zusammenfassung

Im Laufe der Evolution wurde ein Großteil der Gene des cyanobakteriellen Vorläufers der Plastiden in das Kerngenom der Wirtszelle integriert (Endosymbiose). Um die Funktionen der Proteinkomplexe in den Plastiden aufrecht zu erhalten, mussten neue Regulations- und Importmechanismen entwickelt werden. Mehrere kernkodierte Assemblierungsfaktoren, wie zum Beispiel LPA1, LPA2, LPA3, PAM68 und ALB3, wurden identifiziert, die für den einwandfreien Zusammenbau des Photosystem II-Komplexes notwendig sind.

In früheren Veröffentlichungen wurde ein albinotische *Arabidopsis thaliana*-Mutante beschrieben, die bei Anzucht auf Erde im Samenstadium letal ist. Die Thylakoidmembranen von *terc-1* beinhalten keine Kernproteine des Photosystems II und deshalb wird angenommen, dass TerC eine entscheidende Funktion beim Zusammenbau des Photosystems II spielt. Während dieser Arbeit wurde die Funktion von TerC bei der Assemblierung des Photosystems II genau untersucht. Durch die geringere Menge an *AtTerC*-Transkript in *amiR-TerC*-Pflanzen, hervorgerufen durch künstliche Mikro-RNA-Interferenz, wurde die Photosyntheseaktivität, vor allem die des Photosystems II, reduziert. Zusätzlich waren alle plastidären Proteine verringert. Protein-Protein-Interaktionsstudien und Co-Lokalisierungsexperimente zeigten eine spezifische Interaktion von TerC mit Untereinheiten des Photosystems II und dessen Assemblierungsfaktoren. Während des stufenweisen Zusammenbaus des Photosystems II kontrolliert der Einbau von CP43 („chlorophyll binding protein“ mit 43 kDa) in den CP43-freien Komplex die Monomerisierung des Photosystem II-Kernkomplexes. Basierend auf zweidimensionaler Gelanalyse sowie Markierungsexperimenten plastidärer Proteine wird TerC eine entscheidende Funktion in diesem Schritt zugesprochen. Beide Ansätze zeigten eine Verringerung der Menge an freiem CP43 und eine Blockade beim Zusammenbau des Photosystems II im letzten Schritt, der Integration von CP43.

Deshalb wird davon ausgegangen, dass TerC sowohl bei der Integration von CP43 in die Thylakoidmembran, als auch beim Einbau von CP43 in das Photosystem II eine essentielle Rolle spielt, wie es das abschließende Zweistufenmodell aufzeigt: Zunächst inserieren TerC, LPA2 und LPA3 zusammen mit ALB3 das ungefaltete CP43 in die Thylakoidmembran. Anschließend gliedert sich dieser Komplex, bestehend aus TerC, LPA2, LPA3 und CP43, durch Wechselwirkung mit Untereinheiten des Photosystems II an den CP43-freien Photosystem II-Komplex an und der Zusammenbau des monomeren Photosystem II-Komplexes ist abgeschlossen.

Index	
Summary	I
Zusammenfassung	II
Index	III
List of Figures	V
List of Tables	VII
Abbreviations	VIII
1.Introduction	1
1.1 Photosynthesis	1
1.2 Evolutionary impact on chloroplasts	3
1.3 Protein import into chloroplasts and thylakoids	4
1.4 Photosystem II – structure and assembly	9
1.5 Variegated mutants in <i>Arabidopsis thaliana</i>	11
1.6 Previous work on the gene <i>At5g12130</i>	12
1.7 Aims of the thesis	13
2.Materials and Methods	15
2.1 Database analyses and prediction programs	15
2.2 Plant material and growth conditions	15
2.3 Complementation of <i>terc-1</i> with a GFP-tag	16
2.4 Generation of amiRNA lines	16
2.5 Nucleic acid analysis	17
2.6 Chlorophyll fluorescence measurements	18
2.7 Total protein preparation and SDS-PAGE	19
2.8 Blue Native PAGE and 2D SDS-PAGE	19
2.9 Immunoblot analyses	20
2.10 <i>In vivo</i> labelling of <i>Arabidopsis thaliana</i> proteins (pulse-chase labelling)	21
2.11 Sucrose gradient centrifugation	21
2.12 Split Ubiquitin assay	22
2.13 Topology studies of TerC	23
2.14 Electron microscopy	24
2.15 Isolation of protoplasts and fluorescence microscopy	24
2.16 Oligonucleotides	24

3.Results	26
3.1 Phenotype of <i>terc-1</i>	26
3.2 Phenotype of <i>amiR-TerC</i>	27
3.3 Complementation of the mutation	31
3.4 Topology studies on the TerC protein	34
3.5 Photosynthetic performance	35
3.6 Protein profile of <i>terc-1</i> and <i>amiR-TerC</i> plants	38
3.7 Blue native gel analysis of <i>amiR-TerC</i>	42
3.8 Sucrose gradient analysis of <i>terc-1</i> _{TerC-GFP}	44
3.9 Protein-protein interaction studies using the Split Ubiquitin system	46
3.10 <i>In vivo</i> synthesis of chloroplast proteins	47
4.Discussion	51
4.1 Complete knock-out of <i>AtTerC</i> leads to lethality due to a loss of photosystem II	51
4.2 Down-regulation of <i>AtTerC</i> leads to a leaf variegated phenotype and a reduction of thylakoid proteins	52
4.3 Photosynthetic performance of PSII is affected in <i>amiR-TerC</i> plants	53
4.4 Leaf variegation is not caused by oxidative stress in <i>amiR-TerC</i> plants	55
4.5 Putative protein interaction partners of TerC	56
4.6 Integration of CP43 into the thylakoid membrane is impaired in <i>terc-1</i> and <i>amiR-TerC</i> plants	58
4.7 Model for the function of TerC in <i>Arabidopsis thaliana</i>	61
Appendix 1/2	63
References	64
Acknowledgements	82
Curriculum vitae	83
Declaration / Ehrenwörtliche Versicherung	84

List of Figures

Figure 1.1	Structure and components of plant chloroplasts	1
Figure 1.2	Scheme of electron transport across the thylakoid membrane	2
Figure 1.3	Gene transfer during evolution	4
Figure 1.4	Protein import into chloroplasts	5
Figure 1.5	Protein import of nuclear encoded proteins into the thylakoid membrane of chloroplasts	7
Figure 1.6	Assembly steps of PSII subunits	10
Figure 1.7	Characteristic variegated mutants of <i>Arabidopsis thaliana</i>	11
Figure 3.1	Growth phenotype of a 1-week-old wild type plant and a <i>terc-1</i> mutant	26
Figure 3.2	Transmission electron microscopy (TEM) picture of wild type and <i>terc-1</i> mesophyll cells	27
Figure 3.3	Growth phenotype of 3-week-old wild type and <i>amiR-TerC</i> (T2) plants	27
Figure 3.4	Transcript analyses of <i>AtTerC</i> in wild type and <i>amiR-TerC</i> plants	28
Figure 3.5	Growth phenotype of wild type and <i>amiR-TerC</i> (T2) plants	29
Figure 3.6	Growth phenotype of 3-week-old wild type, <i>amiR-TerC</i> (T3) and <i>amiR-TerC</i> (T4) plants	30
Figure 3.7	PCR analyses of plants transformed with pBW7FWG2- <i>TerC</i>	31
Figure 3.8	Transcript analyses of <i>AtTerC</i> in wild type, <i>terc-1</i> _{TerC-GFP} and WT _{TerC-GFP} plants	32
Figure 3.9	Growth phenotype of 3-week-old wild type, <i>terc-1</i> _{TerC-GFP} and WT _{TerC-GFP} plants	33
Figure 3.10	Fluorescence pictures of <i>terc-1</i> _{TerC-GFP} protoplasts	33
Figure 3.11	Salt treatment of isolated thylakoids from <i>terc-1</i> _{TerC-GFP}	34
Figure 3.12	Thermolysin treatment of intact thylakoids of <i>terc-1</i> _{TerC-GFP}	35
Figure 3.13	Photosynthetic performance of wild type, <i>amiR-TerC</i> , <i>terc-1</i> _{TerC-GFP} and WT _{TerC-GFP}	37
Figure 3.14	Parameters of PSI photosynthetic performance in wild type and mutant plants	38
Figure 3.15	Protein content of wild type and <i>terc-1</i> plants	39

Figure 3.16	Protein content of wild type and <i>amiR-TerC</i> plants	41
Figure 3.17	Blue native gel analysis and denaturing second dimension PAGE	42
Figure 3.18	Western analysis of 2D Tris-Tricine gels from Blue-Native PAGE	43
Figure 3.19	Sucrose gradient analysis of wild type and <i>terc-I_{TerC-GFP}</i> thylakoids solubilized with β -DM followed by separation on Tris-Tricine SDS PAGE	45
Figure 3.20	Fractionation of sucrose gradient samples of wild type and <i>terc-I_{TerC-GFP}</i>	46
Figure 3.21	Protein-protein interaction study between TerC and several plastid proteins	47
Figure 3.22	<i>In vivo</i> synthesis (pulse) of plastid encoded proteins from the thylakoid membrane	48
Figure 3.23	<i>In vivo</i> synthesis (pulse) and degradation (chase) of plastid encoded proteins from the thylakoid membrane	49
Figure 3.24	<i>In vivo</i> synthesis (pulse) and degradation (chase) of plastid encoded proteins from the thylakoid membrane separated first on blue native PAGE followed by a denaturing Tris-Tricine SDS-PAGE	51
Figure 4.1	Model for TerC activity on the insertion of CP43 into the thylakoid membrane and the photosystem II	62
Figure Appendix1	Identification of the mutant <i>psb1-2</i>	63

List of Tables

Table 1.1	Summary of identified variegation mutants in <i>Arabidopsis thaliana</i>	12
Table 2.1	<i>Arabidopsis thaliana</i> mutants cultivated for analyses	15
Table 2.2	List of primary antibodies used for immunoblot analyses	20
Table 2.3	List of secondary antibodies used for immunoblot analyses	21
Table 2.4	List of 22 proteins analysed in split ubiquitin interaction studies in <i>Saccharomyces serviciae</i>	22
Table 2.5	List of all primers used for PCR in 5' to 3' orientation	25
Table 3.1	Parameters of chlorophyll a fluorescence obtained from wild type, <i>amiR-TerC</i> , <i>terc-1</i> _{TerC-GFP} and WT _{TerC-GFP} plants	36
Table Appendix 1	List of all primers used for screening for <i>psbO1-2</i> plants and RT-PCR to determine the transcript level of PsbO1 in these Mutants	63

Abbreviations

°C	Degree Celsius	F_M	Maximum fluorescence of PSII
35SCaMV	35S promoter of the Cauliflower Mosaic virus	F_M'	Maximum fluorescence of PSII under illumination
α	anti	FNR	Ferredoxin NADP oxido- reductase
A	Ampere	F_S	Steady state fluorescence of PSII
ADP	Adenosine diphosphate	FTR	Ferredoxin:thioredoxin reductase
amiRNA	Artificial micro RNA	F_V/F_M	Maximum quantum yield of PSII
<i>At</i>	<i>Arabidopsis thaliana</i>	g	Gramm
ATP	Adenosine triphosphate	g	Standard gravity
ATPase	ATP synthase	G3P	Glyceraldehyde 3-phosphate
β -DM	n-Dodecyl β -D-maltoside	GFP	Green fluorescent protein
BN	Blue native	GTP	Guanosine triphosphate
BSA	Bovine serum albumin	h	Hour
$C_6H_{12}O_6$	Glucose	h	Planck constant
$CaCl_2$	Calciumchloride	H_2O	Water
Chl	Chlorophyll	HCl	Hydrochloroc acid
Ci	Curie	HEPES	4-(2-hydroxyethyl)-1- piperazineethanesulfonic acid
CO_2	Carbondioxide	HL	High light
cm	Centimetre	HPLC	High performance liquid chromatography
Col-0	<i>At</i> ecotype Columbia-0	Hz	Hertz
cp	Chloroplast	kDa	Kilodalton
Cub	C-terminus of ubiquitin	KCl	Potasium chloride
Cyt	Cytochrome	KOH	Potasium hydroxyde
DNA	Deoxyribonucleic acid	LB	Left border
DTT	Dithiotreitol	LHC	Light harvesting complex
E	Einstein	LL	Low light
EDTA	Ethylenediaminetetraacetic acid	lmw	Low molecular weight subunit
EMS	Ethyl methane sulphonate	-LT	Synthetic medium lacking leucine, tryptophan
ER	Endoplasmatic reticulum		
EtBr	Ethidium bromide		
ETR	Electron transfer rate		
F_0	Ground fluorescence		
Fe/S	Iron/Sulfur		
Fd	Ferredoxin		

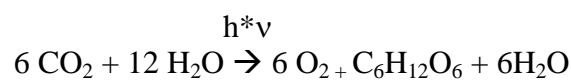
Abbreviations

-LTH	Synthetic medium lacking leucine, tryptophan, histidine	PSII	Photosystem II
M	Molarity	PSII-RC	Photosystem II reaction centre
m	Meter	PVDF	Polyvinylidene Fluoride
MES	2-(<i>N</i> -morpholino)ethanesulfonic acid	Q _{A/B}	Plastoquinon
MgCl ₂	Magnesiumchloride	qP	Photochemical quenching
ML	Moderate light	RNA	Ribonucleic acid
MgSO ₄	Magnesiumsulfate	ROS	Reactive oxygen species
min	Minute	RT	Room temperature
mRNA	messenger RNA	RT-PCR	Reverse transcriptase PCR
MS	Murashige and Skoog	S	Sulfur
ν	Frequency	s	Second
Na ₂ CO ₃	Sodiumcarbonate	SDS	Sodium dodecyl sulphate
NaCl	Sodiumchloride	SRP	Signal recognition particle
NADP ⁺ /H	Nicotinamide adenine dinucleotide phosphate	T-DNA	Transfer-DNA
NaSCN	Sodiumthiocyanate	TEM	Transmission electron microscopy
NDH	NADPH dehydrogenase complex	Tic	Translocon in the inner envelope of chloroplasts
NPQ	Non-photochemical quenching	Toc	Translocon in the outer envelope of chloroplasts
Nub	N-terminus of ubiquitin	TPP	Thylakoidal processing peptidase
O ₂	Oxygen	V	Voltage
OEC	Oxygen evolving complex	WT	Wild type
P ₆₈₀	PSII reaction centre	Φ_{II}	Effective quantum yield of photosystem II
P ₇₀₀	PSI reaction centre	Y(I)	Photochemical quantum yield of PSI
PAM	Pulse amplitude modulation	Y(NA)	Acceptor side limitation of PSI
PC	Plastocyanin	Y(ND)	Donor side limitation of PSI
PCR	Polymerase chain reaction		
PFD	Photon flux density		
P _i	Inorganic phosphate		
P _m	Maximum P ₇₀₀ ⁺ absorption		
P _m '	Maximum P ₇₀₀ ⁺ absorption under illumination		
POR	NADPH:Protochlorophyllid-Oxidoreduktase		
PSI	Photosystem I		

1. Introduction

1.1 Photosynthesis

The planet earth arose about 4.7 billion years ago and about 700 million years later the first life on this planet, single cell organisms, appeared. 3.5 billion years ago the non oxygenic photosynthesis was established and it took another 1 billion years until earth was surrounded by an oxygen containing atmosphere (Great Oxidation Event). During this time the oxygenic photosynthesis must have evolved and established [Bekker et al., 2004]. The oxygenic photosynthesis is a photochemical mechanism that converts inorganic carbon dioxide into organic sugars by light energy delivered from the sun (see equation below) [Campbell, 1997].



In higher plants this photochemical process takes place in organelles called chloroplasts that can be found in all green parts of plants, especially in leaves. Chloroplasts contain in total three different membrane systems, the outer envelope, the inner envelope and thylakoids (**Figure 1.1**).

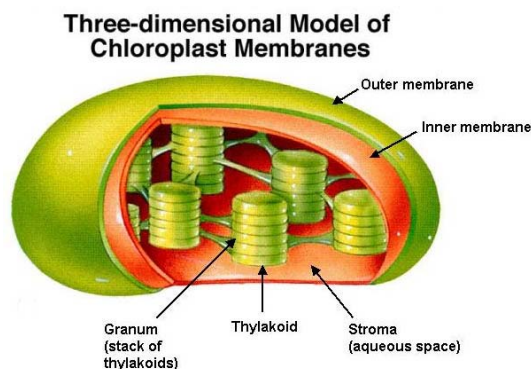


Figure 1.1: Structure and components of plant chloroplasts

Chloroplasts are surrounded by two envelope membranes that separate the plastid stroma from the cytosol of the cell. Inside of the chloroplast another membrane system exists, the so called thylakoid. [Figure taken from Moore, Clark and Vodopich, 1998]

While the outer envelope contains a lot of aqueous channels formed by proteins which make the membrane permeable for metabolites, the inner envelope represents a barrier for these molecules and the uptake and release of metabolites there is controlled by special transporters. The third membrane system, the thylakoids, is the place where photosynthesis takes place. Thylakoids form a compartment that separates the inner space (lumen) from the stroma [Lodish et al., 2000].

Photosynthesis can be divided into two main parts, the so called light reaction and carbon fixation. The light reaction takes place in the thylakoid membrane and lumen where electrons

are transported over the membrane to generate ATP and redox equivalents. This process starts at the photosystem II (PSII), where the absorption of photons by the light harvesting complex of PSII (LHCII) leads to an excitation of chlorophyll a molecules in the reaction centers of PSII (P₆₈₀) (**Figure 1.2**). From these excited P₆₈₀'s electrons are transferred to the primary electron receptor pheophytin a and the generated electron gap is refilled by electrons derived from the water splitting complex, where two H₂O molecules are split into four protons, O₂ and four electrons. From the primary receptor electrons are transferred via a stationary plastoquinone (Q_A) to Q_B which becomes mobile by the uptake of two stromal protons and moves to the Cytochrome *b₆/f* complex (Cyt *b₆/f*). Here, the protons are released to the lumen and the electrons are further transferred via Cyt *b₆/f* to the final mobile carrier protein plastocyanin (PC). PC fills the electron gap at photosystem I. PSI is, like PSII, surrounded by light harvesting complexes (LHCI) and also there excitation of chlorophylls in the reaction center (P₇₀₀) and electron transmission takes place in a similar way as described for PSII. The electron transfer from PSI leads either to the reduction of NADP⁺ by a ferredoxin-NADP-reductase (FNR) via the electron carrier ferredoxin (Fd) (linear electron flow) or electrons are reinjected into the electron transport chain to generate a proton gradient across the thylakoid membrane (cyclic electron flow). This electrochemical potential is used by a protein complex called ATP synthase to generate ATP out of ADP and P_i by releasing protons from the lumen into the stroma of chloroplasts [Campbell, 1997].

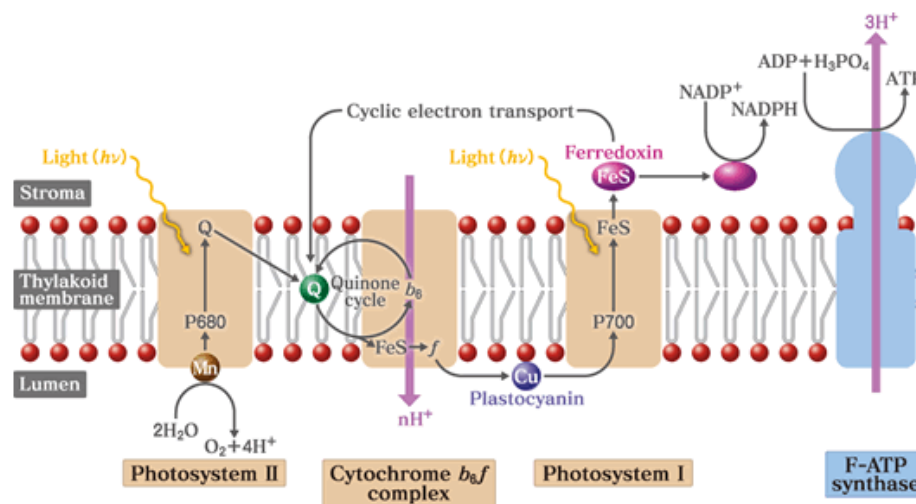


Figure 1.2: Scheme of electron transport across the thylakoid membrane [Figure taken from Shoichi, 2010]

The scheme is showing the structure of thylakoids as a bilayer membrane. Several multi protein complexes are localized in this membrane system contributing to electron transfer along the membrane. Electrons are excited to a higher electric state by sunlight that is collected by light harvesting complexes located to either photosystem II or I. The electrons leaving the PSII reaction center are replaced by new electrons deriving from the water splitting complex in the lumen. During transport of electrons along the thylakoid membrane a proton gradient across the thylakoid membrane is generated that later drives the plastid ATP synthase to generate ATP by release of protons into the stroma.

The second part of photosynthesis, the carbon fixation, is located in the stroma of chloroplasts. Here, ATP and NADPH, produced during the light reaction, are used in the Benson-Calvin cycle to generate a three-carbon phosphate sugar molecule, the so called glyceraldehyde-3-phosphate (G3P), by assimilation of CO₂ [Campbell, 1997]. During this step ATP and NADPH are used in a 3:2 ratio [Allen, 2002]. The linear electron flow delivers these two products of the light reaction in another ratio, thus cyclic electron flow is needed to adjust ATP:NADPH ratio [Eberhard et al., 2008]. To date, there are at least two different pathways of cyclic electron flow known, the NDH-dependent photosystem I cyclic electron transport [Shikanai, 2007] and the PGR5-dependent photosystem I cyclic electron transport [Munekage et al., 2002; DalCorso et al., 2008].

1.2 Evolutionary impact on chloroplasts

In each cell, higher plants contain organelles that fulfill highly specific functions. In present days it is widely accepted that mitochondria and chloroplasts derive from α -proteobacteria and cyanobacteria, respectively. During evolution more than 90% of the genes previously located in the cyanobacterium were transferred to the nucleus of the host cell that is now in control of the protein synthesis of the whole cell [Leister, 2003]. This enables the host to quickly adjust translation of proteins to changing conditions or special needs. But as now all these proteins are synthesised in the cytosol of the cell these proteins must have undergone changes in the amino acid sequence. To make sure that the mature protein will be transferred to the correct destination within the cell it must contain a signal that enables the cell to guide it there. This is achieved by an amino-terminal targeting signal, the so called transit peptide that is cleaved off from the precursor protein after post-translational targeting [Jarvis and Soll, 2002]. The chloroplast genome contains only a few genes compared to their cyanobacterial ancestors [Leister, 2003]. But these genes are coding for the information of some of the most important proteins in this compartment, like the core proteins of PSI and PSII, the Cyt *b₆/f* complex and the ATP-synthase. Therefore, plants must have undergone adaptations to still maintain the physiological activity of these multi protein complexes, that are now composed of nuclear and plastid encoded proteins. To fulfill the task of stoichiometric expression of the subunits and their assembly to multi-protein complexes, new regulatory elements like an import machinery and assembly factors must have evolved [Leister, 2003; Ossenbühl et al., 2004].

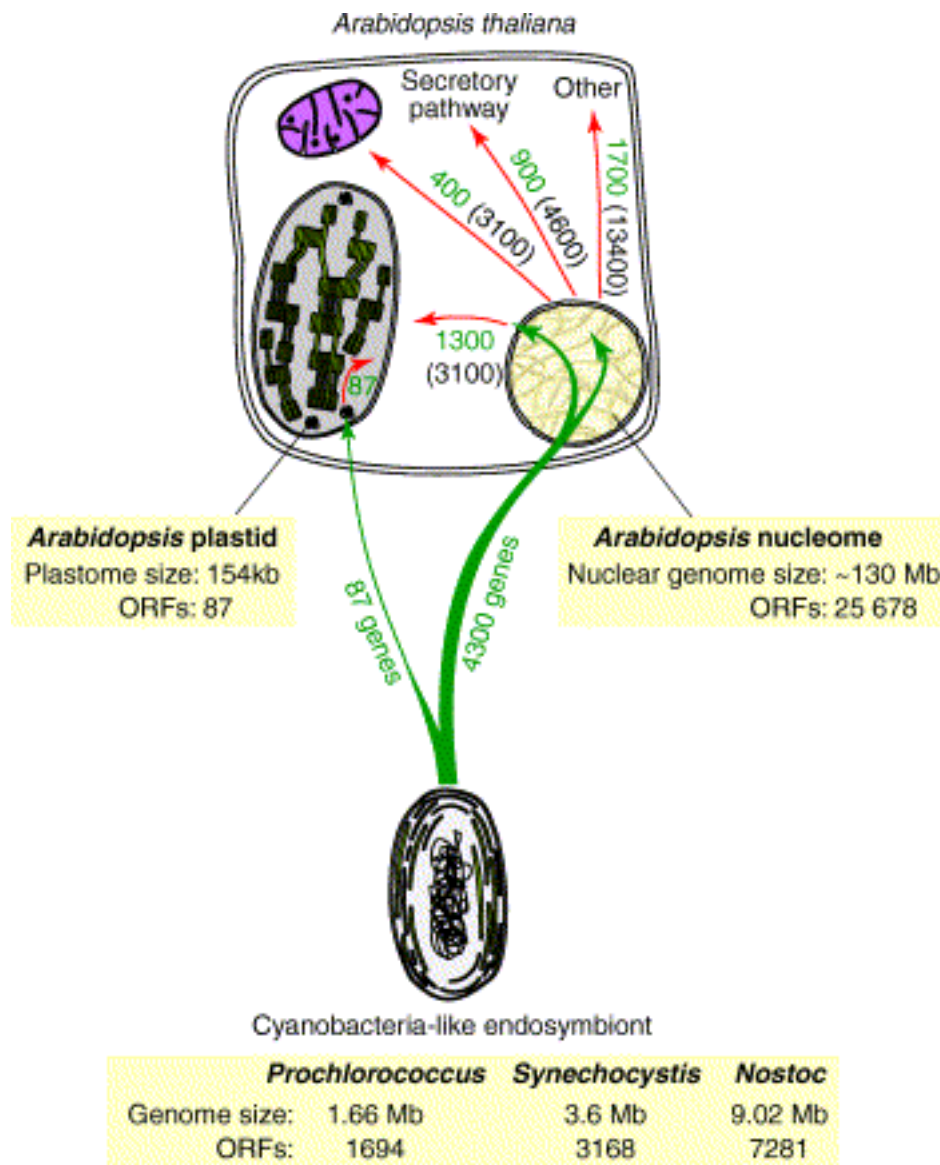


Figure 1.3: Gene transfer during evolution

Genes of cyanobacterial origin are mainly transferred to the nuclear genome of *Arabidopsis thaliana*. The products of these genes are transported into the chloroplast when functions of proteins did not change. But also transport to locations outside of the plastid is possible if the protein gained a new function during evolution. [Figure taken from Leister, 2003]

1.3 Protein import into chloroplasts and thylakoids

Chloroplasts are of prokaryotic origin and are the result of an endosymbiotic event which becomes evident by looking at the three different membrane systems of the organelle. Thylakoids are of prokaryotic and the outer envelope is of eukaryotic origin, whereas the inner envelope is an intermediate product [Gutensohn et al., 2005]. Proteins supposed to be imported to chloroplasts mainly contain an amino-terminal transit peptide that guides the precursor protein across the two envelopes and is afterwards cleaved of by a stromal processing peptidase [Richter and Lamppa, 1998]. Around 10% of the plastid proteins

encoded in the nucleus are imported into the plastids without bearing a transit peptide [Armbruster et al., 2009] The transport across the membranes is mediated by two oligomeric protein complexes (**Figure 1.4**) called Toc complex (translocon at the outer envelope membrane of chloroplasts) [Waegemann and Soll, 1991] and Tic complex (translocon at the inner envelope membrane of chloroplasts) [Kessler and Blobel, 1996]. At first the precursor protein binds to a signal receptor binding protein that guides it to one of the two identified receptors of the Toc complex, Toc159 or Toc34 [Hirsch et al., 1994; Kessler et al., 1994; Jelic et al., 2003]. The interaction of the precursor with the receptor requires binding and hydrolysis of GTP [Schleiff et al., 2002; Becker et al., 2004a]. This is a prerequisite for the transfer through the major translocation channel that is formed by β -sheet structures of Toc75 [Sveshnikova et al., 2000; Baldwin et al., 2006]. Additionally, there are two other proteins attached to this complex, Toc 64 and Toc 12, but so far no crucial function in protein import could be assigned to them [Sohrt and Soll, 2000; Becker et al., 2004b; Rosenbaum-Hofmann and Theg, 2005; Aronsson et al., 2007].

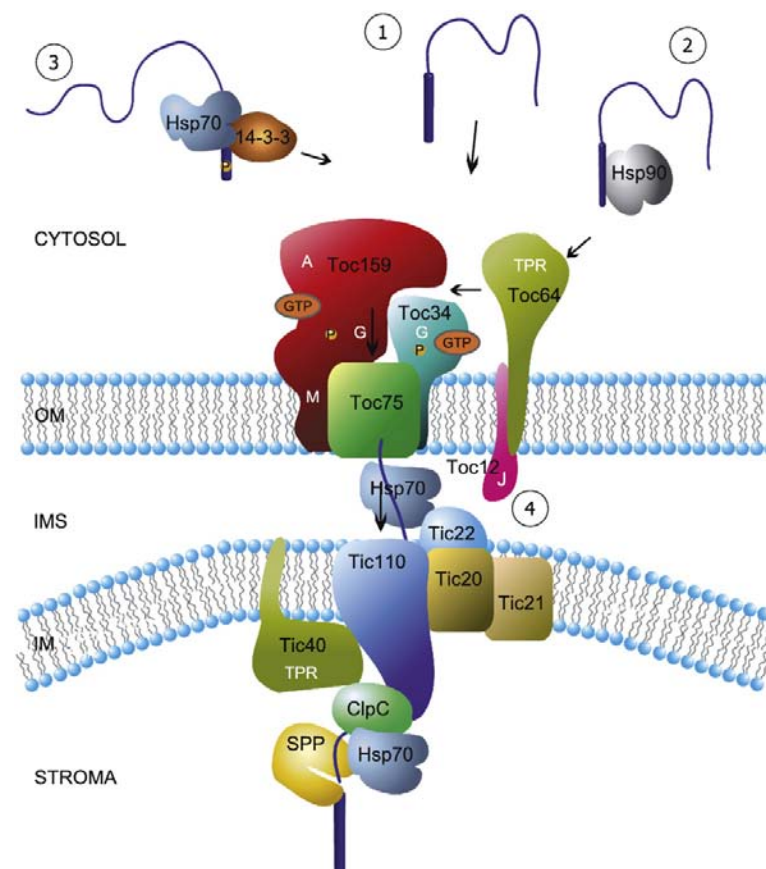


Figure 1.4: Protein import into chloroplasts

Proteins, that are synthesised in the cytosol and have their destination in the chloroplast, must be transferred across the two envelope membranes. Therefore two protein complexes, the Toc and Tic complex, recognise a transit peptide attached to the mature protein and guide the precursor protein across the envelope membranes. [from Andres et al., 2010]

After crossing the first envelope membrane the precursor protein associates with Tic22 in the intermembrane space. Tic22 is a soluble protein that is able to interact transiently with the inner envelope membrane and might represent the receptor for incoming proteins which guides them to the Tic complex [Kouranov and Schnell, 1997; Kouranov et al., 1998]. Tic20 and Tic110, both located in the inner envelope, are supposed to transport precursors across this membrane. But whether they are forming a heteromeric translocon or constituting an import channel by themselves, is not clarified yet [Kouranov et al., 1998; Lübeck et al., 1996; Kessler and Blobel, 1996; van Dooren et al., 2008; Vojta et al., 2009]. The proteins Tic32, Tic55 and Tic62 are proposed redox regulators of protein import across the inner envelope membrane [Caliebe et al., 1997; Kuchler et al., 2002; Hörmann et al., 2004; Chigri et al., 2006; Stengel et al., 2008; Boij et al., 2009], whereas Tic40 contains a stromal chaperon binding domain which is interacting with the stromal chaperone Hsp70 and is necessary for reintegration of proteins into the inner envelope of chloroplasts [Stahl et al., 1999; Chou et al., 2003; Chiu and Le, 2008].

The transport of proteins into or across the thylakoid membrane is mediated by four independent pathways. Two of them, the SRP-dependent pathway and the “spontaneous” pathway, are exclusively used to insert proteins into the membrane, whereas the Sec- and the Tat-pathway are transporting proteins into the lumen of thylakoids [Gutensohn et al., 2005]. The spontaneous insertion is restricted to a specific class of proteins with similar structure and membrane topology. The single membrane span is located closely to the amino-terminus of the mature protein that is facing towards the lumen of thylakoids. Insertion of these proteins into the membrane needs the presence of two hydrophobic domains flanking the hydrophilic amino-terminal end of the protein [Michl et al., 1994; Schleiff and Klösgen, 2001]. The non C-terminal located domain of these two hydrophobic areas functions as the membrane anchor of the mature protein, whereas the other domain closely to the amino end of the protein is cleaved off the mature protein and is only needed as a transit peptide [Michl et al., 1999]. All proteins following this way of insertion into the thylakoid membrane are synthesised in the cytosol of the cell and contain bipartite transit peptides, which mediate both the import into chloroplasts via Toc and Tic complexes and the integration into the thylakoid membrane [Michl et al., 1999]. Examples for proteins using this way of thylakoid integration are CF₀-II, a subunit of the plastidic ATPase [Michl et al., 1994] as well as subunits of photosystem II (PsbW, PsbX and PsbY) [Lorkovic et al., 1995; Kim et al., 1998; Thompson et al., 1999].

The second pathway that is inserting proteins exclusively into the thylakoid membrane is the SRP-dependent pathway. It is the major way to insert polytopic membrane proteins. The main

substrate of this pathway is LHCP, the apoprotein of all LHCs, and this import mechanism is also the best understood one [Gutensohn et al., 2005]. Four stromal factors are needed for proper thylakoid insertion of LHCP, cpSRP54 [Franklin and Hoffman, 1993; Li et al., 1995], cpSRP43 [Schuenemann et al., 1998], cpFtsY [Kogata et al., 1999] and LTD [Ouyang et al., 2001]. The cpSRP54 shows homology to the 54 kDa subunit of the cytosolic signal recognition particle and to its bacterial counterpart Ffh. The cpFtsY is homologous to FtsY, a bacterial SRP-receptor protein. In contrast to these two proteins no homolog in bacteria to cpSRP43 of *Arabidopsis thaliana* is known [Gutensohn et al., 2005]. The fourth stromal factor, LTD, was recently discovered to be located mostly in the stroma of chloroplasts, but also to be slightly attached to the inner envelope. It is binding to the LHCP after transport through the Tic-complex [Ouyang et al., 2001]. In addition to these four stromal factors ALB3, a thylakoid integral protein, is needed for protein insertion. ALB3 is highly homologous to the bacterial YidC and the mitochondrial Oxa1p proteins [Moore et al., 2000]. Additionally to these protein factors the SRP-dependent pathway requires energy delivered by hydrolysis of GTP and a proton gradient across the thylakoid membrane [Jaru-Ampornpan et al., 2007].

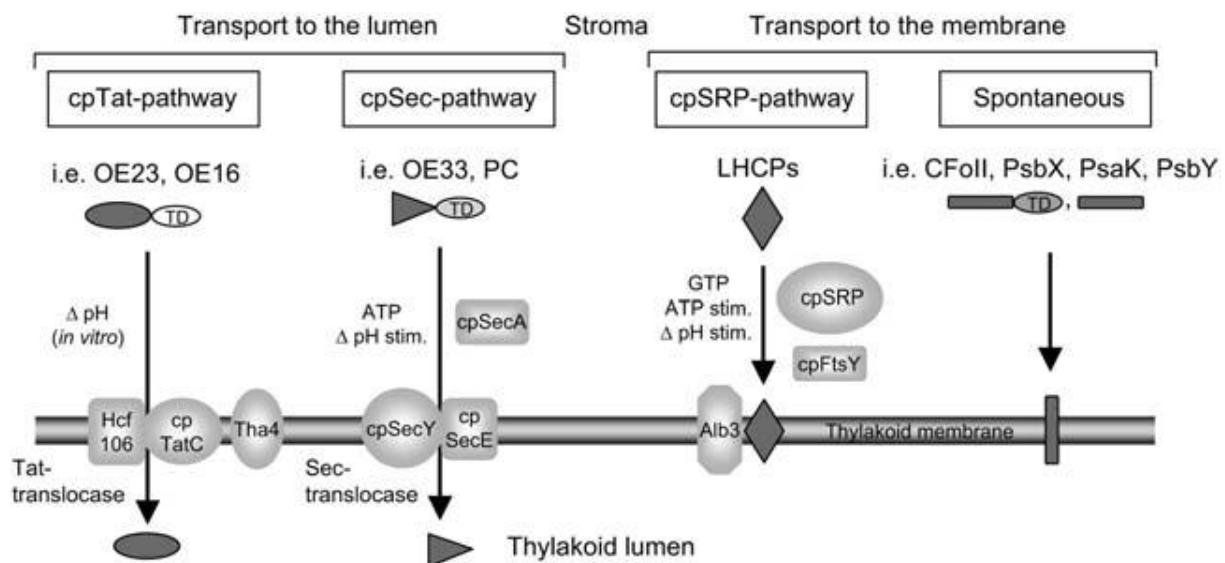


Figure 1.5: Protein import of nuclear encoded proteins into the thylakoid membrane of chloroplasts

Once nuclear encoded proteins reach the stroma of chloroplasts they undergo two possible ways of further processing. If the destination of the imported protein is in the stroma, the transit peptide is cleaved off by stromal peptidases. Proteins with their destination in the thylakoid membrane or lumen can be imported by four different pathways, the SRP-dependent, the Δ pH/Tat-dependent and the Sec-dependent pathways or by spontaneous insertion. [Figure taken from Schünemann, 2007]

The other two protein transport pathways, the Sec-dependent and the Δ pH/Tat-dependent pathways, are mainly translocating hydrophilic proteins in the thylakoid lumen [Di Cola et al.,

2005]. These proteins contain two transit peptide signals, one for the envelopes and another for crossing the thylakoids. The second transit signal is cleaved at the luminal side by a thylakoidal processing peptidase (TPP). Although for both pathways bipartite transit peptide signals are necessary, the amino acid sequence needed for the transport across the thylakoid membrane is conserved among proteins using the same pathway, but differs between proteins using either the Sec-dependent or the Δ pH/Tat-dependent pathway [Robinson et al., 1994].

The Sec-dependent pathway is highly similar to the main secretory pathway in bacteria. The energy for the protein transport derives from hydrolysis of ATP and the three components, SecA, SecE and SecY show significant homology to their bacterial counterparts [Gutensohn et al., 2005]. SecA is located in the stroma and might act as a signal recognition particle [Yuan et al., 1994; Berghöfer et al., 1995] with an ATPase activity [Liu et al., 2010]. The translocation pore is supposed to be formed by the two membrane bound proteins SecE [Schuenemann et al., 1999] and SecY [Laidler et al., 1995; Bergöfer and Klösgen, 1996]. Substrates for the Sec-dependent pathway are plastocyanin, PsaF and PsbO [Hulford et al., 1994; Karnachov et al., 1994; Robinson et al., 1994; Yuan and Cline, 1994].

In contrast to the Sec-dependent protein import the Δ pH/Tat-dependent pathway requires neither energy supplied by triphosphates [Cline et al., 1992] nor soluble factors that recognise the precursor protein in the stroma of chloroplasts [Mould et al., 1991]. In higher plants, the energy for protein import into the lumen is supplied by a pH-gradient across the thylakoid membrane [Braun et al., 2007], which is not true for the green algae *Chlamydomonas reinhardtii* and so still controversially discussed [Finazzi et al., 2003]. The driving force for protein translocation gave rise to the first part of the name of this protein transport pathway. The second part of the name derives from two conserved arginine residues in the respective signal peptide (twin arginine translocation = Tat) [Chaddock et al., 1995]. What is unique about the Δ pH/Tat-dependent pathway in comparison to the other three types of protein import is the ability to translocate mature proteins or fully folded protein domains across the thylakoid membrane [Marques et al., 2004]. The translocase complex itself consists of three protein subunits, TatA (Tha4), TatB (HCF106) and TatC (cpTatC) [Settles et al., 1997; Walker et al., 1999; Motohashi et al., 2001]. It is assumed that in the presence of a proton gradient and the substrate bound to the TatB-TatC-complex TatA transiently joins this aggregate and forms the pore by which proteins are imported [Mori and Cline, 2002; Jakob et al., 2009]. Examples for proteins imported via the Δ pH/Tat-dependent pathway are the 16 and 23 kDa proteins of the OEC [Klösgen et al., 1992; Mould et al., 1991] and the Rieske Fe/S protein of Cytochrome *b₆/f* complex [Molik et al., 2001].

1.4 Photosystem II – structure and assembly

Plant photosystem II is a multi protein-pigment complex located in thylakoid membrane of chloroplasts that works as a light driven water:plastoquinone oxidoreductase. The physiological active form is a dimer formed by two PSII monomers [Nelson and Yocum, 2006]. The reaction center of photosystem II contains the two proteins D1 and D2 with its chromophores (six chlorophylls including the P₆₈₀), two pheophytines and the plastoquinones Q_A and Q_B. The protein CP47 is closely attached to the D2 protein and CP43 is in close proximity to D1. The luminal part of D1 and CP43 is stabilising the proteins of the oxygen evolving complex. CP43 and CP47 are also binding chlorophylls that contribute to energy transfer in PSII and additionally seven β -carotenes necessary for photoprotection [Biesiadka, 2004]. Additionally, several small protein subunits with different functions like assembly, dimer stabilisation and binding of chlorophylls and carotenoids are also constituting the photosystem II [Ferreira, 2004].

Using pulse labelling experiments and native protein complex isolation, five assembly steps of PSII formation could be identified. The first step is the integration of the D1 precursor protein into a receptor complex consisting of D2, PsbE and F, both subunits of Cyt *b*₅₅₉ complex, and PsbI, by that forming the photosystem II reaction center complex (PSII-RC) [Tsiotis et al., 1999; Komenda et al., 2004]. The second step in PSII biogenesis is the insertion of CP47 into the PSII-RC complex [Rokka et al., 2005]. The proper assembly of the so called CP47-RC is necessary as in this state precursor D1 protein is processed, the precursor is cleaved off and the mature D1 is finally present in PSII [Armbruster et al., 2010]. During the next two steps of PSII assembly in total four low molecular weight subunits (lmw) are integrated. At first the insertion of three plastid encoded proteins, PsbH, M and T_C, occurs by which the CP47-RC is stabilised [Rokka et al., 2005]. In the following step the first nuclear encoded protein, PsbR, is integrated [Rokka et al., 2005]. This membrane integral protein is mostly orientated towards the lumen and might play a role in anchoring OEC proteins to photosystem II [Barber et al., 1997]. In the fifth PSII assembly step the last major protein, CP43, is integrated [Rokka et al., 2005]. Directly after the insertion of CP43 another lmw, PsbK, complements the PSII core monomer. This monomer is able to bind PsbO, the first subunit of oxygen evolving complex. So far it is not fully understood whether PsbW, another low molecular weight subunit, binds to photosystem II during its dimerisation [Thidholm et al., 2002] or afterwards to provide binding of LHCII to PSII complexes [Rokka et al., 2005]. More in the periphery of PSII, PsbZ is located that, together with the luminal protein

AtFKBP20, allows binding of LHCII-trimers to PSII to form PSII-supercomplexes [Swiatek et al., 2001; Lima et al., 2006].

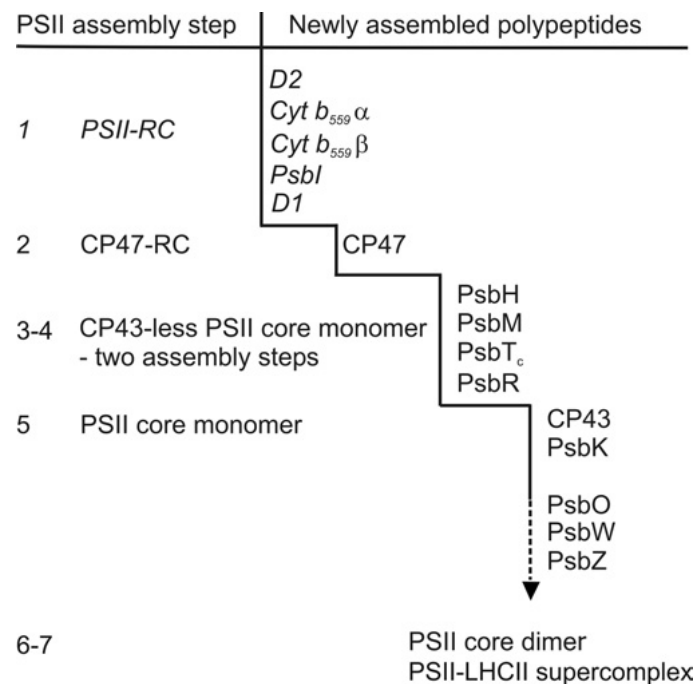


Figure 1.6: Assembly steps of PSII subunits

Incorporation of radioactively labelled subunits into photosystem II was used to determine intermediate states in the order of PSII aggregation. In total four intermediate states were found until in a final fifth step a photosystem II monomer is assembled. After monomer formation a PSII dimer aggregates that binds light harvesting complexes to form up PSII-LHCII-supercomplexes, the photosynthetic active form of photosystem II [from Rokka et al., 2005]

For the first assembly step, the integration of D1, additional factors are necessary that are not structural subunits of PSII. The *Arabidopsis* mutant *hcf136* shows an albinotic phenotype and only trace amounts of D1 protein are detectable whereas the other core proteins are completely missing. Instead of the mature D1 protein an increase in the precursor of the D1 protein can be observed as its integration into the receptor complex is not possible [Meurer et al., 1998; Komenda et al., 2008]. An increase of precursor D1 protein can be detected in *pam68* where either the maturation of D1 is disturbed or the stability of CP47-RC complex that mediates D1 maturation is impaired [Armbruster et al., 2010]. A similar phenotype can be observed in *lpa1* plants. LPA1 might act as a chaperone in the thylakoid membrane together with AtCyp38 and is necessary for proper D1 folding and integration into the receptor complex [Peng et al., 2006; Sirpiö et al., 2008]. Both proteins, PAM68 and LPA1, are interacting *in vitro* with ALB3, an assembly factor that was previously shown to play a role in the SRP-dependent pathway for integration of LHCPs into thylakoid membrane [Bellafiore et

al., 2002]. In *Chlamydomonas* it was observed that the homolog of ALB3, ALB3.1, is necessary for the integration of D1 protein into functional PSII as precursor ALB3.1 and D1 are interacting although it is not affecting the integration into the thylakoid membrane [Ossenbühl et al., 2004].

Two additional assembly factors, LPA2 and LPA3, that are interacting with each other are supposed to contribute to the integration of CP43, as they are also interacting with the PSII core protein. The loss of LPA2 and LPA3 leads to a decrease in CP43 protein and the double mutant *lpa2/lpa3* is completely lacking CP43 [Ma et al., 2007; Cai et al., 2010].

1.5 Variegated mutants in *Arabidopsis thaliana*

Per definition, variegated mutants contain “patches of different colours in its vegetative parts” [Kirk and Tilney-Basset, 1978]. Typically, parts of the plant that used to be green include white or yellow sectors. Cells of the green areas are developed normally whereas the plastids of the abnormal coloured sectors are deficient in chlorophylls and/or carotenoids and appear to be stressed by photooxidation or be blocked in the biogenesis of chloroplasts [Yu et al., 2007].

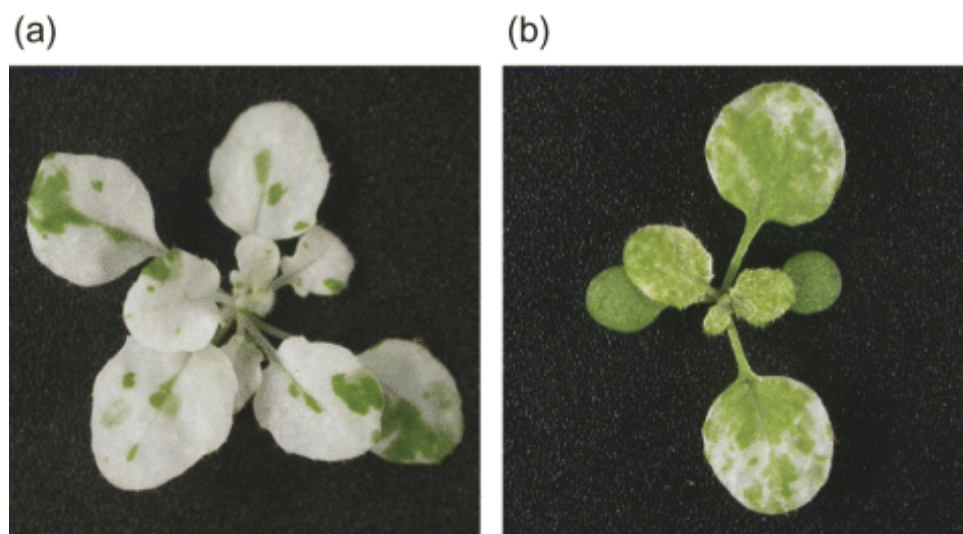


Figure 1.7: Characteristic variegated mutants of *Arabidopsis thaliana*

Variegated mutants contain white or yellow sectors within normal developed green tissue. Here, two typical mutants, *immutants* (*im*) (a) and *variegated2* (*var2*) (b) are shown representatively [from Yu et al., 2007].

Via ethyl methane sulphonate (EMS) and X-ray mutagenesis of *A. thaliana*, several hundred lines showing a variegated phenotype arose, but only a very few genes have been identified whose mutations are responsible for the abnormal leaf colouration. The following table lists all mutants with a variegated phenotype of *Arabidopsis thaliana* characterised so far [Yu et al., 2007].

Table 1.1: Summary of identified variegation mutants in *Arabidopsis thaliana*

mutant	function	author
<i>immutant (im)</i>	plastid terminal oxidase	Aluru et al., 2007
<i>variegated1 (var1)</i>	D1 turnover	Zaltsman et al. 2005
<i>variegated2 (var2)</i>	D1 turnover	Bailey et al. 2002
<i>variegated3 (var3)</i>	carotenoid biosynthesis	Næsted et al., 2004
<i>chloroplast mutator (chm)</i>	control of mitochondrial genome	Abdelnoor et al. 2003
<i>lovastatin-resistant111 (lvr111)</i>	isoprenoid biosynthesis	Estévez et al., 2001
<i>pale cress (pac)</i>	plastid mRNA processing	Meurer et al., 1998
<i>white cotyledons (wco)</i>	16S rRNA maturation	Yamamoto et al., 2000
<i>thylakoid formation1 (thf1)</i>	thylakoid biogenesis	Wang et al., 2004
<i>atase2 deficient (atd2)</i>	purine synthesis	vd Graaff et al., 2004
<i>albomaculans (am)</i>	unknown	Röbbelen, 1968

Variegation in *Arabidopsis thaliana* is caused by defects in several nuclear encoded proteins that are localised preferably in the chloroplast, but also in mitochondria (**Table 1.1**). As all plants listed in Table 1.1 are homozygous for the mutated allele, it is still not clarified why the defect caused by the mutation is not visible in all cells of the plant. It is suggested that in each plant cell there is a threshold in the protein amount or activity that has to be underscored for the variegation phenotype to appear [Yu et al., 2007].

1.6 Previous work on the gene *At5g12130*

Based on a database screen for putative plastid located transmembrane proteins with more than five transmembrane domains the gene *At5g12130* was identified. In his diploma thesis, König [2005] confirmed the predicted plastid localisation of the protein via transformation of protoplasts from *Nicotiana tabacum* with a vector coding for a GFP fusion protein. The fluorescence of the GFP was localised in chloroplasts, but the exact localisation to either envelope membranes or thylakoid membrane could not be clarified. Further database analyses revealed that the highly hydrophobic protein consists of 384 amino acids with a molecular weight of 41 kDa and contains up to eight transmembrane domains. *At5g12130* is a single-copy gene with no paralogs in *Arabidopsis thaliana*. Orthologs of the gene could be found in other plants like rice and maize, in green algae, in cyanobacteria and in archea. Sequence homologies revealed a TerC domain in the protein that is described to function in tellurium resistance in *Escherichia coli* [Burian et al., 2000]]. Knock-out mutants are seedling lethal, so only heterozygous plants could be propagated, and *terc* mutants showed an albino phenotype when grown on MS medium.

During his diploma thesis in 2007, Strissel observed that mutants grown under a very low light intensity ($4 \mu\text{Em}^{-2}\text{s}^{-1}$) turned slightly green in the cotyledon stage. The biogenesis of

plant pigments seemed not to be affected, because chlorophyll a and b, as well as most of the carotenoids, could be detected in these mutant plants via HPLC-analysis. Another fluorescence microscopy study of a GFP-fusion protein suggested localisation of TerC in the thylakoid membrane. Analyses of the photosynthetic protein complexes by mass spectrometry and immunodetection with specific antibodies revealed the presence of thylakoid protein complexes like photosystem I with its light harvesting complexes and LHCBI, as well as extrinsic subunits of PSII. In contrast, proteins of the PSII core complex could never be detected, suggesting a role of At5g12130 in PSII core complex assembly.

Data published in 2008 by Kwon and Cho confirmed the data derived from the two diploma theses. Loss of TerC leads to a pigment defective mutant showing an albino phenotype grown on MS medium under normal light conditions. They also propose that the biosynthetic pathways of chlorophyll and carotenoid biosynthesis are not affected, because precursors of chlorophyll can be found in mutant plants and they also observed the pale green phenotype under dim light. Electron microscopy pictures of albino mutants kept in the dark showed the presence of prolamellar bodies, as in wild type; however, a disorganisation of the prothylakoid membranes was observed. This suggests a defect in the biogenesis of chloroplast due to the loss of TerC protein. Altered plastid gene expression in *terc* seems not to be the reason for the strong effect caused by the loss of this protein as mRNA of *psbA* can still be detected by Northern Blot analysis although the D1 protein cannot be found by immunodetection anymore. In conclusion their results the authors suggest two possible functions for TerC. One possibility is that TerC represents a component of one of the translocation pathways of the thylakoid membrane and assists insertion or translocation of proteins into or across the thylakoid membrane. Another option would be a function in the biogenesis of the thylakoid membrane, due to the abnormal prothylakoid membrane structure in *terc* observed in ultrastructure pictures of etioplasts [Kwon and Cho, 2008].

1.7 Aims of the thesis

In this thesis the exact location and function of TerC in *Arabidopsis thaliana* is characterised. This is achieved by reverse genetics analysis of *AtTerC* knock-out lines and of *amiR-TerC* lines where the transcript of *AtTerC* is down-regulated. These lines are characterised at the physiological and biochemical level.

The role of TerC in photosystem II assembly is analysed in more detailed experiments by identification of putative interaction partners. Furthermore, with the use of GFP-tagged TerC

lines the localisation during PSII assembly is studied. In a final step the obtained data are combined to construct a model of TerC function in *Arabidopsis thaliana*.

2. Materials and methods

2.1 Database analyses and prediction programs

For online sequence analyses and predictions the following homepages and programs were used:

- NCBI (<http://www.ncbi.nlm.nih.gov/>)
- TAIR (<http://www.arabidopsis.org>)
- TargetP (<http://www.cbs.dtu.dk/services/TargetP/>)
- Aramemnon (<http://aramemnon.botanik.uni-koeln.de/>)
- ATTED (<http://atted.jp/>)
- SIGNAL Salk (http://signal.salk.edu/cgi-bin/tdna_express).

For sequence analyses and alignments the Vector NTI software (Invitrogen) was used. For in-house mass spectrometry analyses a database on chloroplast membrane and soluble proteins [Dr. Bernd Müller], as well as other databases of chloroplast sub fractions [Kleffmann et al., 2004; Zybailov et al., 2008], were applied.

2.2 Plant material and growth conditions

Two T-DNA knock out lines for the gene At5g12130 were available. The mutant *terc-1* (SALK_014739) was identified in the SALK collection [Alonso et al., 2003], containing an insertion in the second intron of the gene. The second mutant line *terc-2* (GABI-Kat 844D10) contains a T-DNA insertion in the third exon. Both lines were identified by searching the insertion flanking database SIGNAL (http://signal.salk.edu/cgi-bin/tdna_express). As controls for the measurements of photosynthetic parameters (**Paragraph 2.6**), mutants with defects in either the performance of photosystem II (*psbo1-2*) or in the performance of photosystem I (*psad1-1*) were cultivated. The *psbo1-2* plants behaved exactly like *psbo1-1* [Murakami et al., 2005], thus a defect in PSII can be presumed.

Table 2.1: *Arabidopsis thaliana* mutants cultivated for analyses

name of the mutant	AGI accession number	described by
<i>terc-1</i>	At5g12130	Kwon and Cho, 2008
<i>terc-2</i>	At5g12130	Kwon and Cho, 2008
<i>psad1-1</i>	At4g02770	Ihnatowicz et al., 2004
<i>psbo1</i>	At5g66570	this thesis (Appendix 1/2)

For equal germination and vernalisation seeds were incubated for two days at 4°C in the dark. After sterilization with chlorine gas [Clough and Bent, 1998], *Arabidopsis thaliana* wild type plants (ecotype Col-0) and *terc-1* were grown on 1xMS medium supplemented with 1%

sucrose under $4 \mu\text{Em}^{-2}\text{s}^{-1}$ illumination with a day-night cycle of 16:8 h. Plants on soil were grown in a growth chamber under controlled conditions (PFD: $100\mu\text{Em}^{-2}\text{s}^{-1}$; 16:8 h light-dark cycle). Fertilisation with “Osmocote Plus” (Scotts Deutschland GmbH) was performed according to manufacturer’s instructions.

2.3 Complementation of *terc-1* with a GFP-tag

The coding sequence of *AtTerC* was cloned into the plant expression vector pB7FWG2 (Plant Systems Biology, VIB-Ghent University, Belgium) [Karimi et al., 2002] providing BASTA[®] resistance under the control of a single Cauliflower Mosaic Virus 35S promoter using the Gateway system (Invitrogen) and as the entry vector pDonor201 (Invitrogen). By this, the TerC protein was fused to the N-terminal part of the green fluorescence protein (GFP) from the hydrozoans jellyfish *Aequorea victoria* [Tsien, 1998]. To check the correctness of the sequence, the right orientation and the reading frame, the construct was analysed at an in-house sequencing service (<http://www.genetik.biologie.uni-muenchen.de/sequencing>). The plasmid pBW7FWG2-TerC was transformed into electro competent *Agrobacterium tumefaciens* (strain GV3108) cells and successfully transformed bacteria were selected on YEB medium (beef extract 0.5 g, yeast extract 0.1 g, peptone 0.5 g, sucrose 0.5 g, $\text{MgSO}_4 \cdot 7\text{H}_2\text{O}$ 30.0 mg, distilled water 100.0 ml and agar 2.0 g) containing 100 $\mu\text{g/ml}$ rifampicin, 25 $\mu\text{g/ml}$ gentamicin and 100 $\mu\text{g/ml}$ spectinomycin. Heterozygous *terc-1* plants were transformed by the floral dipping technique [Clough and Bent, 1998] and BASTA[®] resistant plants were screened for GFP fluorescence in chloroplasts with the Axio Imager fluorescence microscope with integrated ApoTome (Zeiss). Homozygous mutants, *terc-1*_{TerC-GFP}, were identified by PCR as later described in paragraph 2.5 and the presence of TerC-GFP was confirmed by probing with a specific GFP antibody as described in 2.9.

2.4 Generation of amiRNA lines

The generation of *amiR-TerC* lines was performed according to Mallory et al. (2004). The interference sequence was cloned into the plant expression vector pGWB2 [Nakagawa et al., 2007] and plant transformation was performed as described above. The ready to use constructs were kindly provided by the group of Prof. Dr. Ingo Flügge from the University of Cologne. If not described otherwise, for all studies performed with the *amiR-TerC* plants the T2 generation was used.

2.5 Nucleic acid analysis

Genomic DNA was isolated by grinding fresh plant leave material in isolation buffer (200 mM Tris-HCL [pH 7.5], 250 mM NaCl, 25 mM EDTA and 0.5% SDS) at RT followed by isopropanol precipitation. Mutant plants were analysed by polymerase chain reaction (PCR) using gene-specific (At5g12130-F and At5g12130-R) and T-DNA-specific primers (SALK-LB and GK-LB) (**Table 2.5**). The following PCR program was applied using a Thermal Cycler (MJ Mini, Biorad):

- | | | | | |
|---|--------|------|---|-----------|
| ➤ | 5 min | 95°C | } | 40 cycles |
| ➤ | 30 sec | 95°C | | |
| ➤ | 30 sec | 55°C | | |
| ➤ | 1 min | 70°C | | |
| ➤ | 10 min | 70°C | | |

The PCR products were separated on a 1% agarose gel containing TAE buffer (0.04 M Tris-HCl [pH 8.0], 1 mM EDTA [pH 8.0] and 0.1% acetic acid) and visualised after EtBr staining under UV light (BioDoc Analyze, Biometra).

Total RNA was extracted from grinded *Arabidopsis* leafs by TRIzol reagent (Invitrogen). First strand synthesis was performed using the SuperScript™ III Reverse Transcriptase according to manufacturer's instructions (Invitrogen, Karlsruhe, Germany). The level of gene expression was quantified via real-time PCR (iQ5™ Multi Colour Real-Time PCR Detection System, Biorad) using specific primers for *AtTerc* (real-time-At5g12130-F2 and real-time-At5g12130-R2) (**Table 2.5**) and for normalisation the primers on the "housekeeping" gene *Ubiquitin* (real-time-Ubiquitin-F and real-time-Ubiquitin-R) (**Table 2.5**) and iQ SYBR Green Supermix (Biorad) as suggest in the user's manual with the following program:

- | | | | | |
|---|--------|------|---|-----------|
| ➤ | 5 min | 95°C | } | 35 cycles |
| ➤ | 20 sec | 95°C | | |
| ➤ | 20 sec | 55°C | | |
| ➤ | 30 sec | 72°C | | |
| ➤ | 1 min | 70°C | | |

The iQ5™ Optical System Software (Bio-Rad) calculated to level of gene expression and the standard deviation according to the following equation [Pfaffl, 2001]:

$$\text{Ratio} = \frac{(E_{\text{target}})^{\Delta\text{Ct, target (calibrator- test)}}}{(E_{\text{ref}})^{\Delta\text{Ct, ref (calibrator- test)}}$$

The amplification efficiencies of the gene of interest and the control gene *Ubiquitin* are indicated as E_{target} and E_{ref} .

2.6 Chlorophyll fluorescence measurements

To measure the *in vivo* chlorophyll a fluorescence in single leaves, the Dual-PAM 100 (Walz GmbH) system was used according to Pesaresi et al. (2009). For standard PSII measurements dark adapted leaves were exposed to a single red light pulse ($5.000 \mu\text{Em}^{-2}\text{s}^{-1}$, 800 ms) and maximum fluorescence (F_M) was determined, as well as the ground fluorescence, with measuring light illumination (F_0). The functionality of PSII (F_V/F_M) was calculated by the equation $F_V/F_M = (F_M - F_0)/F_M$. After a 10 min exposure to actinic red light ($50 \mu\text{Em}^{-2}\text{s}^{-1}$) a second saturation light pulse was applied to measure the maximum fluorescence under illumination (F_M') and the steady state fluorescence (F_S). The values for the effective PSII quantum yield (Φ_{II}) and photochemical quenching (qP) were calculated according to the following equations [Maxwell and Johnson, 2000]:

$$\Phi_{II} = (F_M' - F_S) / F_M'$$

$$qP = (F_M' - F_S) / (F_M' - F_0)$$

In vivo Chl a fluorescence of whole plants was recorded using an imaging chlorophyll fluorometer (Walz Imaging PAM, Walz GmbH) by exposing dark-adapted plants to a pulsed, blue measuring beam (1 Hz, intensity 4; F_0) and a saturating light flash (intensity 4) to obtain F_V/F_M and to actinic light ($50 \mu\text{Em}^{-2}\text{s}^{-1}$) for 10 min to determine Φ_{II} as described before.

PSI activity was monitored using the Dual-PAM 100 according to Klughammer and Schreiber (1994). For maximum oxidation of PSI, a far red light illumination was applied to a single leaf followed by a saturation pulse ($5.000 \mu\text{Em}^{-2}\text{s}^{-1}$ for 800 ms) to determine P_m (maximum P_{700}^+ absorption). Subsequently, actinic light was switched on and every three minutes saturation pulses were applied to determine P_m' , the maximum P_{700}^+ absorption under illumination. The photochemical quantum yield of PSI, $Y(I)$, defined as the fraction of total P_{700} that is reduced in a given state and is not limited by the acceptor side, was calculated as: $Y(I) = 1 - Y(\text{ND}) - Y(\text{NA})$, where $Y(\text{ND})$ represents the fraction of total P_{700} that is oxidised in a given state (as a measure of donor side limitation), and $Y(\text{NA})$ is the fraction of total P_{700} that is not oxidised by a saturation pulse in a given state, calculated as $(P_m - P_m')/P_m$, which provides a measure of acceptor side limitation.

2.7 Total protein preparation and SDS-PAGE

Total proteins were isolated from four week old *Arabidopsis* leaves. Plant material was homogenised in isolation buffer (0.1 M Tris [pH8.0], 50 mM EDTA [pH8.0], 0.25 M NaCl, 1 mM DTT and 0.7% SDS), heated up to 65°C and centrifuged at 15.000 g for 10 min. Prior to electrophoresis, 5x SDS-loading buffer (0.225 M Tris-HCl [pH6.8], 50% glycerol, 5% SDS, 0.05% bromophenol blue and 0.25 M DDT) was added to the samples, that were loaded on an acryl amide Tris-Tricine SDS-PAGE gel containing 10% or 12% acryl amide and separated according to Schaegger and Jagow (1987). Gels were run at a constant current of 20 mA (anode buffer: 0.2 M Tris-HCl [pH 8.9]; cathode buffer: 0.1 M Tris-HCl [pH 8.9], 0.1 M Tricine [pH 8.9], 0.1% SDS and 1 mM EDTA). Afterwards, gels were either stained with Coomassie staining solution (1.8 g Coomassie R250, 50% methanol and 7% acetic acid) followed by a destaining step (40% methanol and 7% acetic acid) until the background of the gels was clear or used for Western analyses (**Paragraph 2.9**).

2.8 Blue Native PAGE and 2D SDS-PAGE

Leaves from four week old plants were homogenised in ice cold buffer 1 (0.4 M sorbitol and 0.1 M Tricine-KOH [pH 7.8]) and filtered through two layers of Miracloth (Calbiochem). Intact chloroplasts were collected by centrifugation at 2.000 g for 10 min at 4°C (Ja-25.50 rotor [Beckmann]), resuspended and lysed in ice cold buffer 2 (20 mM HEPES-KOH [pH 7.5], 10 mM EDTA) for 20 min on ice. Thylakoids were obtained by centrifugation at 12,000 g for 10 min at 4°C and resuspended in TMK (10 mM Tris-HCL [pH 6.8], 10 mM MgCl₂ and 20 mM KCL). The chlorophyll concentration was measured after acetone precipitation of proteins [Porra, 2002] at different wavelengths (A_{750} , A_{664} and A_{646}). For the first dimension of the Blue Native PAGE analysis, proteins equivalent to 50 µg chlorophyll a+b were washed with TMK and solubilised in 750 mM ε-aminocaproic acid, 50 mM Bis-Tris [pH 7.0], 5 mM EDTA [pH 7.0], 50 mM NaCl and 1.0% β-DM for 20 min on ice. After precipitation of non soluble material at 19,000 g for 15 min at 4°C the supernatant was supplemented with 5% Coomassie-blue G250 in 750 mM ε-aminocaproic acid and the samples were loaded onto BN gel (4-12% acryl amide gels, containing 0.5 M ε-aminocaproic acid, 50 mM Bis-Tris [pH 7.0] and 10% glycerol). Overnight electrophoresis was carried out at 4°C (voltage 60 V) with cathode running buffer (50 mM Tricine, 15 mM Bis-Tris [pH 7.0] and 0.02% Coomassie G250) and anode running buffer (50 mM Bis-Tris [pH 7.0]). When the Coomassie front reached half of the gel length the blue cathode buffer was exchanged against a colourless one

and the voltage was increased to 300 V. Gel stripes of the first dimension were either blotted on PVDF membrane (**Paragraph 2.9**) or solubilised in denaturing buffer (0.125 M Tris-HCl [pH 6.8], 4% SDS and 1mM DTT). For protein separation under denaturing conditions one stripe of the blue native gel was incubated for 20 min in SDS loading buffer at room temperature and afterwards placed on top of a Tris-Tricine SDS-Gel (**Paragraph 2.7**).

2.9 Immunoblot analyses

Protein transfer from the acryl amide gel to a PVDF membrane (Millipore, Germany) was performed by use of a semi-dry blotting apparatus [Kyshe-Anderson, 1984] with constant current corresponding to 1 mAcm⁻² according to Martin et al. (2003).

Table 2.2: List of primary antibodies used for immunoblot analyses

name of antibody	target protein	supplier
α -D1	PsbA	Agrisera (Sweden)
α -D2	PsbD	Agrisera (Sweden)
α -CP43	PsbC	Agrisera (Sweden)
α -CP47	PsbB	Agrisera (Sweden)
α -PsbO	PsbO	Agrisera (Sweden)
α -PsbP	PsbP	Agrisera (Sweden)
α -PsbQ	PsbQ	Agrisera (Sweden)
α -PsbS	PsbS	Agrisera (Sweden)
α -LHCB1	LHCB1	Agrisera (Sweden)
α -LHCB2	LHCB2	Agrisera (Sweden)
α -LHCB3	LHCB3	Agrisera (Sweden)
α -LHCB4	LHCB4	Agrisera (Sweden)
α -LHCB6	LHCB6	Agrisera (Sweden)
α -PsaB	PsaB	Agrisera (Sweden)
α -PsaC	PsaC	Agrisera (Sweden)
α -PsaD	PsaD	Agrisera (Sweden)
α -PsaE	PsaE	Agrisera (Sweden)
α -PsaG	PsaG	Agrisera (Sweden)
α -PsaK	PsaK	Agrisera (Sweden)
α -PsaL	PsaL	Agrisera (Sweden)
α -LHCA2	LHCA2	Agrisera (Sweden)
α -LHCA3	LHCA3	Agrisera (Sweden)
α -LHCA4	LHCA4	Agrisera (Sweden)
α -LPA1	LPA1	Peng et al., 2006
α -LPA2	LPA2	Ma et al., 2007
α -ALB3	ALB3	Gerdes et al., 2006
α -ALB4	ALB4	Gerdes et al., 2006
α -PAM68	PAM68	Armbruster et al., 2010
α -PetB	Cyt <i>b</i> ₆	Agrisera (Sweden)
α -POR	POR C	Agrisera (Sweden)
α -RbcL	large subunit of RubisCO	Agrisera (Sweden)

α -Actin	Actin	Dianova (Germany)
α -GFP	eGFP	Invitrogen (Germany)

Successful transfer of proteins from the gel to the PVDF membrane was proved by treating the membrane with a staining solution (0.02% Coomassie R250 and 50% methanol) for 5 min followed by a destaining step with 50% methanol until the background of the membrane was colourless.

Afterwards membranes were probed with specific antibodies raised against several subunits of PSI, PSII, Cyt *b₆/f* and other plastid proteins according to standard protocols [Sambrook et al., 1989].

Table 2.3: List of secondary antibodies used for immunoblot analyses

name of antibody	target protein	supplier
α -rabbit	IgG	Sigma-Aldrich (Germany)
α -chicken	IgY	Sigma-Aldrich (Germany)
α -mouse	IgG	abCAM (UK)

Signals were detected by enhanced chemo luminescence (ECL kit, Amersham Bioscience) using an ECL reader (Fusion FX7, Peqlab) and the Fusion software (Peqlab). The quantification of the signals was performed by the amount of pixels using Photoshop (Adobe).

2.10 *In vivo* labelling of *Arabidopsis thaliana* proteins (pulse-chase labelling)

Leaves from two to three week old plants were cut with a razorblade and infiltrated with TMK buffer containing 20 μ g/ml cycloheximide to block nuclear protein synthesis and 0.2% Tween20. After 30 min of pre incubation [³⁵S]-methionine was added to the reaction (1 mCi final concentration) and the leaves were again infiltrated. Labelling of newly synthesised plastid proteins occurred under illumination with 150 μ Em⁻²s⁻¹ at RT for 20 min (pulse). Plant material was either used for protein analysis as described in paragraphs 2.7 and 2.8 or subjected to a treatment with 10 mM cold methionine (chase) prior to electrophoresis. Protein gels were dried and radioactive signals were quantified using a phosphoimager (Typhoon, GE Healthcare) and the IMAGE Quant program (Molecular Dynamics, version 1.2).

2.11 Sucrose gradient centrifugation

Thylakoids from four week old WT and *terc-I*_{TerC-GFP} plants were isolated as described in 2.8. After washing with 5 mM EDTA [pH7.8], the thylakoids were diluted with water to a final

concentration of 1 mg/ml and solubilized with a final concentration of 0.5% dodecyl- β -D-maltoside (Sigma) for 20 min on ice. The non-solubilized membranes were pelleted by centrifugation at 19,000 *g* for 20 min at 4°C and one milliliter was loaded on top of a sucrose gradient. The sucrose gradients were prepared by freezing 10 ml of 0.4 M sucrose, 20 mM Tricine-NaOH pH7.5, 0.06% β -DM at -80°C for two hours and thawing the solution at 4°C. The gradients were ultra centrifuged at 39,000 rpm (SW40 swing-out rotor) for 21 h at 4°C (Optima MAX-XP, Beckman Coulter). In total 14 fractions were obtained from one gradient. After normalising the fractions to the chlorophyll concentrations of fraction 13 (PSI), all fractions were separated on a 12% Tris-Tricine SDS-gel (**Paragraph 2.7**).

2.12 Split Ubiquitin assay

To analyse putative protein-protein interactions of TerC with other plastid proteins, the coding sequence of *AtTerC* was cloned into pAMBV4 vector and used as a bait protein fused to the C-terminal part of Ubiquitin (Cub) in the Split Ubiquitin assay.

Table 2.4: List of 22 proteins analysed in split ubiquitin interaction studies in *Saccharomyces serviciae*

AGI accession number	name of protein	used vector
At5g12130	TerC	pAMBV4
AtCg00020	D1 (PsbA)	pADSL
AtCg00680	CP47 (PsbB)	pADSL
AtCg00280	CP43 (PsbC)	pADSL
AtCg00270	D2 (PsbD)	pADSL
AtCg00580	PsbE	pADSL
AtCg00710	PsbH	pADSL
At5g66570	PsbO	pADSL
AtCg00350	PsaA	pADSL
AtCg0340	PsaB	pADSL
AtCg00720	PetB	pADSL
AtCg00150	AtpI	pADSL
At1g10960	Fd	pADSL
At1g02910	LPA1	pADSL
At5g51545	LPA2	pADSL
At5g23120	HCF136	pADSL
At4g19100	PAM68	pADSL
At2g28800	ALB3	pADSL
At1g24490	ALB4	pADSL
At2g45770	cpFtsY	pADSL
At4g14870	cpSecE	pADSL
At2g18710	cpSecY	pADSL

The sequence coding for TerC was cloned into pAMBV4 used as bait in the study. All other sequences were cloned into pADSL and acted as the prey.

For interaction studies the coding sequences of several mature thylakoid proteins were cloned in the vector pADSL as prey proteins fused to the modified N-terminal part of Ubiquitin (NubG), which is not able to interact with Cub due to an exchange of an amino acid. Both Cub and NubG are only able to reassemble Ubiquitin if they are fused to proteins that are interacting with each other thus bringing Cub and NubG in close proximity. As a negative control the plasmid pAlg5-NubG, which encodes the ER membrane protein Alg5 fused to NubG, was used for co-transformation. Because NubI, which encodes the WT Nub, and Cub reassemble spontaneously to reconstitute Ubiquitin, Alg5, that is not interacting with any plastid protein, fused to NubI was used as a positive control. The interaction studies were performed in the lab of Prof. Dr. Danja Schünemann at the University of Bochum using the Dual-Membrane kit (Dualsystems Biotech AG) according to manufacturer's instruction as described by Pasch et al. (2005).

2.13 Topology studies of TerC

Thylakoids from four week old WT and *terc-I_{TerC}-GFP* plants were isolated as described in paragraph 2.8. For salt treatments according to Karnauchov et al. (1997) the thylakoids were resuspended in 50 mM HEPES/KOH pH 7.5 at a chlorophyll concentration of 0.5 mg/ml and treated with either 2 M NaCl, 0.1 M Na₂CO₃, 2 M NaSCN, 0.1 M NaOH and as a control no salt for 30 min on ice. Soluble and membrane bound proteins were separated by centrifugation at 10,000 g for 10 min at 4°C, both fractions were separated on 12% Tris-Tricine SDS-gels and proteins were detected by Western analysis using specific antibodies (**Paragraph 2.7**).

For thermolysin treatment, the thylakoids were isolated as described in paragraph 1.8 without adding protease inhibitors and finally resuspended in HM-buffer (10 mM HEPES-KOH [pH 8.0] and 5mM MgCl₂) at a concentration of 50 µg chlorophyll/ml. Thermolysin was added to a final concentration of 50 µg/ml and the thylakoids were incubated for 30 min on ice. The reaction was stopped by adding EDTA [pH 8.0] to final concentration of 20 mM. The thylakoids were pelleted by centrifugation at 15,000 g for 10 min at 4°C, resuspended in 100 µl homogenisation buffer and solubilised by adding SDS to a concentration of 2% [Peng et al., 2006]. After pelleting insoluble material, proteins were loaded on a 12% Tris-Tricine SDS-gel according to equal amounts of chlorophyll (1.5 µg chl) and investigated by immunoblot analysis (**Paragraph 2.7**).

2.14 Electron microscopy

Seeds of wild type and *terc-1* plants were sent to the lab of PD Dr. Stefan Geimer at the University in Bayreuth. 1-week-old plants were taken for transmission electron microscopy and fixed with 2% glutaraldehyde in 50 mM phosphate buffer, pH 7.4, overnight at 4°C. Samples were postfixed in 1% osmium tetroxide for 8 h on ice, dehydrated in a graduated acetone series, including a step with 1% uranylacetate (in 50% acetone, 2 h), embedded in Spurr's resin, and polymerized at 50°C for ~72 h. Ultrathin sections (60 to 70 nm) were cut with a diamond knife (Micro Star, USA) on a Leica Ultracut UCT microtome (Leica Microsystems, Austria) and mounted on pioloform-coated copper grids. The sections were stained with lead citrate and uranyl acetate and viewed with a Zeiss EM 109 transmission electron microscope (Carl Zeiss, Germany) at 80 kV. Micrographs were taken using SO-163 EM film (Kodak, USA).

For scanning electron microscopy, released pollen grains were mounted on stubs and sputter-coated with gold particles (S150A, UK). Specimens were examined with a scanning electron microscope (XL 30 ESEM; Philips, The Netherlands) at an accelerating voltage of 15 kV.

2.15 Isolation of protoplasts and fluorescence microscopy

Leaves of four-week-old *terc-1_{TerC-GFP}* plants were cut into thin strips with a new razor blade and incubated with call wall lysis buffer (20 mM KCl, 10 mM MES pH 5.7, 10 mM CaCl₂, 0.5 M mannitol, 0.1% BSA, 0.1 g/ml macerozyme (Duchefa) and 0.1 g/ml cellulase (Duchefa)) in the dark for three hours. The isolated protoplasts were collected by centrifugation with 50 g for 5 min and afterwards washed with washing buffer (20 mM KCl, 10 mM MES pH 5.7, 10 mM CaCl₂ and 0.5 M mannitol). Protoplasts were analysed using a Axio Imager fluorescence microscope with integrated ApoTome (Zeiss). The X-Cite Series 120 fluorescence lamp (EXFO) was used to excite the GFP fluorescence at a range of wavelength from 505 to 530 nm and the autofluorescence of the chlorophyll at 670 to 750 nm.

2.16 Oligonucleotides

Primers used for genotyping, RT-PCR, real-time analyses and cloning were ordered from Metabion (Germany). The following table shows the sequences of the primers in 5'-3' orientation.

Table 2.5: List of all primers used for PCR in 5' to 3' orientation

name of primer	sequence 5' - 3'
At5g12130-F1	CAGTTATCCACCACGGAATTCTCC
At5g12130-R1	TTGCTCCAATATGTAGCTGCAAGA
Salk-LB	GTCCGCAATGTGTTATTAAGTTGTC
GK-LB	ATATTGACCATCATACTCATT
real-time-At5g12130-F2	TCTTCATCAGTAGATAGTGG
real-time-At5g12130-R2	TATTCTGATACATGAGTGGC
real-time-Ubiquitin-F	GGAAAAAGGTCTGACCGACA
real-time- Ubiquitin R	CTGTTACGGAACCCAAT TC
At5g12130-att-B1	GGGGACAAGTTTGTACAAAAAAGCAGGCTTCATGAGC
At5g12130-att-B1	GGGACCAGCACTTTGTACAAGAAAGCTGGGTGGCTGTCCG
SU- terc-F1	GCTCTAGAAAAAATGAGCTTAGCTTCAGTTATCCACC
SU- terc -F2	GCTCTAGAAAAAATGCTTGCTTCAGCTGCCAATCGTCGT
SU- terc -R	GCCCATGGCTGTCCGCTGGATTTGTTTGTAG

3. Results

3.1 Phenotype of *terc-1*

Two full knock-out T-DNA insertion lines for the gene At5g12130, *terc-1* (SALK_014739) and *terc-2* (GABI-Kat 844D10), could be identified [Strissel, 2007; Kwon and Cho, 2008] showing the same phenotype under all investigated growth conditions. Grown on soil, both lines are seedlings lethal or die after the cotyledon stage (data not shown). Mutants, that were cultivated on MS-medium supplemented with 1% sucrose in a growth chamber with 100 $\mu\text{Em}^{-2}\text{s}^{-1}$ or 40 $\mu\text{Em}^{-2}\text{s}^{-1}$ illumination, showed a full albinotic phenotype [Strissel, 2007; Kwon and Cho, 2008]. Only when grown under 4 $\mu\text{Em}^{-2}\text{s}^{-1}$ illumination, the cotyledons of wild type plants as well as the cotyledons of the mutants turned green (**Figure 3.1**).

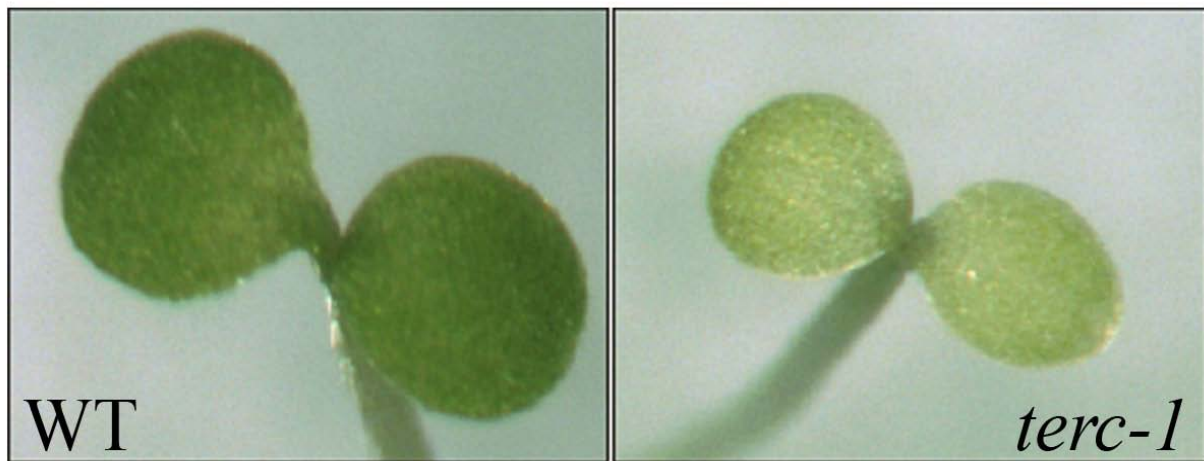


Figure 3.1: Growth phenotype of a 1-week-old wild type plant and a *terc-1* mutant

Both lines were cultivated on MS-medium under controlled conditions in a growth chamber with 4 $\mu\text{Em}^{-2}\text{s}^{-1}$ illumination under a long day light cycle.

Growth of both wild type and *terc-1* plants was arrested in the cotyledon stage under this light condition and did not develop true leaves. The cotyledons of *terc-1* were much paler and smaller compared to wild type.

Cotyledons of both, wild type and *terc-1*, were analysed by transmission electron microscopy (TEM). The mesophyll cells of both lines contained intact chloroplasts, but the structure of the thylakoid membrane differed markedly between wild type and mutant plants (**Figure 3.2**). While thylakoids of wild type plants contained both, grana and stroma lamellae, the thylakoid membrane of *terc-1* consisted only of stroma lamellae.

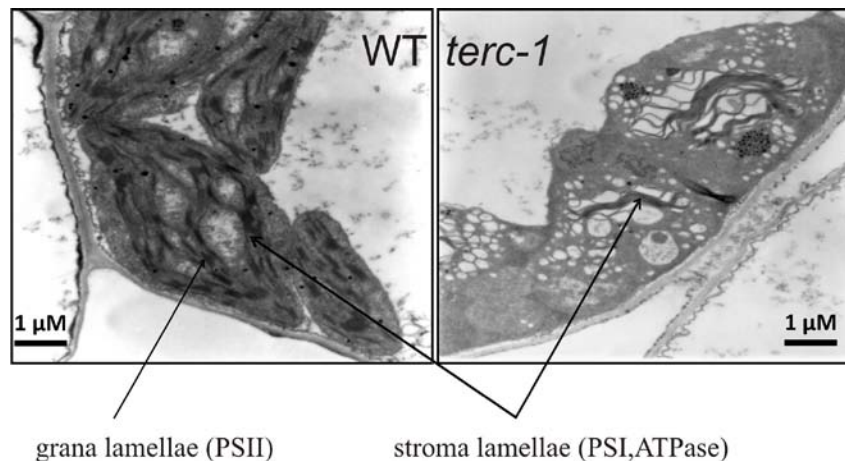


Figure 3.2: Transmission electron microscopy (TEM) picture of wild type and *terc-1* mesophyll cells

Cells of both lines contain intact chloroplasts. The structure of the thylakoid membrane differs between wild type and *terc-1*. Wild type thylakoids contain both grana and stroma lamellae, whereas *terc-1* thylakoid membranes consist exclusively of stroma lamellae. The stroma lamellae contain PSI and ATPase complexes and in the grana lamellae the PSII complexes are located.

3.2 Phenotype of *amiR-TerC*

Since knock-out mutants of *AtTerC* are not viable on soil or on MS-medium, knock-down lines of *AtTerC* were generated. Therefore, a short complementary sequence of *AtTerC* was cloned into the plant expression vector pGWB2 under the control of the 35SCaMV promoter and transformed into 15 wild type plants. All 34 hygromycin resistant transformants (*amiR-TerC*) showed a variegated leaf phenotype in the T1 generation and were able to grow photoautotrophically on soil (**Figure 3.3**). As all independently transformed plants showed the same phenotype, it can be excluded that the variegated phenotype resulted from a T-DNA insertion within the reading frame of an unknown gene.



Figure 3.3: Growth phenotype of 3-week-old wild type and *amiR-TerC* (T2) plants

Plants were grown under controlled conditions in a growth chamber with $100 \mu\text{Em}^{-2}\text{s}^{-1}$ illumination under a long day light cycle (16/8 h light/dark).

To evaluate the degree of down regulation by the artificial micro RNA construct, *amiR-TerC* lines were analysed regarding the transcript level of *AtTerC*. For that, real-time PCR analyses on cDNA derived from wild type and *amiR-TerC* plants were performed. The transcript level of *AtTerC* was down-regulated to less than 10% in the T2 generation of *amiR-TerC* compared to wild type (**Figure 3.4**).

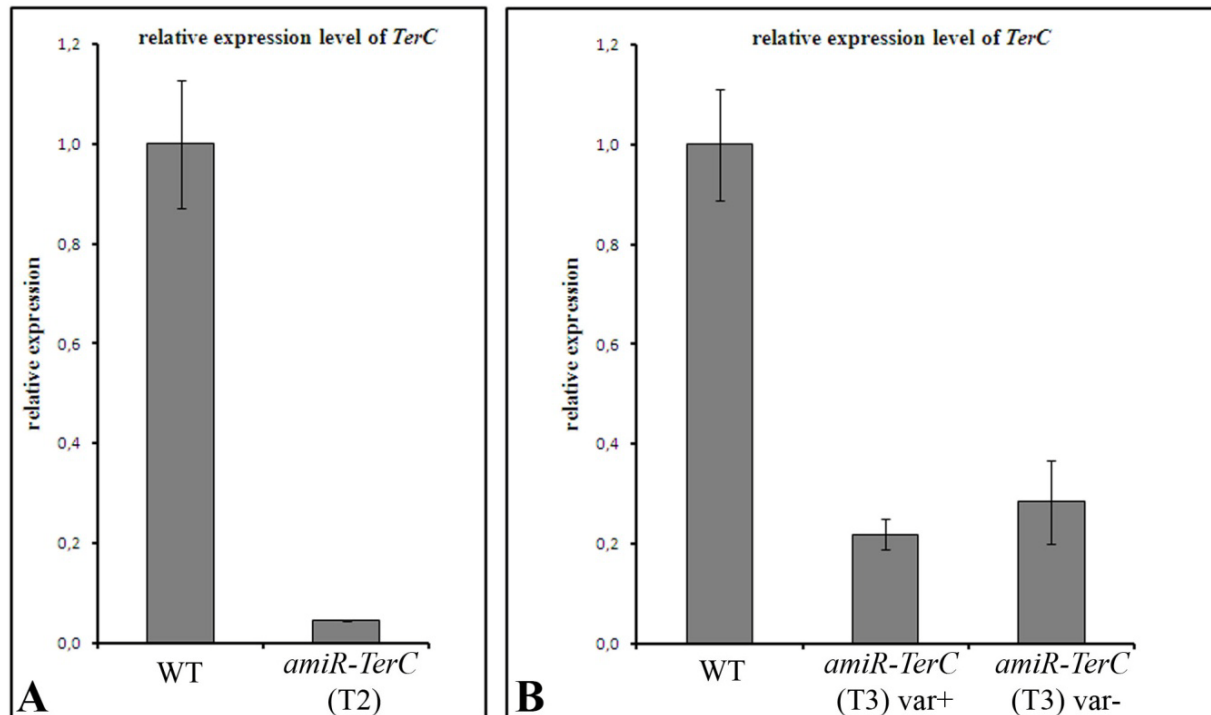


Figure 3.4: Transcript analyses of *AtTerC* in wild type and *amiR-TerC* plants

Real-time PCR analyses revealed the relative transcript level of *AtTerC*. In the T2 generation of *amiR-TerC* the amount of transcript is reduced to less than 10% compared to wild type (A). In the T3 generation the transcript level of *AtTerC* in variegated leaves (*amiR-TerC* (T3) var+) was about 20% compared to wild type whereas the transcript levels were only reduced to around 30% in non variegated leaf tissue (*amiR-TerC* (T3) var-) (B).

However, an increase of *AtTerC* transcript levels in the T3 generation of *amiR-TerC* compared to plants of the T2 generation was observed.

To investigate the effect of light intensity on the growth of *amiR-TerC* (T2), plants were grown for one week under $100 \mu\text{Em}^{-2}\text{s}^{-1}$ illumination in a growth chamber under controlled conditions. Afterwards plants were separated and further cultivated under high light (HL: $1000 \mu\text{Em}^{-2}\text{s}^{-1}$), moderate light (ML: $100 \mu\text{Em}^{-2}\text{s}^{-1}$) or low light (LL: $5 \mu\text{Em}^{-2}\text{s}^{-1}$) for another 16 days. After the first week, during which all plants were grown under $100 \mu\text{Em}^{-2}\text{s}^{-1}$, a slight reduction in plant growth was observed for the *amiR-TerC* plants compared to wild type plants (**Figure 3.5**).

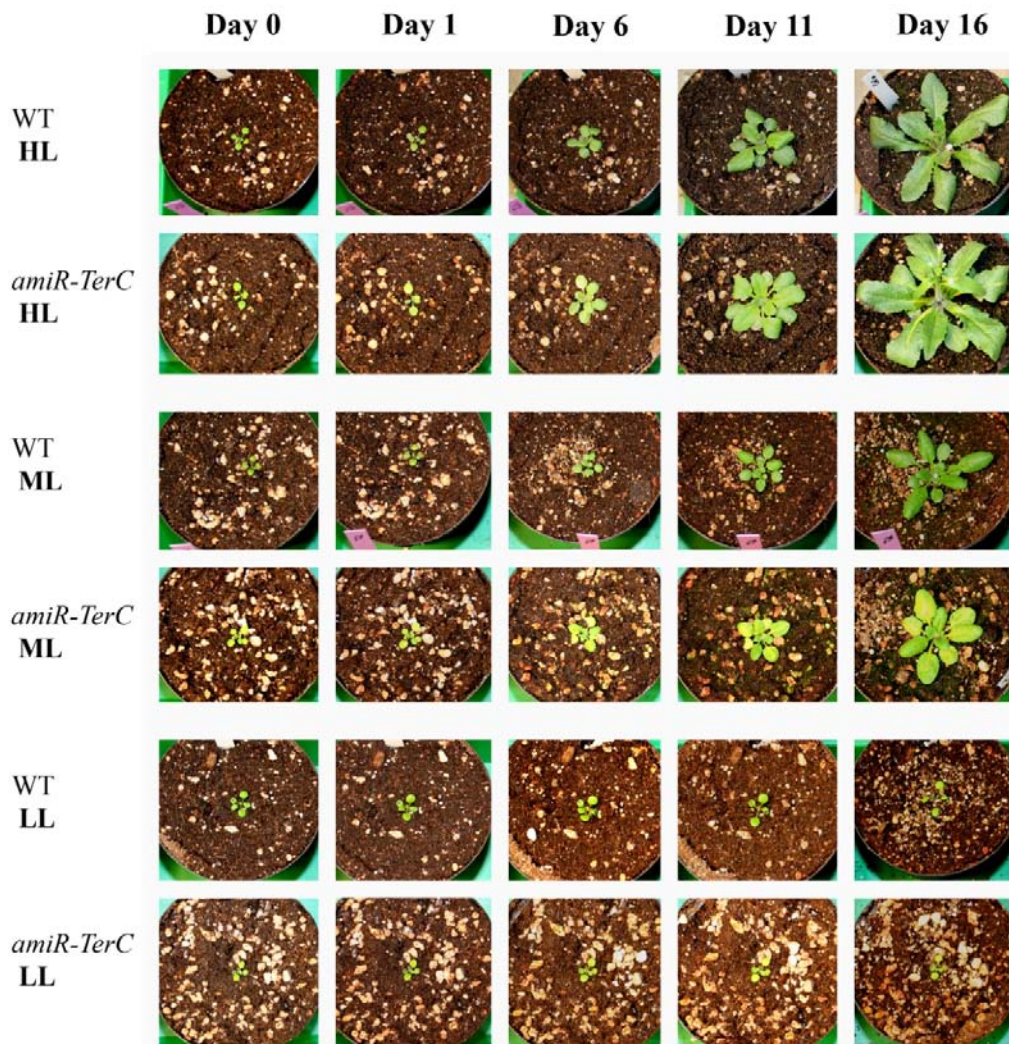


Figure 3.5: Growth phenotype of wild type and *amiR-TerC* (T2) plants

Plants were first grown under controlled conditions in a growth chamber with $100 \mu\text{Em}^{-2}\text{s}^{-1}$ illumination for one week. Afterwards plants were either illuminated with $1000 \mu\text{Em}^{-2}\text{s}^{-1}$ (HL), $100 \mu\text{Em}^{-2}\text{s}^{-1}$ (ML) or $5 \mu\text{Em}^{-2}\text{s}^{-1}$ (LL).

After switching the plants to LL and ML conditions, this difference in plant size stayed for the following 16 days and the variegated leaf phenotype in *amiR-TerC* persisted. After the first day of high light treatment, leaves of wild type plants obtained a purple colouration due to anthocyanine production, indicating a stress reaction. This effect could not be observed in *amiR-TerC* plants. In contrast to the maintenance of leaf variegation under low light and moderate light conditions, the leaf variegation phenotype decreased under HL after 11 days. After another 5 days, only the midribs of the *amiR-TerC* leaves were paler compared to those of wild type plants.

As mentioned above, the *amiR-TerC* plants grown under LL and ML stayed smaller compared to wild type plants until the end of the 16 days of light treatment. Interestingly, the *amiR-TerC*

plants under high light were slightly bigger than wild type plants and flowering started earlier in the *amiR-TerC* plants.

Additionally, wild type and *amiR-TerC* plants were grown under different light-dark cycles. Plants that grew under a 16/8 h light/dark rhythm (long day) showed a stronger increase in biomass production for all lines (WT, *amiR-TerC* (T3) and *amiR-TerC* (T4)) compared to 12/12 h and 8/16 h light/dark. After reducing the light period to 12 h the size of wild type plants was only slightly reduced, whereas the size of the *amiR-TerC* plants was drastically decreased. This effect was even more pronounced under short day conditions (8/16 h light/dark cycle) (**Figure 3.6**).

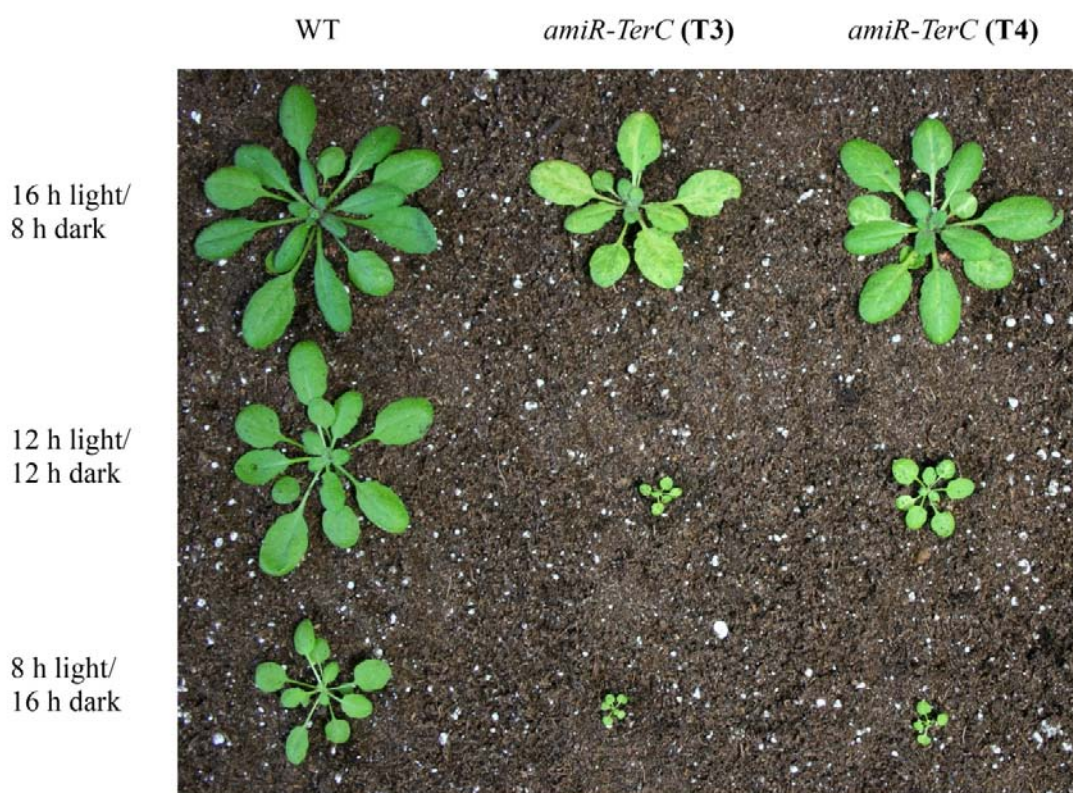


Figure 3.6: Growth phenotype of 3-week-old wild type, *amiR-TerC* (T3) and *amiR-TerC* (T4) plants

Plants were grown under controlled conditions in a growth chamber with $100 \mu\text{Em}^{-2}\text{s}^{-1}$ illumination under different light/dark cycles.

Similar to the effect on the expression level of *AtTerC*, where an increase of *AtTerC* expression in the *amiR-TerC* plants could be observed from one generation to the next (**Figure 3.4**), the decrease in biomass production was also declined. In addition, in plants of the T2 generation, where the expression of *AtTerC* is reduced most strongly, every leaf of a mature plant showed the variegated phenotype (**Figure 3.3**), whereas plants of the T3 generation produced some leaves that were indistinguishable from wild type leaves. T4 generation plants produced 50% variegated and non variegated leaves (**Figure 3.6**). Another

effect observed between the different generations of *amiR-TerC* plants was the better growth performance of the T4 generation compared to the T3. After shortening light period, the size of the *amiR-TerC* (T3) plants was reduced drastically compared to wild type plants whereas growth deficiency in the T4 generation was less severe.

The increasing *AtTerC* transcript levels, the higher biomass production from one generation to the other and the decrease of white sectors in the leaves suggest a silencing of the artificial micro RNA interference in subsequent generations. Transcript analyses from the levels of *AtTerC*-mRNA in the variegated and non variegated leaf tissue of the T3 generation plants (**Figure 3.4**), suggest that a transcript level of about 25% compared to wild type constitutes a threshold that, if fallen below, causes the leaf variegation phenotype in *amiR-TerC* plants.

3.3 Complementation of the mutation

Since knock out lines of *AtTerC* are not able to grow photoautotrophically, heterozygous *terc-1* plants as well as wild type plants were used for transformation with a plant expression vector bearing the coding sequence of *AtTerC* N-terminal fused to GFP under the control of a 35SCaMV promoter (pBW7FWG2-TerC). Basta[®] resistant plants were screened by PCR to identify complemented lines that were homozygous for *terc-1* and contained the GFP coding sequence fused to TerC (**Figure 3.7**).

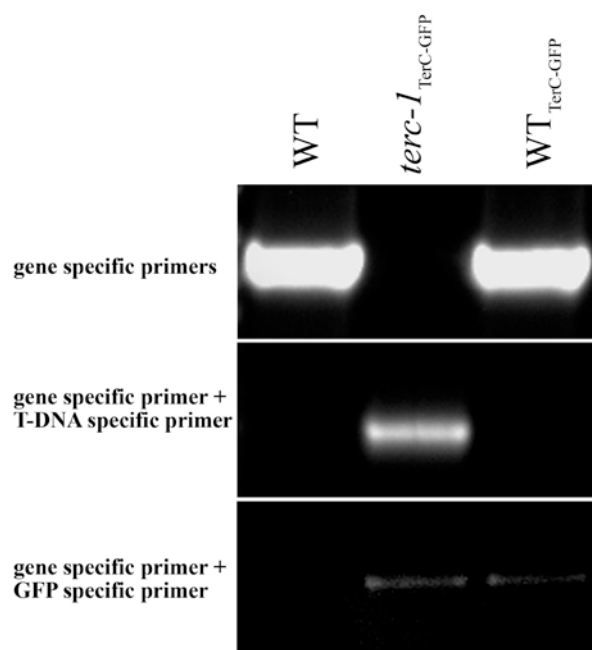


Figure 3.7: PCR analyses of plants transformed with pBW7FWG2-TerC

Wild type and *terc-1* plants transformed with pBW7FWG2-TerC were analysed by PCR. The homozygosity of *terc-1* was confirmed using gene specific and T-DNA specific primers. The presence of the transformed construct was confirmed using a GFP specific primer.

To verify that TerC-GFP is complementing the *terc-1* mutation on transcript level, real-time PCR analyses were performed to measure the amount of *AtTerC* transcript in *terc-1*_{TerC-GFP} and in WT_{TerC-GFP}. The transformation of wild type plants with pBW7FWG2-TerC lead to a 20 fold accumulation of *AtTerC* compared to non-transformed wild type plants. The *terc-1*_{TerC-GFP} plants showed double the amount of *AtTerC* transcript as the wild type (**Figure 3.8**).

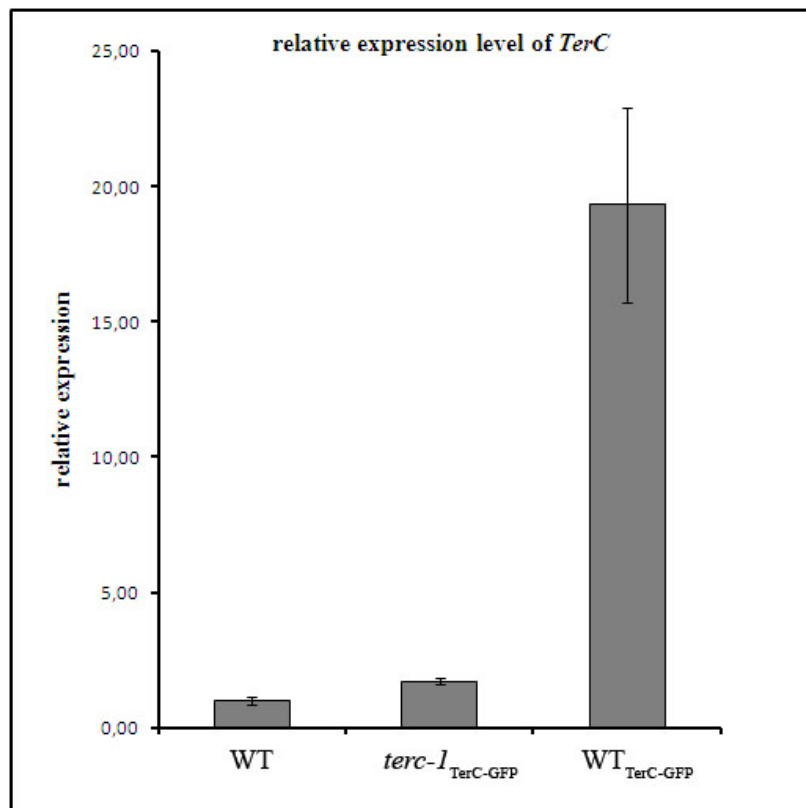


Figure 3.8: Transcript analyses of *AtTerC* in wild type, *terc-1*_{TerC-GFP} and WT_{TerC-GFP} plants

Real-time PCR analyses revealed the relative transcript level of *AtTerC*. In *terc-1*_{TerC-GFP} plants the amount of transcript was twice as high as in wild type. The WT_{TerC-GFP} plants revealed a 20 fold overexpression of *AtTerC* compared to wild type plants.

Regarding the visual phenotype, the WT_{TerC-GFP} plants did not show any difference in growth or colouration compared to wild type. In contrast, the *terc-1*_{TerC-GFP} plants had a variegated phenotype similar to the one of *amiR-TerC* plants (**Figures 3.3 and 3.9**), and were able to grow photoautotrophically.

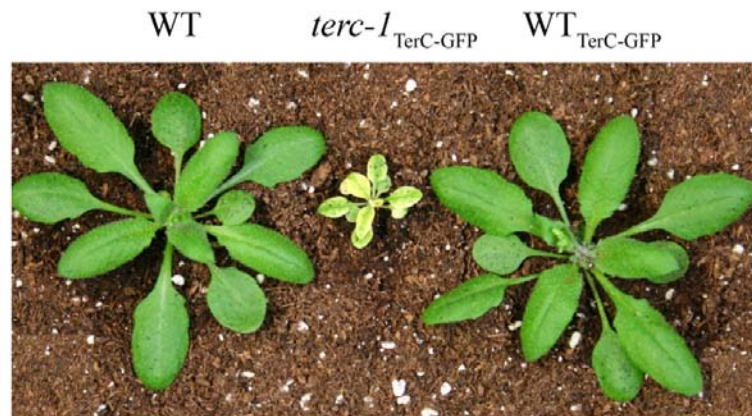


Figure 3.9: Growth phenotype of 3-week-old wild type, *terc-I*_{TerC-GFP} and WT_{TerC-GFP} plants

Plants were grown under controlled conditions in a growth chamber with $100 \mu\text{Em}^{-2}\text{s}^{-1}$ illumination under a long day light/dark cycle.

To verify the expected thylakoid membrane localisation of the TerC-GFP fusion protein, protoplasts were isolated from leaves of *terc-I*_{TerC-GFP} and WT_{TerC-GFP} plants. In both cases, a GFP specific signal could be detected in the chloroplasts of the isolated protoplasts (**Figure 3.10**).

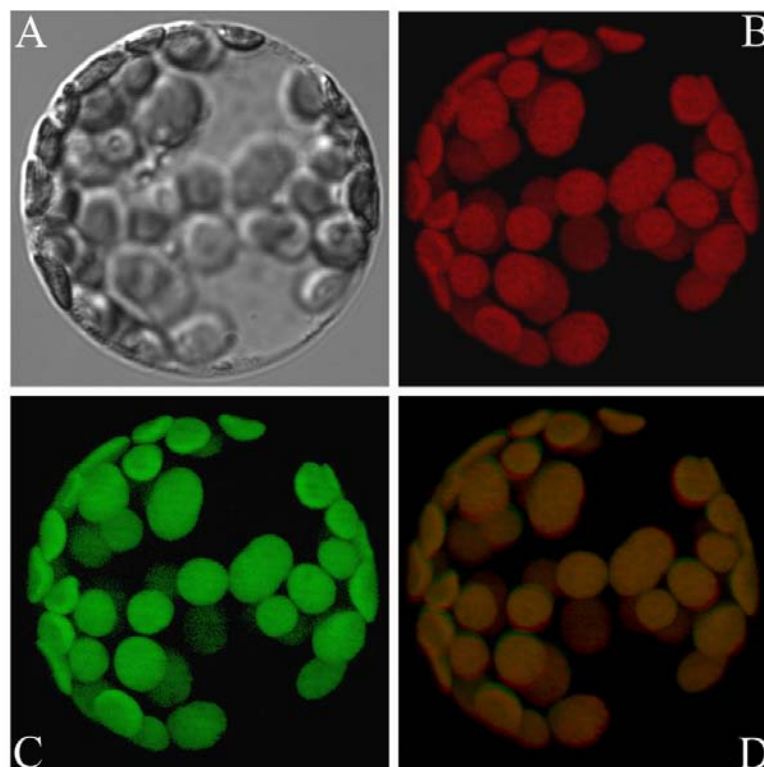


Figure 3.10: Fluorescence images of *terc-I*_{TerC-GFP} protoplasts

Intact protoplasts (**A**) were analyzed with an Axio Imager fluorescence microscope. The autofluorescence of chlorophyll is shown in red (**B**) and the GFP fluorescence in green (**C**). The merged picture (**D**) indicates the overlap of both signals. In this figure only protoplasts isolated from *terc-I*_{TerC-GFP} are shown. The analysis of protoplasts from WT_{TerC-GFP} revealed the same results.

The merged signals of the GFP fluorescence and the autofluorescence of chlorophyll in the isolated chloroplasts (**Figure 3.10**) verified the expected localization of the fusion protein in the thylakoid membrane.

3.4 Topology studies on the TerC protein

TerC is predicted to be an integral membrane protein with up to 8 transmembrane domains (Aramemnon: <http://aramemnon.botanik.uni-koeln.de/>). Due to its high hydrophobicity, it was not possible to generate a functional antibody. Thus, the TerC-GFP fusion protein was used for topology studies. To clarify whether the fusion protein behaves as an integral membrane protein, salt treatment experiments with isolated thylakoids from *terc-I*_{TerC-GFP} were performed using 2M NaCl, 0.1 M Na₂CO₃, 2M NaSCN, 0.1 M NaOH or no salt.

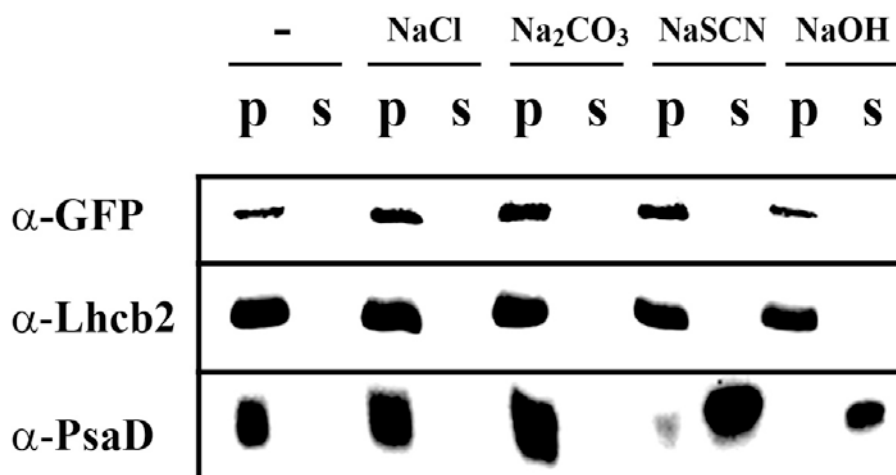


Figure 3.11: Salt treatment of isolated thylakoids from *terc-I*_{TerC-GFP}

The GFP-antibody was used to localise the TerC-GFP fusion protein in either the pellet (p) or the supernatant (s) after salt treatment. Antibodies against Lhcb2 (membrane integral protein) and PsaD (membrane extrinsic protein) were used as controls.

Regardless of the salt treatment, the GFP specific signal always derived from the pellet fraction, indicating a very strong association of TerC with the thylakoid membrane (**Figure 3.11**). The same result was obtained for Lhcb2 which is known to be a membrane spanning protein. In contrast to Lhcb2 and TerC, the PsaD protein could be partially washed off the membrane with NaSCN, a chaotropic salt, and completely with alkaline NaOH, indicating that it is located more peripheral in the thylakoid membrane.

In the TerC-GFP fusion protein, the GFP-tag is fused to the C-terminus of TerC. This constellation allowed the investigation of the membrane orientation of the GFP-tag. By adding thermolysin to intact thylakoids of *terc-I*_{TerC-GFP} plants, the orientation of the C-

terminal part of TerC could be determined as it is either digested by thermolysin facing the stroma or protected by the thylakoid membrane if facing the lumen.

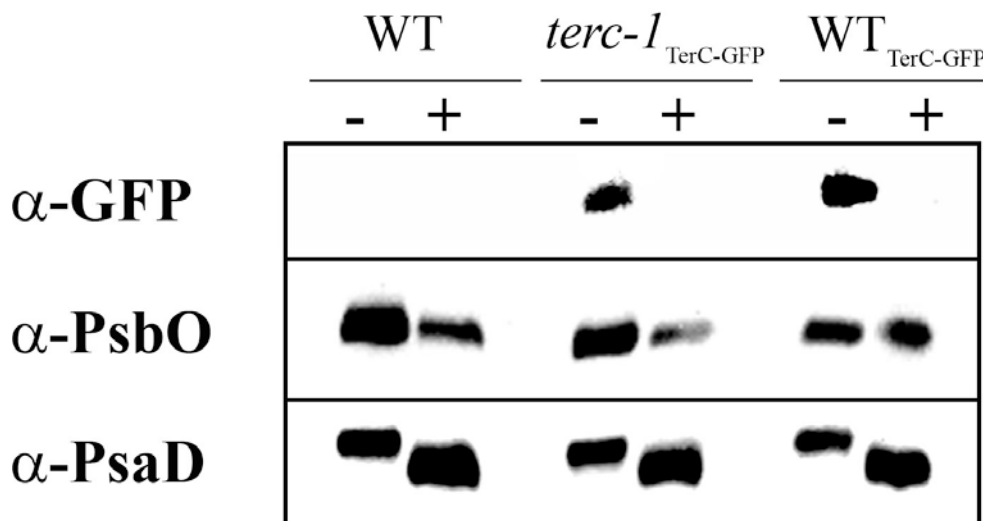


Figure 3.12: Thermolysin treatment of intact thylakoids of *terc-I*_{TerC-GFP}

The GFP-antibody was used to detect the C-terminal part of the TerC-GFP fusion protein. As controls, the luminal protein PsbO and the stroma exposed extrinsic protein PsaD were analysed.

As expected, no GFP signal was detectable in the wild type sample. Both, *terc-I*_{TerC-GFP} and WT_{TerC-GFP} samples showed a GFP signal only in the non thermolysin-treated samples (**Figure 3.12**). The presence of PsbO in the thermolysin-treated samples indicated that thermolysin was not able to cross the intact lipid bilayer leading to a partial digestion of PsbO. The accessible stromal part of PsaD was digested completely by thermolysin leading to shift in the protein size. Altogether, these findings suggest a stromal orientation of the GFP at the C-terminus of TerC.

3.5 Photosynthetic performance

The photosynthetic parameters of *amiR-TerC*, *terc-I*_{TerC-GFP} and WT_{TerC-GFP} plants were determined using the Dual-PAM 100 and compared to values of wild type plants. In the knock down-line *amiR-TerC* the maximum quantum yield (F_v/F_M), the effective quantum yield (Φ_{II}) and the non photochemical quenching (NPQ) were reduced compared to wild type, whereas the reduced state of the primary electron receptor (Q_A), measured on 1-qP, was not significantly changed (**Table 3.1**). These results suggest a defect in the electron flow through PSII in *amiR-TerC*. The defect in the F_v/F_M could be complemented by expressing TerC-GFP in *terc-I* mutant plants under the control of the 35SCaMV promoter (*terc-I*_{TerC-GFP}), but the Φ_{II} stayed decreased and the fraction of reduced Q_A (1-qP) was about twice as high in *terc-I*_{TerC-GFP} compared to wild type plants (**Table 3.1**).

Table 3.1: Parameters of chlorophyll a fluorescence obtained from wild type, *amiR-TerC*, *terc-I_{TerC-GFP}* and WT_{TerC-GFP} plants

Parameter	wild type	<i>amiR-TerC</i>	<i>terc-I_{TerC-GFP}</i>	WT _{TerC-GFP}
F_v/F_M	0.82 ± 0.03	0.70 ± 0.08	0.81 ± 0.01	0.81 ± 0.01
Φ_{II}	0.78 ± 0.04	0.52 ± 0.08	0.66 ± 0.03	0.74 ± 0.01
1-qP	0.07 ± 0.02	0.09 ± 0.03	0.15 ± 0.02	0.07 ± 0.01
NPQ	0.18 ± 0.03	0.08 ± 0.03	0.13 ± 0.03	0.17 ± 0.03

For each genotype the mean values and standard deviation of 5 plants are shown. Actinic light intensity was $70 \mu\text{Em}^{-2}\text{s}^{-1}$. For plants transformed with the pBW7FWG2-TerC construct, the data of one individual transformed line are listed. (F_v/F_M : maximum quantum yield of PSII; Φ_{II} : effective quantum yield of PSII; 1-qP: excitation pressure on PSII; NPQ: non photochemical quenching)

Supporting evidences were obtained using an Imaging PAM where the chlorophyll a fluorescence can be measured *in vivo* across a whole plants leaf surface. The *amiR-TerC* plants showed a moderately reduced F_v/F_M and Φ_{II} in the green sectors of the leaves (**Figure 3.13 (A)**). The white leaf sectors showed a stronger reduction in these values. Vice versa, the ground fluorescence (F_0) was increased in *amiR-TerC* plants. These observations are in accordance with the graphs recorded by the Dual-PAM 100. The value for F_0 was increased in *amiR-TerC* compared to wild type and additionally some characteristic features of the wild type graph were missing in the knock-down line. After switching on the actinic light a strong increase in chlorophyll fluorescence could be observed that was quickly reduced with two short intermediate rises in chlorophyll a fluorescence. The first intermediate rise derived from limitations downstream of PSI due to the light dependent regulation of the FNR (ferredoxin NADP oxidoreductase) [Ilik et al., 2006]. The second intermediate rise is coming from a delay due to light activation of FTR (ferredoxin:thioredoxin reductase), a key enzyme of the Calvin cycle [Lindahl et al., 2009]. These two intermediate increases in fluorescence were absent in *amiR-TerC* and instead a drop of the fluorescence below the F_0 level was observed. The increase in F_0 fluorescence could be resored after switching off the actinic light for 5 min (**Figure 3.13 (B)**).

In contrast to the *amiR-TerC* plants, *terc-I_{TerC-GFP}* and WT_{TerC-GFP} did not show any difference compared to wild type plants regarding the *in vivo* chlorophyll measurement using the Imaging PAM (**Figure 3.13 (C)**). This supports the suggestion above, that in *terc-I* the TerC-GFP fusion protein is fully complementing the defect in F_v/F_M .

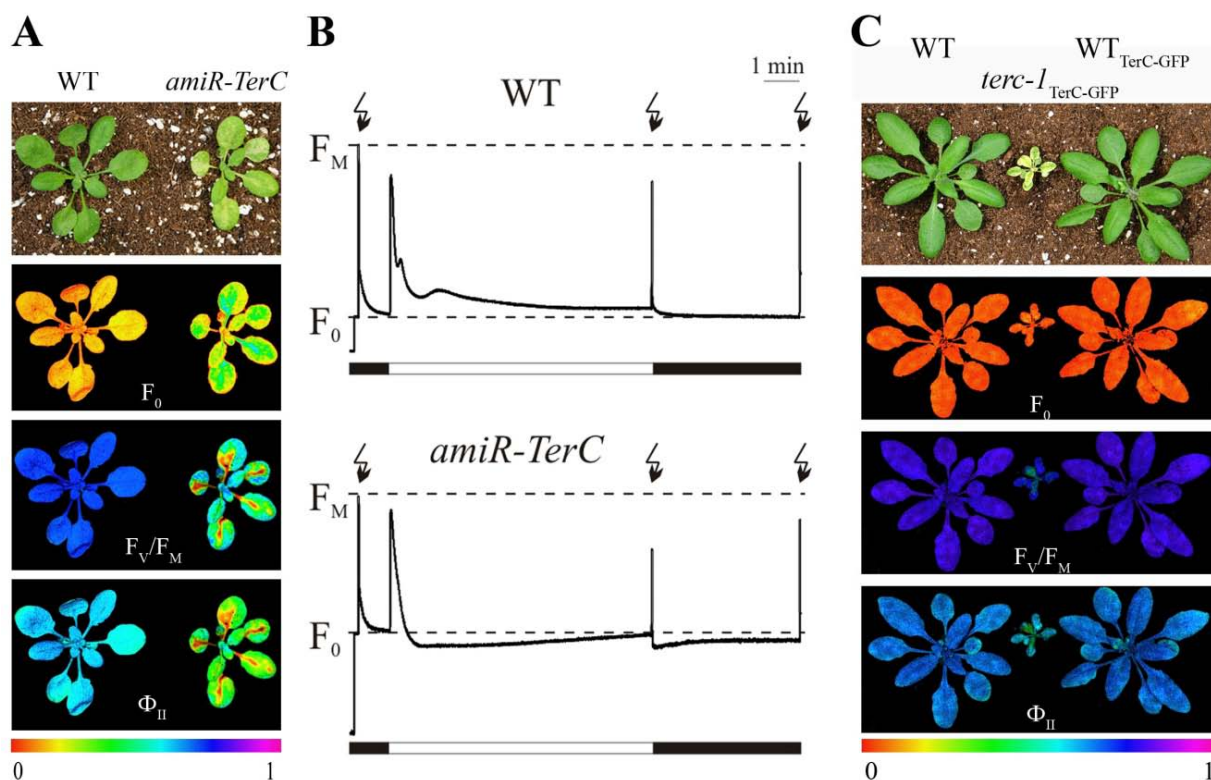


Figure 3.13: Photosynthetic performance of wild type, *amiR-TerC*, *terc-1*_{TerC-GFP} and WT_{TerC-GFP}

In vivo chlorophyll a fluorescence measurement of WT, *amiR-TerC*, *terc-1*_{TerC-GFP} and WT_{TerC-GFP} were performed using the imaging PAM (A and C) (F_v/F_M : maximum quantum yield of PSII; Φ_{II} : effective quantum yield of PSII and F_0 : ground fluorescence) or the fluorescence of WT and *amiR-TerC* was recorded with the Dual-PAM 100 (B).

The previous measurements mainly focused on the PSII activity. Further spectroscopic analyses were performed to investigate the photosynthetic parameters of PSI. The maximum absorption value of P_{700}^+ (P_m) from the fully reduced to the fully oxidized state and the change of P_{700} absorption under steady state fluorescence (P_m') in *amiR-TerC* were reduced by 50% compared to wild type, indicating a decreased amount of PSI present in the mutants (Figure 3.14). The photochemical quantum yield of PSI ($Y(I)$) and the electron transport rate around PSI ($ETR(I)$) were only slightly reduced in *amiR-TerC*.

The increase of about 50% in the donor side limitation in *amiR-TerC* compared to wild type and the not altered value for the acceptor side limitation in these two genotypes further suggests a defect upstream of PSI in the knock-down mutant (Figure 3.14).

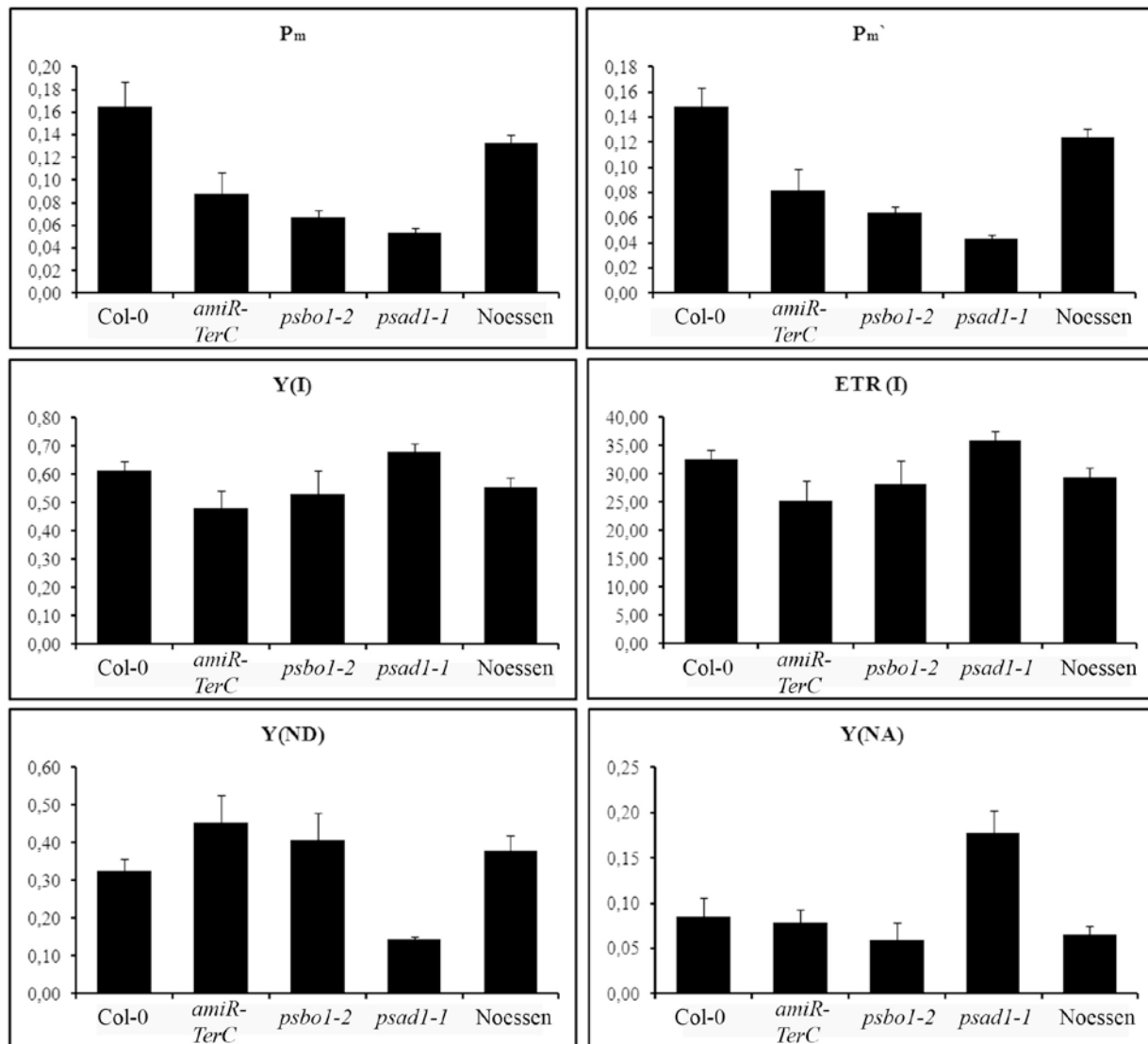


Figure 3.14: Parameters of PSI photosynthetic performance in wild type and mutant plants

P_{700}^+ absorption measurements of photosynthetic parameters from PSI were performed on wild type (Col-0 and Noessen), *amiR-TerC*, *psbO1* [this thesis] and *psad1-1* [Ihnatowicz et al., 2004] plants. Mean values and standard deviation for five plants each genotype are presented. P_m , the maximal change of the P_{700} signal upon quantitative transformation of P_{700} from the fully reduced to the fully oxidized state; $Y(I)$, the photochemical quantum yield of PSI; ETR (I), the electron transport rate around PSI; $Y(ND)$, the fraction of overall P_{700} that is oxidized in a given state (provides a measure of PSI donor side limitation); $Y(NA)$, the fraction of overall P_{700} that cannot be oxidized by a saturation pulse in a given state (provides a measure of PSI acceptor side limitation).

3.6 Protein profile of *terc-1* and *amiR-TerC* plants

As the knock-out of the *AtTerC* gene led to albinotic mutants which were only able to produce green cotyledons under very low light intensities (Figure 3.1). The presence of chloroplast localized proteins localized in the chloroplasts was investigated via immunodetection. Therefore, total protein extracts of both wild type and *terc-1* plants were separated on Tris-Tricine SDS gels, blotted on PVDF membranes and probed with specific antibodies against

subunits of PSII, PSII, LHCI, LHCII and the Cytochrome *b₆/f* complex, as well as proteins involved in PSII assembly, the POR protein, ferredoxin and the large subunit of the RubisCO. The protein loading was adjusted on the basis of equal amounts of Actin (**Figure 3.15**).

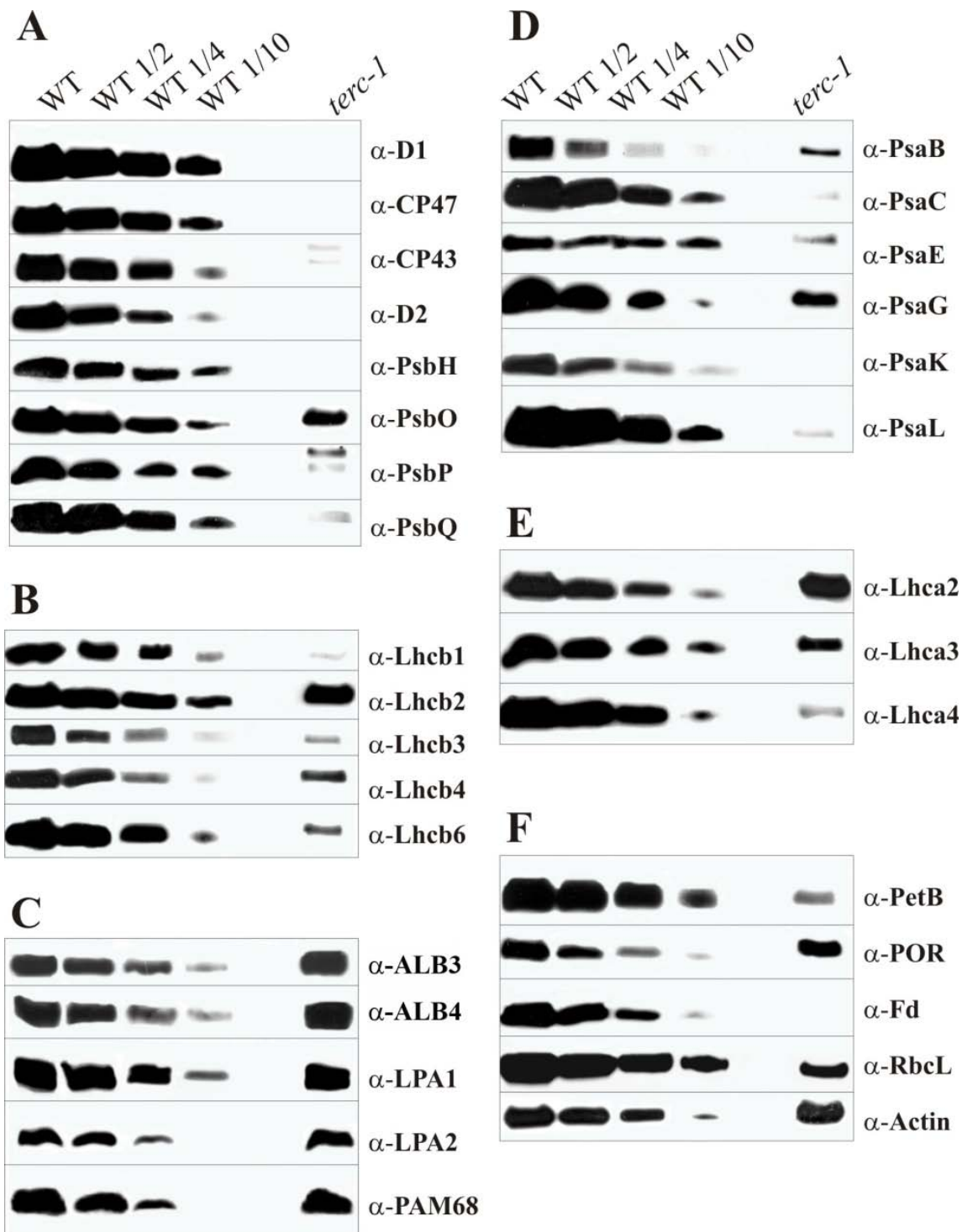


Figure 3.15: Protein content of wild type and *terc-1* plants

Total protein extracts of wild type and *terc-1* were separated via Tris-Tricine SDS-PAGE and afterwards immunoblot analyses were performed. Specific antibodies against proteins of the PSII (**A**), the Lhcb (**B**), assembly factors of PSII (**C**), the PSI (**D**), the Lhca (**E**) and miscellaneous proteins (**F**) were used for protein detection.

The detection of subunits of the photosystem II revealed that the four core proteins, D1, D2, CP43 and CP47, as well as PsbH were completely absent in *terc-1* plants. In contrast, the three proteins PsbO, PsbP and PsbQ which are located in the lumen and build up the water splitting complex were present in the knock-out mutant, although the protein amount was decreased compared to wild type plants. The additional bands on the Westerns against CP43 and PsbP derived from unspecific binding of the respective antibody (**Figure 3.15 (A)**). Except for PsaK and ferredoxin (Fd), all other analysed proteins could be detected in *terc-1* plants. This result shows that *terc-1* is able to synthesize LHCII (**Figure 3.15 (B)**), PSI (**Figure 3.15 (D)**) and LHCI (**Figure 3.15 (E)**) as well as assembly factors of PSII (**Figure 3.15 (C)**) and other proteins (**Figure 3.15 (F)**). However, the protein complex that is most drastically affected by the knock-out of *AtTerC* is the photosystem II.

To confirm the observations made in the knock-out mutant *terc-1* the same analyses were performed with the knock-down line *amiR-TerC* (**Figure 3.16**). The interpretation was mainly focused on the subunits of photosystem II, as the previous results suggested a major defect in the protein composition of this complex. The main difference of *amiR-TerC* and *terc-1* was the presence of the core proteins of PSII in *amiR-TerC* (**Figure 3.16 (A)**). Although the amount of the tested proteins was still decreased compared to wild type plants, the effect of *AtTerC* down-regulation was not as strong as the complete knock-out of the gene. As the protein amount of wild type and *amiR-TerC* samples was adjusted to the same amount of chlorophyll a+b, the signals derived from immunodetection were quantified and calculated on the basis of Actin (100%) in wild type and *amiR-TerC* samples (**Figure 3.16 (G)**). Interestingly, after this recalculation most of the analysed proteins, especially the subunits of PSI, LHCI, LHCII and the miscellaneous proteins, showed a decrease in their amount of around 30% compared to the wild type signal. In total, three proteins, D2, ALB4 and LPA1, were identified to be up-regulated in *amiR-TerC* plants. As the main focus was on the subunits of PSII, it was interesting to see, that the amounts of D1 (88%) and the CP47 (79%) were only slightly decreased, whereas the amount of CP43 in *amiR-TerC* plants was severely decreased to only 45% compared to wild type level.

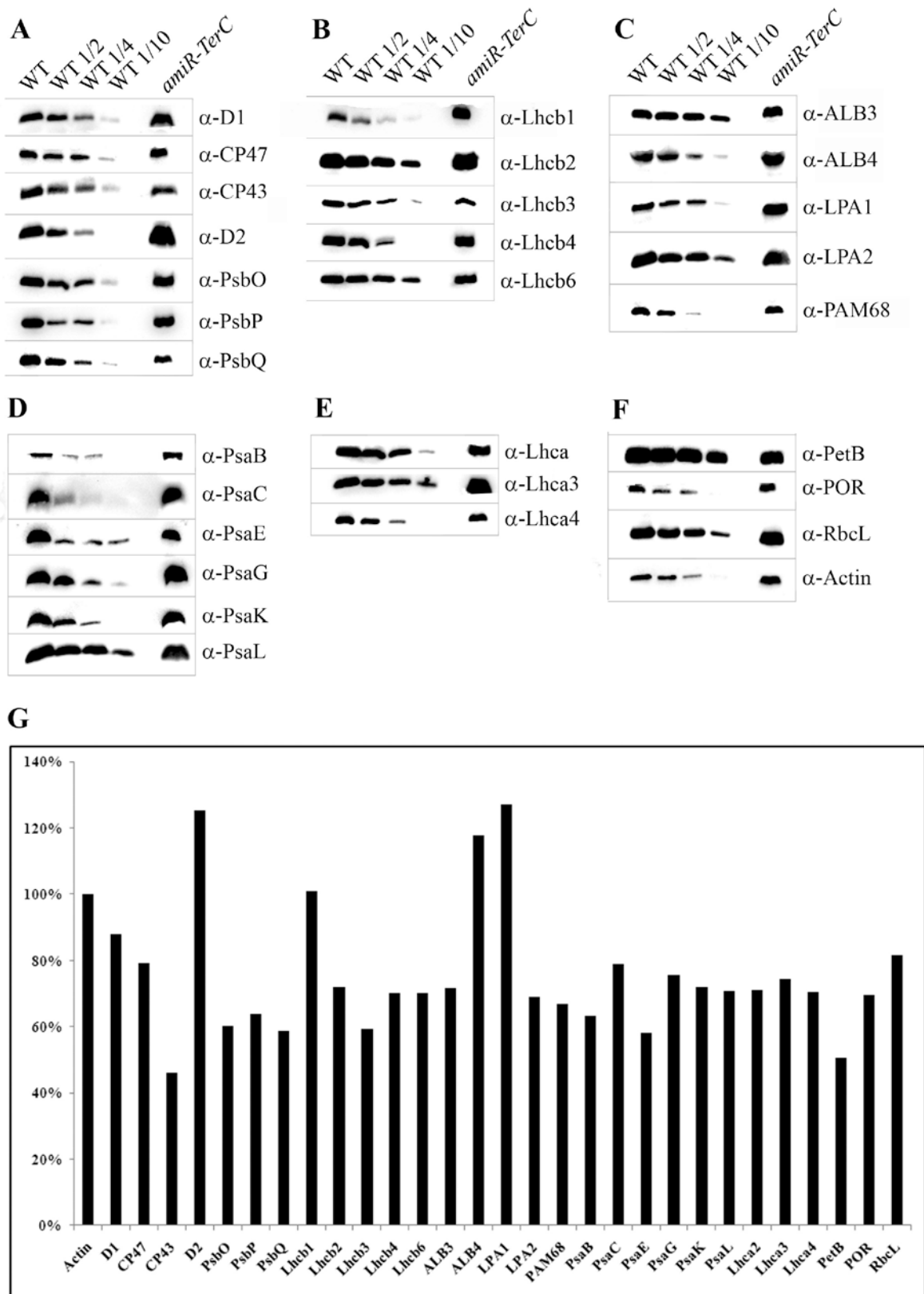


Figure 3.16: Protein content of wild type and *amiR-TerC* plants

Total protein extracts of wild type and *amiR-TerC* were separated via Tris-Tricine SDS-PAGE and afterwards immunoblot analyses were performed. Specific antibodies against proteins of the PSII (A), of the Lhcb (B), known to be assembly factors of PSII (C), of the PSI (D), of the Lhca (E) and miscellaneous proteins (F) were used for protein detection. Signals from A to F were quantified and adjusted to equal levels of Actin in wild type and *amiR-TerC* samples (100%) (G).

3.7 Blue native gel analysis of *amiR-TerC*

A decrease in the yield of photosystem II, the complete absence of PSII core proteins in *terc-1* and a reduction of these proteins in *amiR-TerC* led us to study the composition of photosynthetic complexes in the knock-down line. To investigate these complexes, blue native PAGE and second dimension gels under denaturing conditions were performed (**Figure 3.17 (A)**). The trimeric LHCII (V), the monomeric PSII (III), the dimeric PSII (II) and the PSII-supercomplexes were slightly reduced in *amiR-TerC*. In contrast to these complexes, the amount of the CP43-PSII complex was enriched in *amiR-TerC* plants compared to wild type after solubilisation of thylakoids with 1% β -DM. This severe difference between wild type and *amiR-TerC* became evident in the Coomassie stained denatured second dimension gel (**Figure 3.17 (B)**), too.

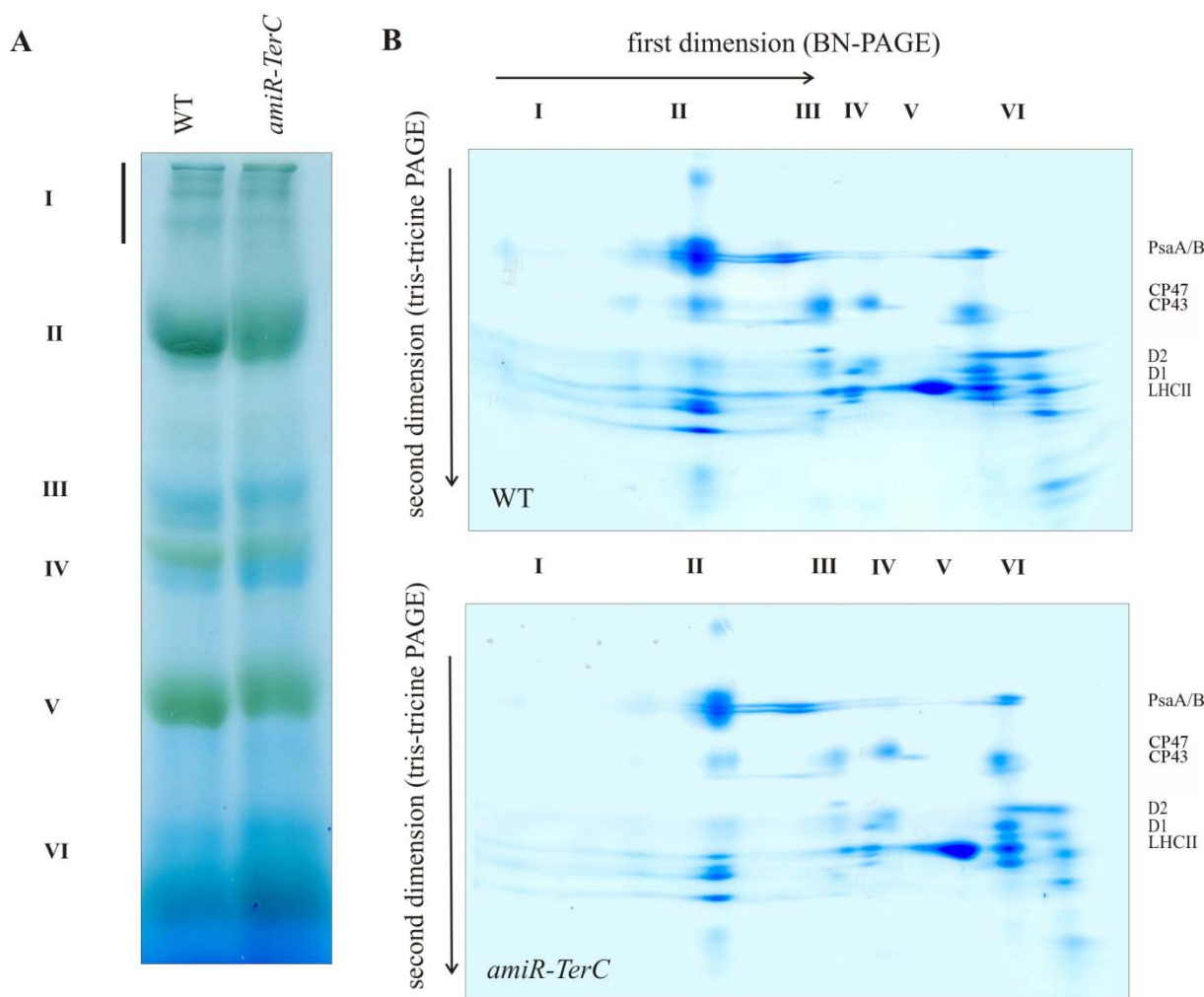


Figure 3.17: Blue native gel analysis and denaturing second dimension PAGE

Protein complexes in the thylakoid membrane were solubilized with 1% β -DM and separated under native conditions (**A**). Thylakoid protein complexes are indicated as **I** (PSII-supercomplexes), **II** (monomeric PSI and dimeric PSII), **III** (monomeric PSII), **IV** (CP43-PSII), **V** (trimeric LHCII) and **VI** (unassembled proteins). Gel slices from the first dimension were separated under denaturing conditions in a Tris-Tricine PAGE (**B**).

In the wild type gel, the spots representing CP47 (IV) and CP43 (III) showed equal intensities. In the *amiR-TerC* gel, the intensity of the CP43 (III) spot was decreased drastically compared to the CP47 (IV) spot. As a consequence, all spots derived from PSII proteins from the monomeric PSII (III) to the high molecular weight PSII-supercomplexes (I) were reduced. In the *amiR-TerC* gel the amount of unassembled CP43 was additionally decreased compared to the wild type gel (**Figure 3.17 (B)**).

To verify this observation, second dimension gels of wild type and *amiR-TerC* were blotted onto PVDF membranes and immunodetection analyses of the D2, CP43, CP47, Lhcb2 and PsaB proteins using specific antibodies was performed (**Figure 3.18**). In *amiR-TerC* plants, an accumulation of unassembled D2 protein compared to D2 integrated in PSII complexes was observed. Additionally, the PSII-supercomplexes were only hardly detectable in the knock-down lines, whereas in wild type plants several signals representing the D2 protein in high molecular weight complexes were detectable. The reduction of PSII-supercomplexes in *amiR-TerC* plants was confirmed by immunodetection of Lhcb2, CP47 and CP43. In contrast to the increase of unassembled D2 in *amiR-TerC* plants compared to wild type, the amount of unassembled CP43 was reduced compared to the assembled protein. For the PsaB protein, only a slight reduction in the supercomplex region of PSI was observed.

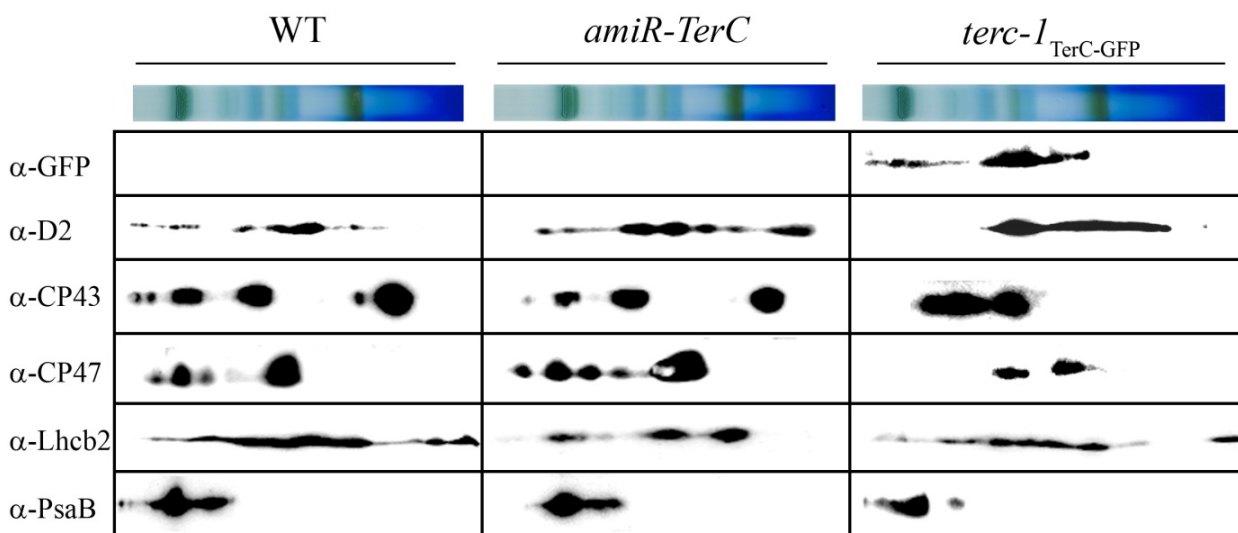


Figure 3.18: Western analysis of 2D Tris-Tricine gels from Blue-Native PAGE

Gel stripes of the Blue native PAGE were run on a 12% Tris-Tricine SDS-Gel under denaturing conditions. For immunological detection of subunits of the PSII, the LHCII and the PSI, specific antibodies raised against D2, CP43 and CP47 for the photosystem II, Lhcb2 for the LHCII complex and PsaB as a subunit of photosystem I were probed on the PVDF membranes after blotting of the gels.

Additionally, a Blue-Native PAGE was performed with thylakoids isolated from *terc-1*_{TerC-GFP} plants. The first dimension did not show any difference compared to the wild type (**Figure**

3.18). To analyze, whether the TerC-GFP fusion protein co-migrates with any major thylakoid complexes, immunodetection analyses with the respective antibodies and a GFP specific antibody were performed. The signal derived from the TerC-GFP fusion protein co-migrated with the CP43-PSII, the monomeric and dimeric PSII and the PSII-supercomplexes, indicating a co-localization with photosystem II. The most abundant signal of TerC-GFP was observed in the region of monomeric PSII, the assembly step where the integration of CP43 into photosystem II occurs. Interestingly, in *terc-I_{TerC-GFP}* plants the fraction of unassembled CP43 protein was not at all detectable.

3.8 Sucrose gradient analysis of *terc-I_{TerC-GFP}*

Because the data derived from the spectroscopic measurements with the Dual- and imaging PAM indicated fully functional PSII complexes in *terc-I_{TerC-GFP}* (**Figure 3.13 (C) and Table 3.1**), thylakoids from wild type and *terc-I_{TerC-GFP}* plants were isolated and solubilized with 0.5% β -DM and used for additional co-migration experiments. The protein complexes were separated on a sucrose gradient by ultra centrifugation (**Figure 3.19 (A)**). After centrifugation, the gradient was divided into 14 fractions which were separated on a Tris-Tricine SDS-PAGE and afterwards blotted on a PVDF membrane. Staining of the membrane with Coomassie blue revealed no changes in protein distribution (**Figure 3.19 (B)**).

Both wild type and *terc-I_{TerC-GFP}* gradients contained three green bands (**Figure 3.19 (A)**), which represented LHCII, PSII and PSI from top to bottom. This was confirmed by immunodetection with specific antibodies against subunits of these protein complexes. The PsaB protein, representing a subunit of photosystem I, was mainly detectable in the fractions 13 and 14 and only to a minor extent in fraction 12. This result confirmed the location of photosystem I in the bottom region of the sucrose gradient. The D2 protein, a subunit of the PSII reaction center, could be found in fractions 8 to 12, indicating that the middle bands of the sucrose gradients consisted mainly of PSII complexes. Another subunit of the PSII, the CP43 protein, was detected in the same fractions like the D2 protein. Interestingly, CP43 was also detectable in fractions 4 to 7. This finding indicates the presence of unassembled CP43 protein in both wild type and *terc-I_{TerC-GFP}* plants. The light harvesting complex of photosystem II, represented by the Lhcb2 protein, was detectable in fraction 3 to 10 with the highest concentration of the protein in fractions 8 and 9. This observation suggested that the upper green band of the sucrose gradients contained preferentially Lhcb proteins.

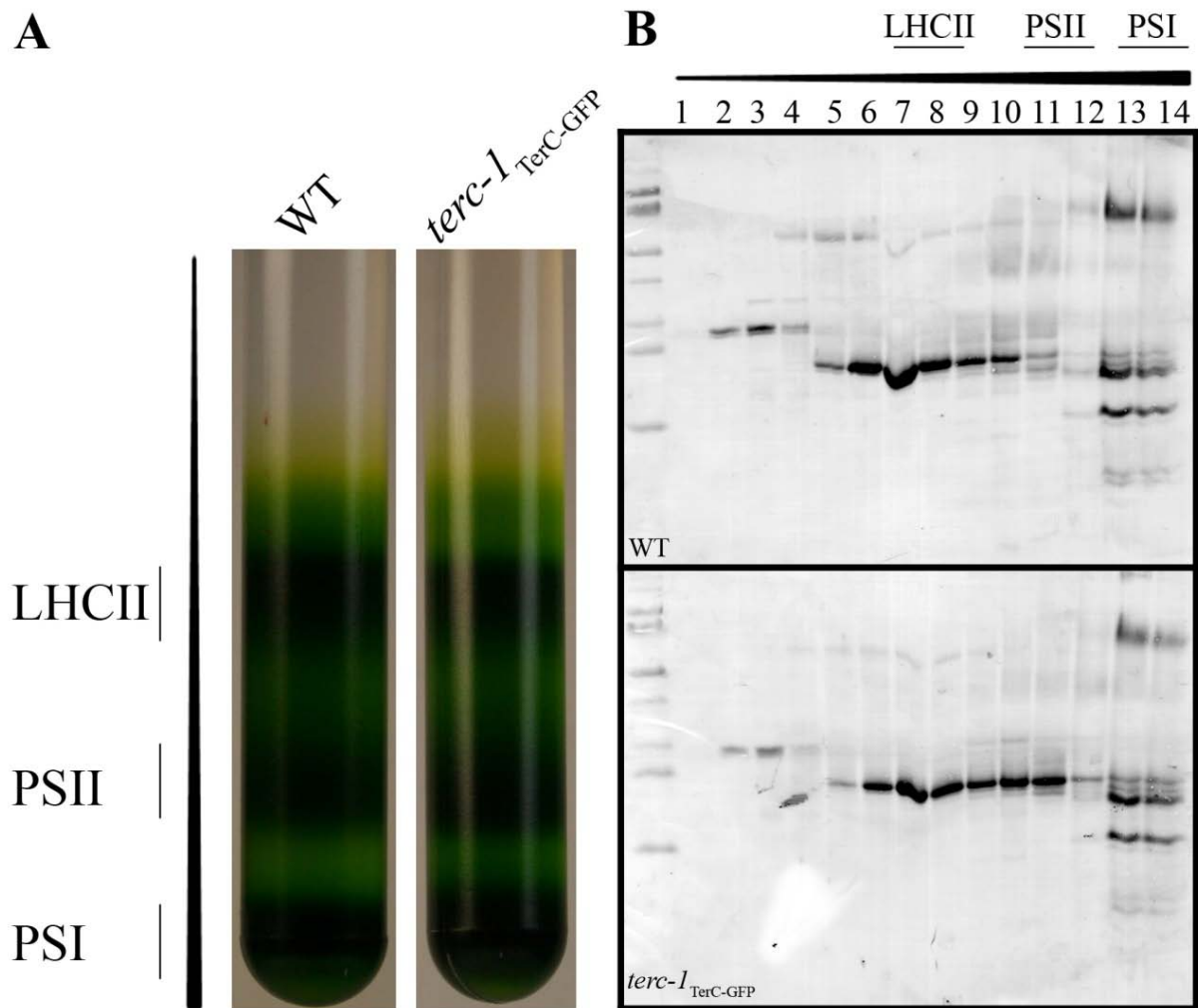


Figure 3.19: Sucrose gradient analysis of wild type and *terc-1*_{TerC-GFP} thylakoids solubilized with β -DM followed by separation via Tris-Tricine SDS-PAGE

Isolated thylakoid protein complexes were separated by ultra centrifugation (A). Afterwards, the gradients were partitioned into 14 fractions and separated via Tris-Tricine SDS-PAGE followed by blotting onto PVDF membrane and staining with coomassie blue (B).

To investigate the localization of the TerC-GFP fusion protein, PVDF membranes with wild type and *terc-1*_{TerC-GFP} proteins were probed with an antibody that specifically recognized the GFP protein. While there was no detectable signal on the wild type membrane, a chemiluminescence signal corresponding to the TerC-GFP fusion protein was found in the samples from *terc-1*_{TerC-GFP} plants. The GFP signal overlapped with the CP43 signal as it could be found in fractions 5 to 12 like the CP43 protein. This observation suggests a co-localization of TerC-GFP and CP43 in the respective sucrose gradient.

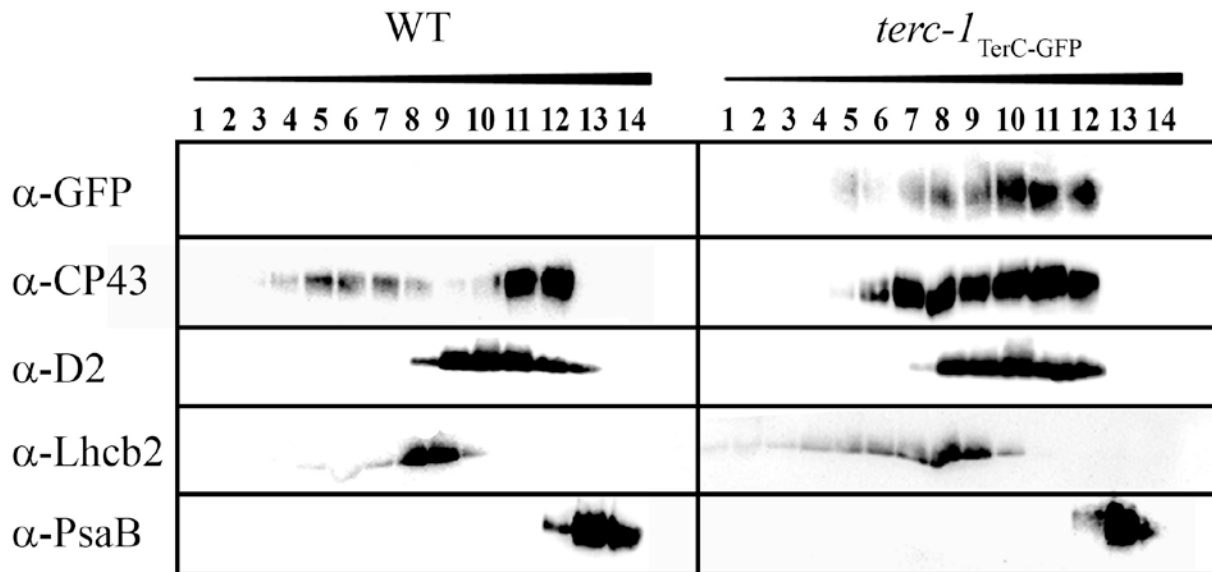


Figure 3.20: Fractionation of sucrose gradient samples of wild type and *terc-1*_{TerC-GFP}

The 14 fractions of the sucrose gradients were separated on a 12% Tris-Tricine SDS-PAGE followed by blotting onto PVDF membrane. The localization of CP43, D2, Lhcb2, PsaB and the TerC-GFP fusion protein was performed by immunodetection with specific antibodies raised against these proteins.

3.9 Protein-protein interaction studies using the Split Ubiquitin system

As the previous experiments revealed an involvement of TerC in either the assembly of photosystem II or the integration of subunits of PSII into the thylakoid membrane, a yeast Split Ubiquitin study for integral membrane proteins was performed to identify putative interaction partners of TerC. Various proteins were considered for direct interaction studies, like proteins of PSII, known assembly factors of PSII, proteins involved in transport of proteins into or across the thylakoid membrane and proteins of other complexes in the thylakoid membrane like PSI, Cytochrome *b₆/f* complex, the ATPase and the electron transporter ferredoxin. The coding sequence of *AtTerC* was cloned into the vector pAMBV4 and by this fused to the C-terminus of Ubiquitin acting as a bait protein. The putative interactors were cloned into the vector pADSL fused to the modified N-terminus of Ubiquitin (NubG) acting as prey proteins. After co-transformation of the yeast strain DSY-1 with different combinations of bait and prey constructs, the ability of the yeast cells to grow on selective medium indicates a successful interaction of bait and prey proteins.

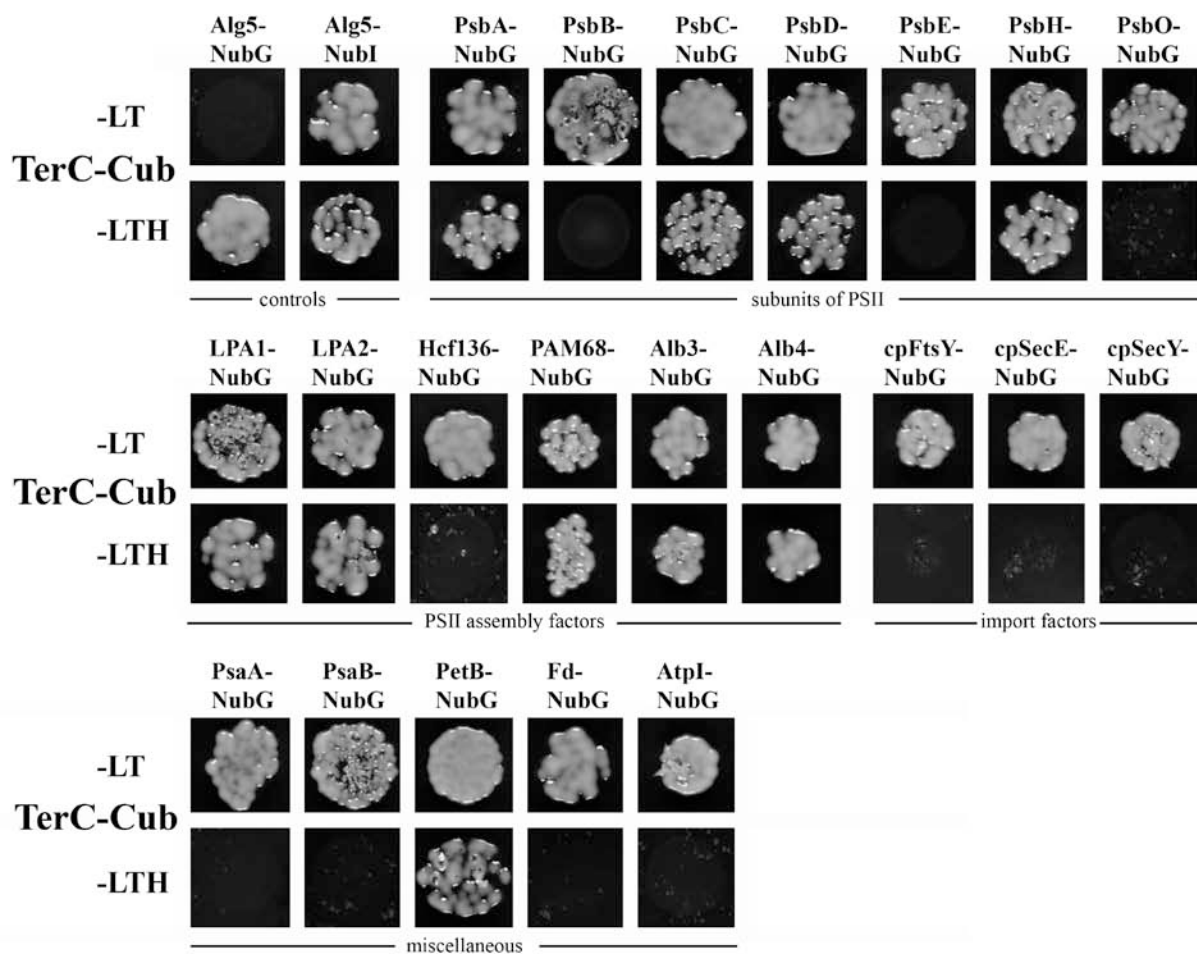


Figure 3.21: Protein-protein interaction study between TerC and several plastid proteins

Co-transformed *DSY-1* yeast cells were grown on either permissive (-LT) or non-permissive medium (-LTH). On permissive medium all co-transformed yeast cells were growing except of the negative control with Alg5. On non-permissive medium only the strains containing interacting proteins were able to grow. TerC fused to the C-terminus of Ubiquitin was used as bait and proteins of the PSII, assembly factors of PSII, import factors and some miscellaneous proteins were used as preys.

According to the results of the Split Ubiquitin assay (**Figure 3.21**), TerC interacted with PsbA, PsbC, PsbD and PsbH, subunits of photosystem II, but not with PsbB, PsbE and PsbO. An interaction could also be confirmed for the assembly factors LPA1, LPA2, PAM68, ALB3 and ALB4, but not for HCF136. An interaction with factors involved in protein import (cpFtsY, cpSecE and cpSecY), subunits of photosystem I (PsaA and PsaB), AtpI (a subunit of the ATPase) and ferredoxin could not be observed. The only putative interaction partner of TerC that is not related to the PSII or its assembly was PetB, a subunit of the Cytochrome *b_{6/f}* complex.

3.10 *In vivo* synthesis of chloroplast proteins

To investigate the biosynthesis, insertion ability and stability of plastid encoded thylakoid proteins, pulse-chase experiments on wild type, *terc-1* and *amiR-TerC* plants were performed.

The pale green plants of *terc-1* together with wild type plants were harvested from MS plates after one week of illumination with $4 \mu\text{Em}^{-2}\text{s}^{-1}$ and incubated with radioactively labeled methionine for 20 min. The presence of newly synthesized radioactively labeled proteins was investigated after SDS-PAGE and scanning a phosphoscreen after two days of exposure to the dried gel. In the wild type sample all prominent bands like PsaA/B, CF1 α/β , CP43, CP47, D1 and D2 were detectable after labeling, whereas in *terc-1* the bands representing the core subunits of PSII, D1, D2, CP43 and CP47, were missing, although the other bands were present. The only protein related to the PSII core complex, that was present in *terc-1*, was the precursor of the D1 protein (pD1) (**Figure 3.22**).

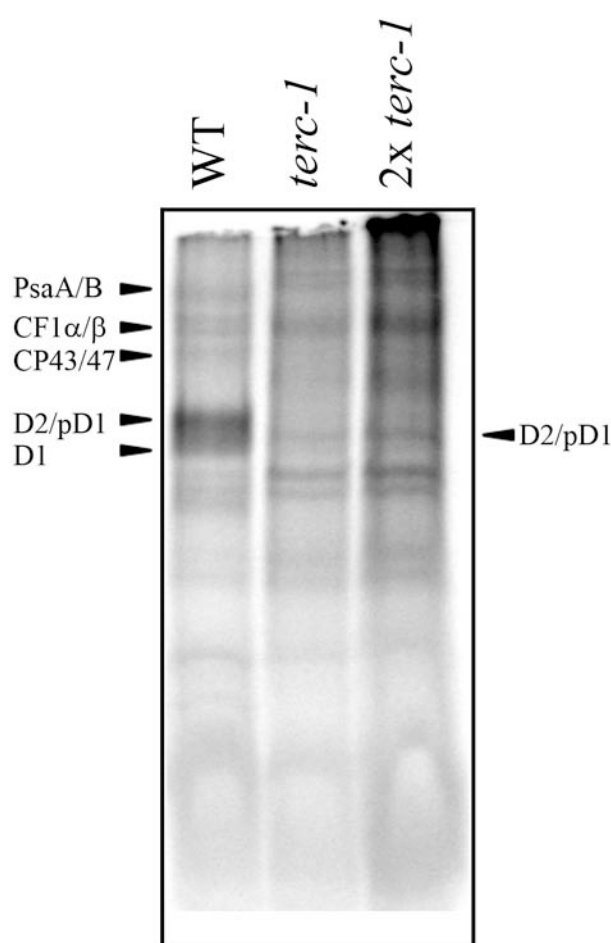


Figure 3.22: *In vivo* synthesis (pulse) of plastid encoded proteins from the thylakoid membrane

Radioactive labeling (pulse) of one week old WT and *terc-1* plants in the presence of cyclohexamide for 20 min was performed. After the pulse thylakoid membranes were isolated and the proteins were separated by Tris-Tricine SDS-PAGE and visualized autoradiographically.

To verify the result obtained from the [^{35}S]-methionine radioactive protein labeling of *terc-1* and to see a less drastic effect, the labeling of plastid proteins was also performed in the

amiR-TerC plants. This labeling revealed a decrease of labeled CP43 protein in *amiR-TerC* to about 80% of the wild type level, whereas the other proteins related to photosynthesis were present in almost double the amount as in wild type (**Figure 3.23 (A)**).

To exclude a function of TerC in the stability of photosystem II, one hour of chase with cold methionine followed the 20 min pulse. Again, a reduction in the amount of radioactively labeled CP43 could be observed in *amiR-TerC*, whereas the other proteins were synthesized in an at least equal amount as in wild type (**Figure 3.23 (B)**). The chase with cold methionine revealed no faster degradation of proteins in *amiR-TerC* than in wild type, indicating that TerC is not involved in the stability of photosystem II.

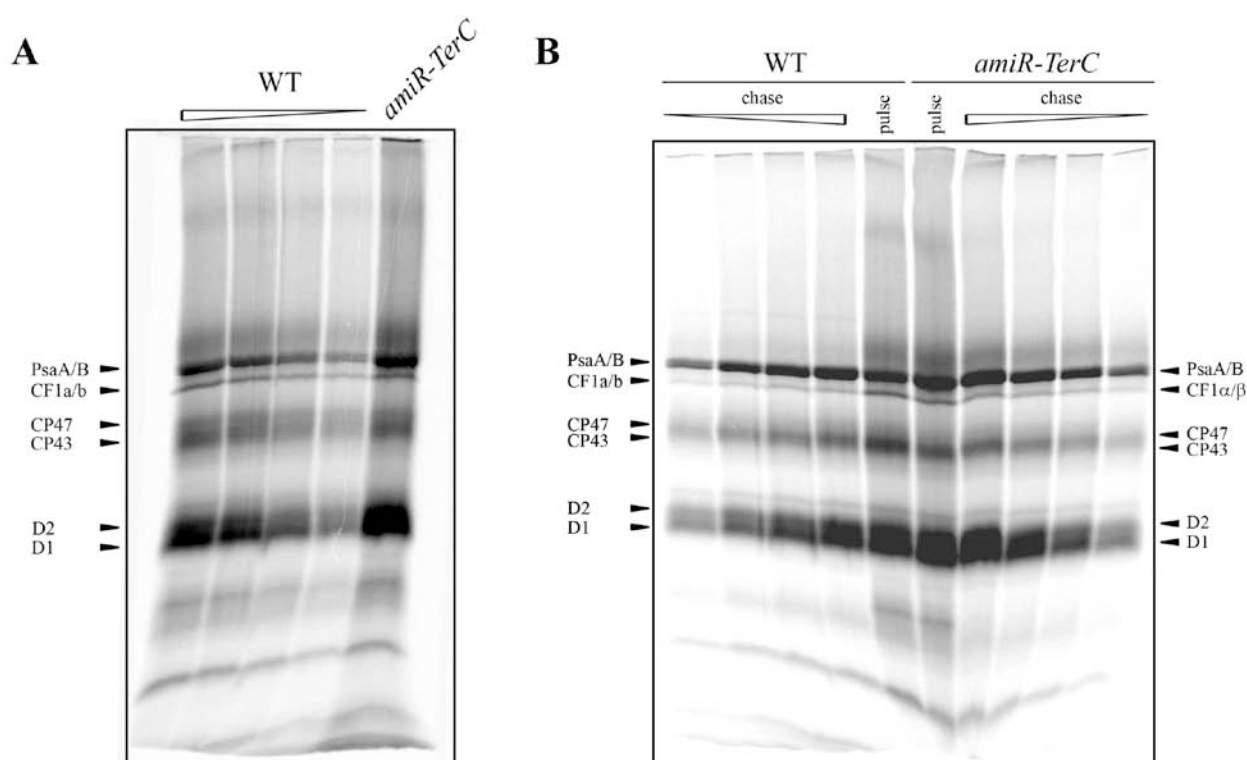


Figure 3.23: *In vivo* synthesis (pulse) and degradation (chase) of plastid encoded proteins of the thylakoid membrane

Radioactive labeling (pulse) of three week old WT and *amiR-TerC* plants in the presence of cyclohexamide for 20 min (**A** and **B**) followed by a chase with cold methionine for one hour (**B**) was performed. After pulse and chase thylakoid membranes were isolated and the proteins were separated by Tris-Tricine SDS-PAGE and visualized autoradiographically.

Due to the reduced amount of CP43 after the pulse labeling (**Figure 3.23 (B)**), the assembly of the PSII complex was analysed by blue native PAGE with radioactively labeled thylakoid proteins from wild type and *amiR-TerC*. Therefore, thylakoids were solubilized with 1% β -DM after pulse and chase and separated under non denaturing conditions. Afterwards, gel stripes of the first dimension were separated under denaturing conditions on a Tris-Tricine

SDS-PAGE. The dried gels were exposed to a phosphoscreen for two day and visualized using a phosphoimager. The most striking difference in the second dimension of the pulse labeled thylakoids was the reduction of CP43 in *amiR-TerC* (**Figure 3.24 (A)**). Already the unassembled CP43 in fraction VI was strongly affected. In fraction I (PSII-supercomplexes), fraction II (PSII dimer) and fraction III (PSII monomer) the amount of CP43 was reduced. This indicates a reduction in the overall assembly of PSII, however D1 and D2 behaved different. The amount of D1/D2 in fraction VI (unassembled proteins), in the PSII-RC in fraction V, in the CP47-RC (IV) and in fraction III, the PSII core monomer, was not reduced. Thus, only the newly synthesized PSII complexes were affected in the knock-down mutant, whereas the turnover of photo-damaged PSII seems not to be impaired.

The chase with cold methionine following the pulse labeling showed the ability of *amiR-TerC* to assemble complete photosystem II complexes, although the speed of assembly is slowed down (**Figure 3.24 (B)**). While after the 20 min of pulse in *amiR-TerC* there were almost no radioactively labeled PSII-supercomplexes visible compared to wild type, these high molecular complexes became more prominent after one hour of chase, during which almost all labeled proteins were assembled into the high molecular complexes. Thus, the overall amount of unassembled radioactively labeled proteins in fraction VI was reduced and the PSII dimer and the PSII-supercomplexes were labeled stronger.

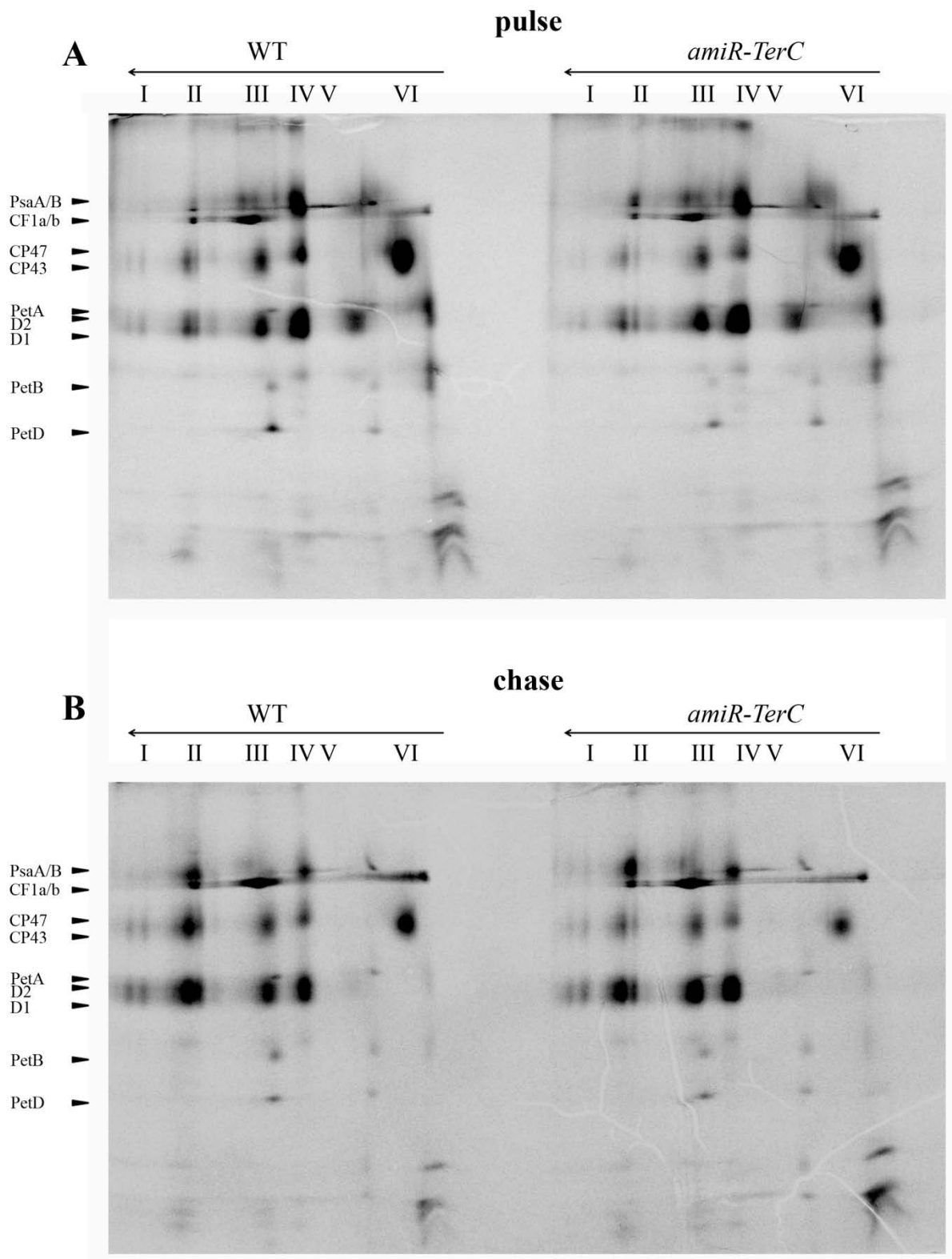


Figure 3.24: *In vivo* synthesis (pulse) and degradation (chase) of plastid encoded proteins from the thylakoid membrane separated first on blue native PAGE followed by a denaturing Tris-Tricine SDS-PAGE

Radioactive labeling (pulse) of three week old WT and *amiR-TerC* plants in the presence of cyclohexamide for 20 min (**A**) followed by a chase with cold methionine for one hour (**B**) was performed. After pulse and chase thylakoid membranes were isolated and the proteins were separated first in a blue native gel followed by Tris-Tricine-SDS-PAGE and visualized autoradiographically.

4. Discussion

4.1 Complete knock-out of *AtTerC* leads to lethality due to a loss of photosystem II

For *terc* knock-out mutants, an albinotic phenotype on soil was observed previously [König, 2005; Strissel, 2007; Kwon and Cho, 2008]. Therefore, *terc* mutant lines were not viable beyond the seedling stage. The albinotic phenotype of *terc* could not be rescued on MS medium supplemented with sucrose and it was not caused by a defect in chlorophyll biogenesis, as *terc-1* plants grown under very low light intensities ($4 \mu\text{Em}^{-2}\text{s}^{-1}$) turned slightly green in the cotyledon stage [Strissel, 2007; Kwon and Cho, 2008]. Further, Kwon and Cho (2008) could exclude a defect in the plastid transcription in *terc* plants, as they were able to detect e.g. the mRNA of *psbA* via Northern Blot analyses, whereas the D1 protein was never detected in *terc-1* [Strissel, 2007; Kwon and Cho, 2008].

Transmission electron microscopy (TEM) analyses revealed the presence of thylakoid membranes in chloroplasts of *terc-1* mutant plants grown under dim light conditions (**Figure 3.2**). But interestingly, only the formation of stroma lamellae was found in these chloroplasts. It is well known that PSI complexes and the ATP-synthase are located in the stroma lamellae, whereas PSII is functionally present in the grana lamellae. This membrane structure, consisting of stacked thylakoid membranes, is completely absent in *terc-1* plants suggesting that mainly photosystem II might be affected by the functional loss of *AtTerC*.

In agreement with the suggested defect in PSII observed by transmission electron microscopy (TEM), *terc-1* plants were devoid of the core proteins of PSII, D1, D2, CP43 and CP47, and the low molecular weight subunit PsbH involved in early PSII assembly (**Figure 3.15**). In contrast to the observations for the PSII core proteins, some luminal proteins of PSII, PsbO, PsbP and PsbQ, as well as assembly factors of PSII and subunits of other thylakoid localized protein complexes, like LHCII, PSI, LHCI and the Cytochrome *b₆f* were present in the knock-out mutant. These results suggest an involvement of TerC in the assembly of photosystem II.

Compared to other mutants that are defective in PSII assembly, e.g. *hcf136* [Meurer et al., 1998] that is able to generate pale green leaves when grown on MS medium supplemented with sucrose under moderate light conditions ($20 \mu\text{Em}^{-2}\text{s}^{-1}$), *terc-1* shows a more severe phenotype. The only known mutant affected in PSII assembly with a severe phenotype similar to *terc-1*, is the *alb3* mutant. ALB3 is not only involved in the integration of D1 into the PSII core complex but also necessary for the import of LHCII proteins into the thylakoid

membrane [Bellafiore et al., 2002; Ossenbühl et al., 2004]. The difference in the phenotypic between *terc-1* and other known mutants involved in PSII assembly, like *lpa1* [Peng et al., 2006], *lpa2* [Ma et al., 2007], *lpa3* [Cai et al., 2010], *pam68* [Armbruster et al., 2010] and *hcf136* [Meurer et al., 1998] suggests that TerC bears multiple functions during thylakoid biogenesis. One might speculate that TerC is not only involved in PSII assembly, but also in the assembly of other thylakoid complexes. An additional function of TerC could be a role the assembly of the Cytochrome *b₆f* complex. The amount of PetB protein was severely reduced in both, the *terc-1* knock-out mutants (**Figure 3.15**) and in the *amiR-TerC* plants (**Figure 3.16**). Additionally, a protein-protein interaction of TerC with PetB was confirmed by *in vitro* Split Ubiquitin analyses (**Figure 3.21**). However, the following discussion will focus mainly on the impact of TerC during the assembly of photosystem II in *Arabidopsis thaliana*.

4.2 Down-regulation of *AtTerC* leads to a leaf variegated phenotype and a reduction of thylakoid proteins

Since *terc-1* revealed a severe phenotype, an artificial micro RNA line was produced to be able to perform biochemical analyses. The *amiR-TerC* plants were generated by transformation of wild type plants (Col-0) with the plasmid pGWB2-TerC. The generated *amiR-TerC* plants were able to grow photoautotrophically on soil, but showed a variegated leaf phenotype with white sectors embedded in the green leaf tissue (**Figure 3.3**). The successful down-regulation of *AtTerC* was confirmed by real-time PCR analysis. The transcript level of *AtTerC* was reduced in the T2 generation of *amiR-TerC* plants to less than 10% of the wild type level (**Figure 3.4 (A)**). In the T3 generation of *amiR-TerC* plants, most of the leaves still displayed the variegated phenotype, but some leaves resembled wild type leaves (**Figure 3.6**). Therefore, the transcript level of *AtTerC* was also analysed in the T3 generation of *amiR-TerC* plants. Both variegated and non variegated leaves showed a decrease in *AtTerC* transcript compared to wild type (**Figure 3.4 (B)**). In the variegated leaves (var+) the transcript level of *AtTerC* was reduced to around 20% and in the non variegated leaves (var-) the transcript level was down to around 30%. These different transcription levels of *AtTerC* suggest a threshold level of around 25% that, if fallen below, leads to the variegated leaves or to leaves that resemble those of wild type plants. The diminished effect of the artificial micro RNA from the T2 to the T3 generation of *amiR-TerC* plants suggests that an endogenous silencing mechanism is acting on the amiRNA effect.

The *amiR-TerC* plants were analysed with respect to their protein content like the *terc-1* plants (**Figure 3.15**). All investigated proteins were detectable in *amiR-TerC* plants,

indicating that all protein complexes (PSI, PSII, LHCI, LHCII and the Cytochrome *b₆/f* complex), as well as the PSII assembly factors, were present in the knock-down mutants (**Figure 3.16 (A to F)**). The specific signals derived from the immunoblot analyses were quantified and adjusted to equal amounts of Actin in both wild type and *amiR-TerC* samples. The quantification revealed that protein levels, especially those of the PSI, LHCI and LHCII, were down-regulated to 60-70% in *amiR-TerC* plants compared to wild type (**Figure 3.16 (G)**). Interestingly, D2, ALB3 and LPA1, were up-regulated to around 125% in the knock-down mutant. In contrast to that, the amount of D1 (88%) and CP47 (80%) was slightly above the average value of 60-70% and only two analysed proteins were reduced below the average value in *amiR-TerC* being CP43 (45%) and PetB (50%). This reduction in the amount of CP43 and PetB is a hint for the involvement of TerC in the assembly of CP43 into the photosystem II and maybe also in the assembly of the Cytochrome *b₆/f* complex.

4.3 Photosynthetic performance of PSII is affected in *amiR-TerC* plants

Because of the lack of the photosystem II core proteins in *terc-1* and the severe reduction of CP43 in *amiR-TerC*, spectroscopic measurements addressing the intactness and efficiency of PSI and PSII were performed.

The *amiR-TerC* plants showed a severe increase in ground fluorescence (F_0) (**Figure 3.13 (A and B)**) and a decrease in the maximum quantum yield of PSII (F_V/F_M) and in the effective quantum yield of PSII (Φ_{II}) (**Table 3.1; Figure 3.13 (A and B)**). These observations resemble spectroscopic data from mutants that are affected in photosystem II assembly and/or stoichiometry like *hcf136* [Meurer et al., 1998], *lpa1* [Peng et al., 2006], *lpa2* [Ma et al., 2007], *lpa3* [Cai et al., 2010] and *pam68* [Armbruster et al., 2010]. After rise of chlorophyll a fluorescence due to actinic light exposure, when recording fluorescence curves for F_V/F_M and Φ_{II} determination a drop of the fluorescence below the F_0 level was observed for the *amiR-TerC* plants (**Figure 3.13 (B)**). Additionally, two intermediate rises in chlorophyll a fluorescence, that occur in wild type plants during the relaxation of the initial chlorophyll a fluorescence as a consequence of limitations within photosystem I and the calvin cycle, were not detectable in *amiR-TerC* plants. These are specific characteristics of mutants with a reduced PSII/PSI ratio and can be explained by the higher activity of PSI relative to PSII [Armbruster et al., 2010]. The decrease of the effective quantum yield of PSII (Φ_{II}) suggests an additional defect in the electron transport chain downstream of PSII either at the position of PSI [Ihnatowicz et al., 2004] or the Cytochrome *b₆/f* complex [Meierhoff et al., 2003].

As the immunoblot analyses of *amiR-TerC* plants revealed a decrease in the amount of PSI proteins to about 60-70% compared to wild type plants (**Figure 3.16 (G)**), further spectroscopic measurements regarding the functionality of photosystem I were performed on *amiR-TerC* plants and compared to wild type, *psbI-2*, a mutant defective in PSII [this thesis (**Appendix 1/2**)] and *psad1-1*, a mutant defective in PSI, [Ihnatowicz et al., 2004]. The P_m value, representing the maximum absorption of P_{700}^+ (transition from a fully reduced to a fully oxidized state), and the P_m' value (the absorption of P_{700}^+ during illumination) were reduced to around 60% in *amiR-TerC* plants compared to its corresponding wild type (Col-0) (**Figure 3.14**). This correlated with the reduced PSI protein amounts that were already observed in previous analyses (**Figure 3.16 (G)**) demonstrating that the reduced activity of PSI in *amiR-TerC* plants is not directly caused by the down-regulation of *AtTerC* transcript. This assumption is supported by the measured efficiency of PSI shown by the photochemical quantum yield of PSI (Y(I)) and the electron transfer rate around PSI (ETR) which were both only slightly decreased compared to wild type. A proof for the proper functionality of PSI in *amiR-TerC* plants was obtained by measurements on the donor side (Y(ND)) and acceptor side limitation (Y(NA)) of photosystem I. While in *psad1* a severe decrease in the donor side limitation and a strong increase in the acceptor side limitation compared to wild type plants could be observed, the *amiR-TerC* plants behaved exactly like *psbI*. Both, *amiR-TerC* and *psbI*, showed an increase in the donor side limitation compared to their corresponding wild type backgrounds. The acceptor side limitation remained unaltered in wild type, *amiR-TerC* and *psbI* plants. This proves the intactness of photosystem I and a defect upstream of this protein complex in *amiR-TerC* plants, located in the photosystem II and/or the Cytochrome *b₆/f* complex.

In addition, the plants stably expressing the TerC-GFP fusion protein, *terc-I_{TerC-GFP}* and *WT_{TerC-GFP}*, were spectroscopically analysed to investigate the functionality of the photosynthetic complexes in both genotypes (**Table 3.1**). The *WT_{TerC-GFP}* plants behaved exactly like wild type plants which showed that the GFP-tag does not affect the fluorescence recorded by the Dual PAM100. In *terc-I_{TerC-GFP}* plants the functionality of the photosystem II seemed to be restored. The expressed fusion protein TerC-GFP could complement the defect in the PSII of *terc-I* knock-out mutants as the maximum quantum yield of PSII (F_v/F_m) showed the same value as wild type plants. The non photochemical quenching (NPQ) in *terc-I_{TerC-GFP}* plants resembled the wild type value, too. However, the TerC-GFP fusion protein could not complement all defects of the *terc-I* knock-out mutant as the effective quantum yield of PSII (Φ_{II}) was decreased and the excitation pressure on PSII represented by the value

1-qP was increased in *terc-I_{TerC}-GFP* plants compared to wild type. This increased excitation pressure might be due to the involvement of TerC in the dimerisation of the Cytochrome *b₆f* complex (**Figure 3.24 (A)**).

Altogether, the *terc-I_{TerC}-GFP* lines seem suitable for colocalisation experiments with respect to TerC and CP43. If the GFP-tag abolishes other functions of TerC remains to be determined, especially an involvement of TerC in the assembly process of the Cyt *b₆f* complex has to be addressed in future studies (**Figure 3.9**).

4.4 Leaf variegation is not caused by oxidative stress in *amiR-TerC* plants

The *amiR-TerC* plants clearly showed a leaf variegated phenotype as they displayed white sectors within the normal green leaf tissue (**Figure 3.3**). From other leaf variegated mutants (**Table 1.1**) it is known that the transcription of plastid or mitochondrial encoded genes is disturbed or that in most of these mutants, an increase of oxidative stress in the leaf tissue is observed [Yu et al., 2007]. Since the level of leaf variegation in oxidative stress affected mutants, like in *im* [Aluru et al., 2007], *var1* [Zaltsman et al. 2005], *var2* [Bailey et al. 2002] and *var3* [Næsted et al., 2004], increased after high light treatment [Yu et al., 2007], *amiR-TerC* plants were also grown under high light (1000 $\mu\text{Em}^{-2}\text{s}^{-1}$). Additionally, low light conditions (5 $\mu\text{Em}^{-2}\text{s}^{-1}$) were applied to investigate the level of leaf variegation (**Figure 3.5**). The growth of *amiR-TerC* plants under high light revealed an opposite effect as observed for other variegated mutants. Instead of an increase in the level of leaf variegation, the leaves of *amiR-TerC* plants turned completely green after 16 days of high light treatment. Only the midribs of the *amiR-TerC* leaves stayed paler compared to wild type plants. This indicates, that in contrast to other variegated mutants [Aluru et al., 2007; Zaltsman et al. 2005; Bailey et al. 2002; Næsted et al., 2004] *amiR-TerC* plants can cope better with high irradiance and do not accumulate higher amounts of reactive oxygen species (ROS) which leads to an enhanced bleaching of the leaves. Another proof that the leaf variegated phenotype in *amiR-TerC* plants is not caused by ROS can also be found upon high light treatment of these plants. Upon the first day of high light treatment, the leaves of wild type plants produced a purple colouration which is indicative of an enhanced anthocyanine production to prevent oxidative damage in the leaf tissue. In contrast, leaves of *amiR-TerC* plants did not show an altered leaf colouration which indicates that the oxidative stress in *amiR-TerC* is not as high as in wild type plants.

If one would expect an increase of leaf variegation under high light, one would also expect a decrease of leaf variegation under low light. However, for *amiR-TerC* plants this was not the

case. The *amiR-TerC* plants maintained their leaf variegation phenotype even under prolonged light treatment.

Since increased light intensities did not enhance the leaf variegation and prolonged low light treatment did not attenuate this effect, plants were cultivated under different day/night cycles to investigate the effect of the light period on the growth of *amiR-TerC* plants (**Figure 3.6**). The reduction of the light period to 12 h or even 8 h had no effect on the leaf variegation in *amiR-TerC* plants of the T3 and T4 generation. The plants maintained their leaf variegation, but instead the biomass production of the plants was severely affected. By reducing the light period to either 12 h or 8 h the plant size of the *amiR-TerC* mutants decreased drastically. These observations together with the loss of leaf variegation under high light treatment are in accordance with the defects in the photosynthetic performance of *amiR-TerC* plants. It seems as if *amiR-TerC* plants grown under 16 h of light with an illumination of $100 \mu\text{Em}^{-2}\text{s}^{-1}$ do not produce enough metabolites during the day to supply the entire plant. A shortening of the light period even enhances the deficiency in metabolite supply leading to a severe decrease in plant biomass production. This deficiency could be complemented by increasing the light intensity to $1000 \mu\text{Em}^{-2}\text{s}^{-1}$.

Referring to results from Kwon and Cho (2008), who ruled out a defect on the transcript level for *terc*, and the observation, that the leaf variegated phenotype in *amiR-TerC* plants is not caused by high oxidative stress, another mechanism is operating in *amiR-TerC* plants. This mechanism causing the variegated phenotype was elucidated by decreasing the transcript level of *AtTerC* to less than approximately 25% via artificial micro RNA interference. Some mesophyll cells seem to express TerC above this threshold level and thus turn green. Other mesophyll cells seem to express TerC below this threshold level and thus turn white leading to a leaf variegated phenotype.

4.5 Putative protein interaction partners of TerC

Due to the absence of PSII core proteins in *terc-1*, the reduced photosynthetic performance of PSII in *amiR-TerC* plants and the different amounts of PSII core proteins, interaction studies of the TerC protein with PSII core proteins were performed.

One method to investigate protein-protein interactions of membrane bound proteins is the Split Ubiquitin assay. The TerC protein fused to the C-terminus of Ubiquitin acted as a bait protein in yeast cells that were co-transformed with vectors coding for the proteins of interest fused to the N-terminus of Ubiquitin and thus acting as prey proteins. The growth of yeast cells on non-permissive medium indicated an interaction of the two proteins expressed in the

cells. Upon interaction of the two proteins the C- and N-terminal halves of Ubiquitin are assembled and can be cleaved off by a protease leading to the induction of a reporter gene. The TerC protein interacted specifically with subunits of the photosystem II, especially with the core proteins D1 (PsbA), D2 (PsbD), CP43 (PsbC) and additionally with PsbH (**Figure 3.21**). No interaction could be confirmed with CP47 (PsbB) and other subunits of PSII. Furthermore, the tested PSII assembly factors, LPA1, LPA2, PAM68, ALB3 and ALB4, but not HCF136, showed an interaction with TerC. There was no interaction with proteins of other protein complexes observed in this assay, except for an interaction with PetB. A similar complex interaction pattern was observed in studies of other PSII assembly factors. For ALB3 interactions with various thylakoid proteins like D1, D2, CP43, PsaA and CF₀III, a subunit of the ATPase, were shown, indicating an important role of ALB3 in the assembly of several protein complexes in the thylakoid membrane [Pasch et al., 2005]. Also PAM68 exhibited interactions with various subunits and assembly factors of PSII [Armbruster et al., 2010]. The LPA protein family, on the other hand, showed only interactions with specific subunits of the photosystem II. For the LPA1 protein an explicit interaction with the D1 protein was observed [Peng et al., 2006] and LPA2 and LPA3 interacted specifically with CP43, ALB3 and with each other [Ma et al., 2007; Cai et al., 2010]. Based on the results of the interaction assays, an involvement of TerC in the assembly of PSII and/or the integration of PSII subunits into the thylakoid membrane is suggested.

As it was not possible to create a functional antibody against TerC due to its high hydrophobicity [<http://aramemnon.botanik.uni-koeln.de/>], WT_{TerC-GFP} and *terc-I*_{TerC-GFP}, both expressing the TerC-GFP fusion protein, were generated to perform immunological analyses of TerC-FDP. The *terc-I*_{TerC-GFP} plants showed a leaf variegated phenotype like the *amiR-TerC* plants, although they showed a two-fold expression of the *AtTerC-GFP* transcript compared to the *AtTerC* expression in wild type (**Figure 3.8**). To analyse the topology and functionality of the TerC-GFP fusion protein, thylakoids of *terc-I*_{TerC-GFP} plants were isolated and treated with different salt solutions. The TerC-GFP fusion protein behaved as an integral membrane protein in *terc-I*_{TerC-GFP} as it could not be washed off the membrane with neither chaotropic nor alcalic salts (**Figure 3.11**). The digestion of proteins in the thylakoid membrane of wild type, *terc-I*_{TerC-GFP} and WT_{TerC-GFP} with thermolysin, a metalloprotease that is not able to cross lipid bilayers, reveals that the C-terminus of TerC-GFP is facing the stroma side of the thylakoids because the GFP-tag was digested upon thermolysin treatment (**Figure 3.12**). Although the TerC-GFP fusion protein behaved as expected and it is able to complement the maximum quantum yield defect of PSII in *terc-I*, *terc-I*_{TerC-GFP} still showed

the leave variegated phenotype. This could be due to the GFP-tag fused to the C-terminus of TerC preventing the protein to fulfil its additional functions.

As the TerC-GFP fusion protein behaved as an integral membrane protein and the stable transformed *terc-I_{TerC-GFP}* plants complemented the defect of the photosystem II, these plants were used for Blue native PAGE and sucrose gradient fractionation to investigate the localisation of the TerC-GFP fusion protein in more details. The first dimension of the Blue native PAGE with thylakoids isolated from *terc-I_{TerC-GFP}* plants did not show any major differences compared to wild type. This indicates that in the green sectors of *terc-I_{TerC-GFP}* leaves, the composition of the photosynthetic complexes is similar to the one of the wild type. The immunodetection analyses conducted on second dimension gels revealed a co-localisation of TerC-GFP with all PSII assembly states, the PSII reaction center, the CP43-PSII, the PSII monomer and dimer and the PSII-supercomplexes. The most intense GFP signal was detected in the fraction of CP43-PSII and the monomeric form of PSII. The co-localisation of TerC with these complexes is a prerequisite for the proposed role of TerC in the assembly of CP43 into photosystem II.

In accordance with the observations from the native gel analyses, similar observations derived from sucrose gradient fractionation. The gradients loaded with solubilised thylakoids from wild type and *terc-I_{TerC-GFP}* plants did not differ after ultracentrifugation. The Coomassie staining of the 14 fractions showed the same distribution pattern and protein amounts in both wild type and *terc-I_{TerC-GFP}* plants. The immunodetection against CP43, D2, Lhcb2 and PsaB revealed no major difference in the distribution of those proteins in wild type and *terc-I_{TerC-GFP}*. The signal derived from the TerC-GFP fusion protein overlapped perfectly with the signal derived from CP43. This confirms a co-localisation of TerC-GFP with CP43. The distribution of D2 was slightly different compared to CP43, however D2 and TerC-GFP did not co-localise.

Based on these observations, one can conclude that TerC-GFP and CP43 are interacting and TerC-GFP might be necessary to integrate CP43 into the thylakoid membrane and photosystem II.

4.6 Integration of CP43 into the thylakoid membrane is impaired in *terc-1* and *amiR-TerC* plants

So far, the results show that the loss or reduction of the TerC protein leads to a severe defect in photosystem II which indicates a putative function of TerC in the assembly of PSII or the integration of its subunits into the thylakoid membrane. To further clarify an involvement of

TerC in these processes, Blue native PAGE analyses and second dimension SDS PAGE were performed with wild type and *amiR-TerC* plants. Under native conditions, an accumulation of the CP43-PSII complex (IV) in *amiR-TerC* could be observed, whereas all other protein complexes seemed to be slightly reduced in the knock-down mutant (**Figure 3.17 (A)**). This observation was never made before in mutants affected in PSII assembly [Pasch et al., 2005; Peng et al., 2006; Ma et al., 2007; Cai et al., 2010; Armbruster et al., 2010]. The specific accumulation of the CP43-PSII complex is another hint for a putative role of TerC in the integration of CP43 into photosystem II. To separate the single subunits of the different PSII assembly states [Rokka et al., 2005], the protein complexes were separated under denaturing conditions. The protein composition in wild type and *amiR-TerC* revealed some drastic differences between the two genotypes (**Figure 3.17 (B)**). The first difference between wild type and *amiR-TerC* was the reduced amount of unassembled CP43 protein in *amiR-TerC* (VI). The second major difference was the altered stoichiometries of the CP43-PSII complex (IV) and the monomeric PSII complex (III). In wild type, the D1, D2 and CP47 proteins revealed similar amounts in both complexes. The *amiR-TerC* lines showed a different distribution of these three proteins. For all three proteins the amount in the CP43-PSII complex (IV) was increased compared to the monomeric PSII complex (III). This indicates a block in the assembly of PSII in the step during which the CP43 protein is integrated into the CP43-PSII complex. This block led to an accumulation of this complex under steady state conditions in *amiR-TerC* plants.

A role of TerC in the assembly of CP43 into the PSII monomer is supported by the different amounts of the PSII core proteins detected in *amiR-TerC* plants (**Figure 3.16**). The assembly of PSII occurs in five steps. At first, a precomplex consisting of the D2 protein and the Cytochrome *b₅₅₉* complex appears in the thylakoid membrane. The precursor form of the D1 protein is then integrated into the precomplex forming the PSII reaction center. The next step is the integration of CP47 into the PSII reaction center representing the CP43-PSII complex, the first stable complex of PSII that can be detected via Blue native PAGE analysis. After processing of the D1 precursor and the integration of some low molecular weight subunits, the final PSII core protein, CP43, is incorporated resulting in the monomeric PSII complex [Rokka et al., 2005]. Regarding a block in the assembly of CP43, all previous complexes should accumulate under steady state conditions in *amiR-TerC* comparable to the accumulation of the CP43-PSII complex. Therefore, a “gradient” in the amount of the PSII core proteins following their assembly steps is proposed. Indeed, after quantification of the four PSII core proteins this “gradient” was determined (**Figure 3.16 (G)**). D2, the first core

protein which is present in PSII assembly was up-regulated to 125% compared to wild type. The next proteins that are integrated during PSII assembly are D1 and CP47 with 88% and 79% respectively, compared to wild type. The final of the four proteins that is assembled into the PSII is CP43. This protein showed the strongest reduction in *amiR-TerC* with only 45% protein amount compared to wild type.

Taken together the assembly of PSII is impaired in *amiR-TerC*. However, it has to be clarified whether TerC is needed for proper assembly of CP43 into the photosystem II and/or is involved in the integration of CP43 into the thylakoid membrane. To discriminate between these two possibilities, pulse/chase experiments with wild type, *terc-1* and *amiR-TerC* plants were performed. After [³⁵S]-methionine labelling of thylakoid proteins in wild type and *terc-1* plants, a dramatic decrease in newly synthesised proteins was observed in *terc-1* (**Figure 3.22**). Regarding the core proteins of PSII, only the precursor form of D1 and/or D2 could be identified in *terc-1*. The other proteins were missing completely as it was expected from the steady state protein measurement (**Figure 3.15**). The [³⁵S]-methionine labelling of thylakoid proteins in wild type and *amiR-TerC* plants did not show such a severe difference (**Figure 3.23 (A)**). Both samples were loaded according to 10 µg of chlorophyll, but almost all proteins, especially the D1 protein, were overexpressed in *amiR-TerC*. The only protein that was less abundant in *amiR-TerC* plants compared to wild type was the CP43 protein. To analyse, if the decrease of CP43 protein in *amiR-TerC* plants is due to an impaired integration of the protein into the thylakoids or due to stability problems, the 20 min pulse with radioactively labelled methionine was followed by one hour of chase with cold methionine (**Figure 3.23 (B)**). Again, after 20 min labelling a reduction in the amount of newly synthesised CP43 was observed in *amiR-TerC* compared to the wild type. But once CP43 was integrated into the thylakoid membranes, it was as stable in the mutant as it was in the wild type plants. This excludes the possibility, that TerC is involved in stabilising the PSII complex and proves that in *amiR-TerC* plants the integration of CP43 into the thylakoid membrane is disturbed.

To verify the suggested function of TerC in integrating CP43 into the thylakoid membrane and by this into the photosystem II, newly synthesised and radioactively labelled thylakoid proteins were isolated in their native complexes followed by a separation of the respective subunits according to their molecular weight (**Figure 3.24 (A)**). Again, like in the steady state (**Figure 3.17**), a strong reduction in the amount of unassembled CP43 protein (VI) in the *amiR-TerC* sample compared to the wild type was observed. Due to the reduced amount of unassembled protein, which general could be assembled into the high molecular protein

complexes, the amount of newly synthesised CP43 proteins was constantly less abundant in *amiR-TerC* complexes compared to the wild type complexes. The integration of CP43 into the PSII-supercomplexes was almost not detectable in *amiR-TerC* plants. The PsaA/B proteins of PSI and subunits of the ATPase were present in equal amounts in wild type and *amiR-TerC*. Only the amount of newly synthesised CP47 seemed to be reduced in *amiR-TerC* plants. The equal amounts of radioactively labelled D1/D2 protein in *amiR-TerC* and wild type plants most likely derived from the high turnover rate of D1 due to photodamage. In addition to the reduction of the CP43 and CP47 proteins, the formation of the dimeric Cytochrome *b₆f* complex seemed to be disturbed in *amiR-TerC*. The subunits of the monomeric Cytochrome *b₆f* complex were present in almost equal amounts in wild type and in *amiR-TerC* plants. While in wild type thylakoids most radioactively labelled proteins of these subunits could be detected in the dimeric Cytochrome *b₆f* complex, *amiR-TerC* thylakoids retained most of the radioactively labelled subunits of the Cytochrome *b₆f* complex in the monomeric form. After the pulse labelling step, leaves of *amiR-TerC* and wild type plants were incubated with cold methionine (**Figure 3.24 (B)**). Once proteins were synthesised in *amiR-TerC* plants, they were properly integrated into the thylakoid membrane and their stability was not affected. The integration of newly synthesised CP43 into the high molecular weight complexes was slowed down in *amiR-TerC* plants due to the reduction of unassembled CP43 protein.

4.7 Model for the function of TerC in *Arabidopsis thaliana*

From the results gained during this work, an important role of TerC during the integration of CP43 into the thylakoid membrane and into the photosystem II is proposed. As *terc-1* is albino and seedling lethal and the mutants are completely devoid of the four PSII core proteins D1, D2, CP43 and CP47, a function of TerC related to PSII assembly is proposed. This hypothesis is strengthened by the photosynthetic performance of *amiR-TerC* plants which shows a clear defect in photosystem II, but a functionally active photosystem I. Additionally, Blue native PAGE and second dimension gels of radioactively labelled and non labelled proteins reveal a reduction of unassembled CP43 protein and a block during the integration of this CP43 protein into the PSII monomer. The following model suggests a function of TerC during the integration of CP43 into the thylakoid membrane and its assembly into photosystem II. Additionally, the putative protein-protein interactions of TerC with other proteins localised in the thylakoid membrane are considered (**Figure 4.1**). The model suggests a two step mechanism. During the first step, TerC, LPA2 and LPA3 together with the ALB3 protein are integrating the unfolded form of the CP43 protein into the

thylakoid membrane. In a second step, the complex consisting of TerC, LPA2, LPA3 and CP43 joins the CP43-PSII complex and mediated by interaction of TerC with D1, D2, PsbH and the PSII assembly factors LPA1 and PAM68 the formation of the monomeric PSII complex is completed.

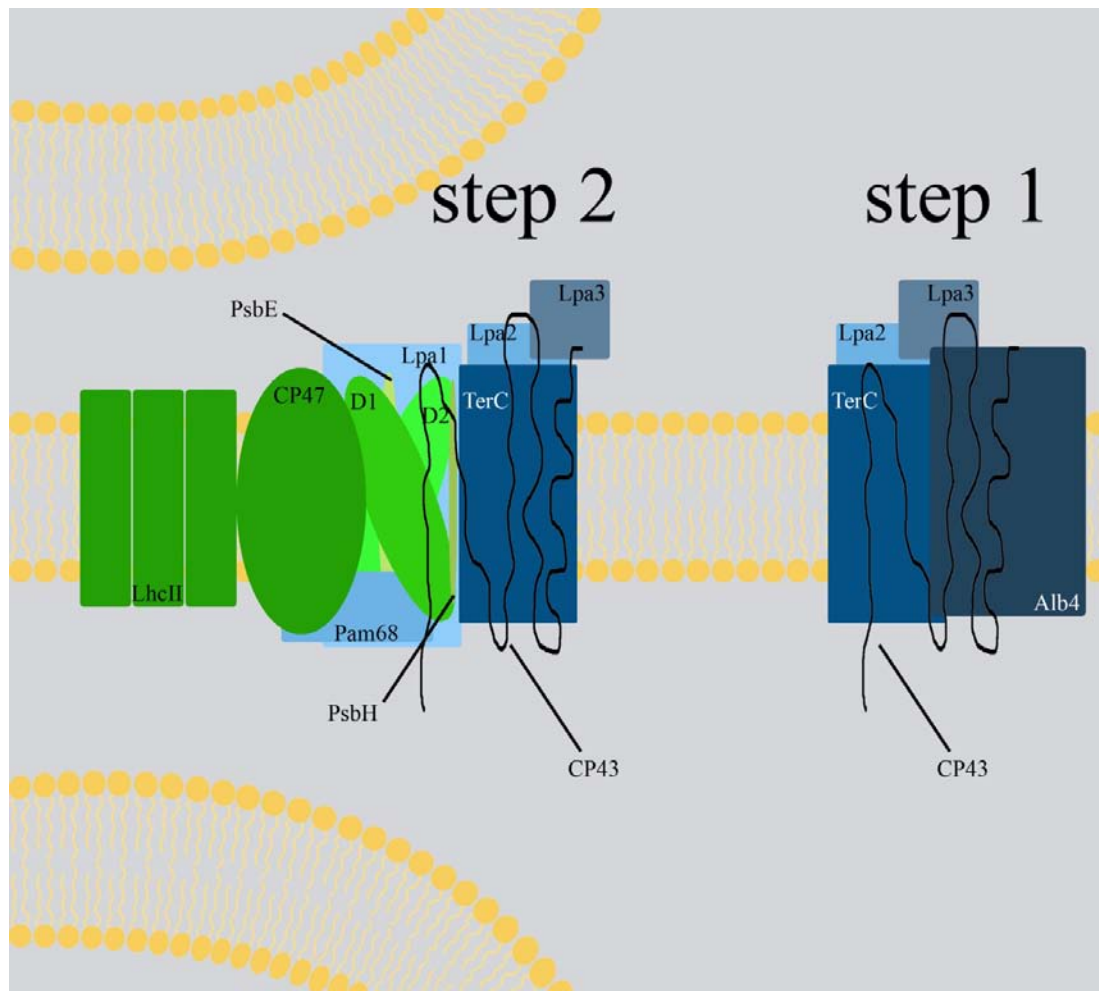


Figure 4.1: Model for TerC activity on the insertion of CP43 into the thylakoid membrane and the photosystem II

The TerC protein is supposed to act in a two step process of CP43 integration. In the first step the integration of CP43 into the thylakoid membrane occurs, followed by the integration of CP43 into the CP43-PSII complex. The photosynthetic proteins are displayed in green colour and the PSII assembly factors are indicated in blue.

Most probably, the insertion of CP43 into the thylakoid membrane occurs co-translationally, like the insertion of D1. For D1 it was shown that thylakoid bound ribosomes interact cpSecY, a subunit of a thylakoid translocation complex [Zhang et al., 2001]. Maybe TerC is the corresponding docking station for CP43 like cpSecY for D1.

Another function of TerC could be the formation of the dimeric Cytochrome *b₆/f* complex. Some preliminary results like the interaction of TerC with PetB were obtained during this study. However, more detailed analyses are needed to shed light on this aspect of TerC functionality.

Appendix 1

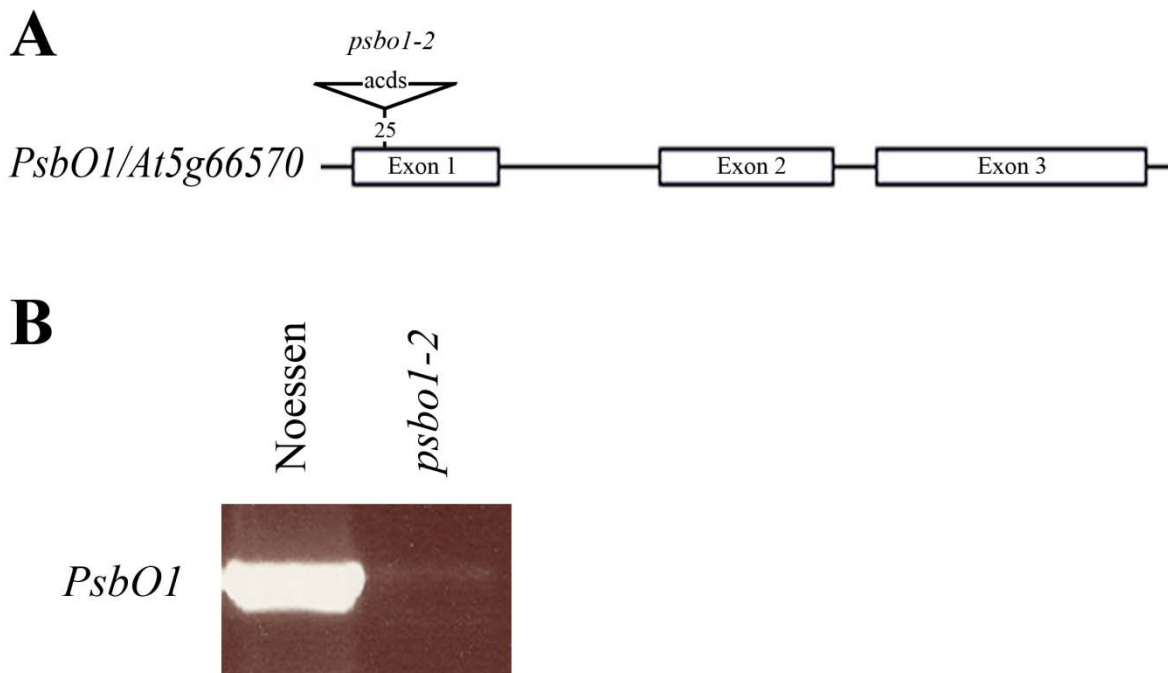


Figure Appendix 1: Identification of the mutant *psbo1-2*

The transposon mutant *psbo1-2* contains an *acds*-transposon at position 25 in the first exon of the gene. Exons are numbered and shown as white boxes. Introns, as well as 5' and 3' UTR, are shown as a black line. The *psbo1-2* allele was found in the Riken line RATM12-1816-1_G. The *acds*-transposon insertion is not drawn in scale (A). The *acds*-transposon insertion effects the steady state level of *PsbO1* RNA. In total 2 µg of RNA of both, Noessen and *psbo1-2*, was isolated and transcribed into cDNA. PCR with cDNA specific primers (Table Appendix 2) was performed and a strong decrease in the *PsbO1* transcript was observed. But the *acds*-transposon insertion did not lead to a complete knock out of the gene *At5g66570*.

Appendix 2

Table Appendix 1: List of all primers used for screening for *psbo1-2* plants and RT-PCR to determine the transcript level of *PsbO1* in these mutants

name of primer	sequence 5' - 3'
At5g66570-F	tgttgtgaagatcaattggaca
At5g66570-R	tgaatcgaagattacagaattgga
RATM-Ds5-2a	tccgttccgttttcgtttttac
PsbO1-cDNA-F	AAGTTCTCACCTCCGATCGAC
PsbO1-cDNA-R	CAGTGTTCTTCACGTTCTCCT

References**A**

Abdelnoor R.V., Yule R., Elo A., Christensen A.C., Meyer-Gauen G. and Mackenzie S.A. (2003). Substoichiometric shifting in the plant mitochondrial genome is influenced by a gene homologous to muts. *Proceedings of the National Academy of Sciences of the USA* **100**, 5968–5973

Allen J. (2002). Photosynthesis of ATP-electrons, proton pumps, rotors, and poise. *Cell* **110**, 273-276.

Alonso J.M., Stepanova A.N., Leisse T.J., Kim C.J., Chen H., Shinn P., Stevenson D.K., Zimmerman J., Barajas P., Cheuk R., Gadrinab C., Heller C., Jeske A., Koesema E., Meyers C.C., Parker H., Prednis L., Ansari Y., Choy N., Deen H., Geralt M., Hazari N., Hom E., Karnes M., Mulholland C., Ndubaku R., Schmidt I., Guzman P., Aguilar-Henonin L., Schmid M., Weigel D., Carter D.E., Marchand T., Risseuw E., Brogden D., Zeko A., Crosby W.L. Berry, C.C. and Ecker J.R. (2003). Genome-wide insertional mutagenesis of *Arabidopsis thaliana*. *Science* **301**, 653-657

Aluru M.R., Stessman D.J., Spalding M.H. and Rodermel S.R. (2007). Alterations in photosynthesis in *Arabidopsis* lacking IMMUTANS, a chloroplast terminal oxidase. *Photosynth Res* **91**, 11–23

Andrès C., Agne B. and Kessler F. (2010). The TOC complex: Preprotein gateway to the chloroplast. *Biochimica et Biophysica Acta* **1803**, 715–723

Armbruster U., Hertle A., Makarenko E., Zühlke J., Pribil M., Dietzmann A., Schliebner I., Aseeva E., Fenino E., Scharfenberg M., Voigt C. and Leister D. (2009). Chloroplast Proteins without Cleavable Transit Peptides: Rare Exceptions or a Major Constituent of the Chloroplast Proteome? *Molecular Plant* **2**, 1325–1335

Armbruster U., Zühlke J., Rengstl B., Kreller R., Makarenko E., Rühle T., Schünemann D., Jahns P., Weisshaar B., Nickelsen J. and Leister D. (2010). The *Arabidopsis* thylakoid

protein PAM68 is required for efficient D1 biogenesis and photosystem II assembly. *Plant Cell* **22**, 3439-60

Aronsson H. and Jarvis P. (2002). A simple method for isolating import-competent *Arabidopsis* chloroplasts. *FEBS Lett* **529**, 215-220

Aronsson H., Boij P., Patel R., Wardle A., Topel M. and Jarvis P. (2007). Toc64/OEP64 is not essential for the efficient import of proteins into chloroplasts in *Arabidopsis thaliana*. *Plant J.* **52**, 53–68.

B

Baldwin A.J. and Inoue K. (2006). The most C-terminal tri-glycine segment within the polyglycine stretch of the pea Toc75 transit peptide plays a critical role for targeting the protein to the chloroplast outer envelope membrane. *FEBS J.* **273**, 1547–1555

Bailey S., Thompson E., Nixon P.J., Horton P., Mullineaux C.W., Robinson C. and Mann N.H. (2002). A critical role for the Var2 FtsH homologue of *Arabidopsis thaliana* in the photosystem II repair cycle *in vivo*. *Journal of Biological Chemistry* **277**, 2006–2011

Barber J., Nield J., Morris E.P., Zheleva D. and Hankamer B. (1997). The structure, function and dynamics of photosystem II. *Plant Physiol.* **100**, 817–827

Becker T., Jelic M., Vojta A., Radunz A., Soll J. and Schleiff E. (2004a). Preprotein recognition by the Toc complex. *Embo J* **23**, 520–30

Becker T., Hritz J., Vogel M., Caliebe A., Bukau B., Soll J. and Schleiff E. (2004b). Toc12, a novel subunit of the intermembrane space preprotein translocon of chloroplasts. *Mol. Biol. Cell* **15**, 5130–5144.

Bekker A., Holland H.D., Wang P.L., Rumble D. 3rd, Stein H.J., Hannah J.L., Coetzee L.L., Beukes N.J. (2004). Dating the rise of atmospheric oxygen. *Nature* **427**, 117-120

Bellafiore S., Ferris P., Naver H., Göhre V. and Rochaix J.D. (2002). Loss of Albino3 leads to the specific depletion of the light-harvesting system. *Plant Cell* **14**, 2303-14.

Berghöfer J. and Klösgen R.B. (1996). Isolation and characterization of a cDNA encoding the SecY protein from spinach chloroplasts. *Plant Physiol* **112**, 863

Berghöfer J., Karnauchov I., Herrmann R.G. and Klösgen R.B. (1995). Isolation and characterization of a cDNA encoding the SecA protein from spinach chloroplasts: evidence for azide-resistance of Sec-dependent protein translocation across thylakoid membranes of spinach. *J Biol Chem* **270**, 18341–6

Biesiadka J., Loll B., Kern J., Irrgang K.D. and Zouni A. (2004). Crystal structure of cyanobacterial photosystem II at 3.2 ° Å resolution: a closer look at the Mn-cluster. *Phys. Chem. Chem. Phys.* **6**, 4733–36

Boij P., Patel R., Garcia C., Jarvis P. and Aronsson H. (2009). In vivo studies on the roles of Tic55-related proteins in chloroplast protein import in *Arabidopsis thaliana*. *Molecular Plant* **2**, 1397–1409

Braun N.A., Davis A.W. and Theg S.M. (2007). The chloroplast Tat pathway utilizes the transmembrane electric potential as an energy source. *Biophys. J.* **93**, 1993–1998

Burian J., Tu N., Klucar L., Guller L., Lloyd-Jones G., Stuchlik S., Fejdi P., Siekel P. and Turna J. (2000). In vivo and in vitro cloning and phenotype characterization of tellurite resistance determinant conferred by plasmid pTE53 of a clinical isolate of *Escherichia coli*. *Folia Microbiol* **13**

C

Cai W., Ma J., Chi W., Zou M., Guo J., Lu C. and Zhang L. (2010). Cooperation of LPA3 and LPA2 Is Essential for Photosystem II Assembly in *Arabidopsis*. *Plant Physiology* **154**, 109-120

Caliebe A., Grimm R., Kaiser G., Lübeck J., Soll J. and Heins L. (1997). The chloroplastic protein import machinery contains a Rieske-type iron–sulfur cluster and a mononuclear iron-binding protein. *EMBO J* **16**, 7342–50

Campbell, N.A. (1997). *Biologie*. Heidelberg; Berlin; Oxford: Spektrum Akademischer Verlag GmbH

Chaddock A.M., Mant A., Karnauchov I., Brink S., Herrmann R.G. and Klösgen R.B., et al. (1995). A new type of signal peptide: central role of a twin-arginine motif in transfer signals for the DpH-dependent thylakoidal protein translocase. *EMBO J* **14**, 2715–22

Chigri F., Hörmann F., Stamp A., Stammers D.K., Bölder B., Soll J. and Vothknecht U.C. (2006). Calcium regulation of chloroplast protein translocation is mediated by calmodulin binding to Tic32. *Proc. Natl. Acad. Sci. U. S. A.* **103**, 16051–16056

Chiu C.C. and Li H. (2008). Tic40 is important for reinsertion of proteins from the chloroplast stroma into the inner membrane. *Plant J.* **56**, 793–801

Chou M.L., Fitzpatrick L.M., Tu S.L., Budziszewski G., Potter-Lewis S., Akita M., et al. (2003). Tic40, a membrane-anchored co-chaperone homolog in the chloroplast protein translocon. *EMBO J* **22**, 2970–80

Cline K., Ettinger W.F. and Theg S.M. (1992). Protein-specific energy requirements for protein transport across or into thylakoid membranes. Two luminal proteins are transported in the absence of ATP. *J Biol Chem* **267**, 2688–96

Clough S.J. and Bent A.F. (1998). Floral dip: a simplified method for *Agrobacterium*-mediated transformation of *Arabidopsis thaliana*. *Plant J* **16**, 735-743

D

DalCorso G., Pesaresi P., Masiero S., Aseeva E., Schünemann D., Finazzi G., Joliot P., Barbato R. and Leister D. (2008). A complex containing PGRL1 and PGR5 is involved in the switch between linear and cyclic electron flow in *Arabidopsis*. *Cell* **132**, 273-285.

Di Cola A., Klostermann E. and Robinson C. (2005). The complexity of pathways for protein import into thylakoids: it's not easy being green. *Biochemical Society Transactions* **33**, 1024–1027

E

Eberhard S., Finazzi G. and Wollman F.A. (2008). The dynamics of photosynthesis. *Annu Rev Genet* **42**, 463-515

Estévez J.M., Cantero A., Reindl A., Reichler S. and León P. (2001). 1-deoxy-d-xylulose 5-phosphate synthase, a limiting enzyme for plastidic isoprenoid biosynthesis in plants. *Journal of Biological Chemistry* **276**, 22901–22909

F

Ferreira K.N., Iverson T.M., Maghlaoui K., Barber J. and Iwata S. (2004). Architecture of the photosynthetic oxygen-evolving center. *Science* **303**, 1831–1838

Finazzi G., Chasen C., Wollman F.A. and de Vitry C. (2003). Thylakoid targeting of Tat passenger proteins shows no DpH dependence in vivo. *EMBO J* **22**, 807–15

Franklin A.E. and Hoffman N.E. (1993). Characterization of a chloroplast homologue of the 54-kDa subunit of the signal recognition particle. *J Biol Chem* **268**, 22175–80.

G

Gerdes L., Bals T., Klostermann E., Karl M., Philippar K., Hünken M., Soll J. and Schünemann D. (2006). A Second Thylakoid Membrane-localized Alb3/OxaI/YidC Homologue Is Involved in Proper Chloroplast Biogenesis in *Arabidopsis thaliana*. *The Journal of Biological Chemistry* **281**, 16632–16642

Gutensohn M., Enguo Fan E., Frielingsdorf S., Peter Hanner, Hou B., Hust B. and Klösigen R.B. (2006). Toc, Tic, Tat et al.: structure and function of protein transport machineries in chloroplasts. *Journal of Plant Physiology* **163**, 333-347

van der Graaff E., Hooykaas P., Lein W., Lerchl J., Kunze G., Sonnewald U. and Boldt R. (2004). Molecular analysis of 'de novo' purine biosynthesis in solanaceous species and in *Arabidopsis thaliana*. *Frontiers in Bioscience* **9**, 1803–1816

H

Hirsch S., Muckel E., Heemeyer F., von Heijne G. and Soll J. (1994). A receptor component of the chloroplast protein translocation machinery. *Science* **266**, 1989–92

Hörmann F., Kückler M., Sveshnikov D., Oppermann U., Li Y. and Soll J. (2004). Tic32, an essential component in chloroplast biogenesis. *J Biol Chem* **279**, 34756–62

Hulford A., Hazell L., Mould R.M. and Robinson C. (1994). Two distinct mechanisms for the translocation of proteins across the thylakoid membrane, one requiring the presence of a stromal protein factor and nucleotide triphosphates. *J Biol Chem* **269**, 3251–6

I

Ihnatowicz A., Pesaresi P., Varotto C., Richly E., Schneider A., Jahn P. Salamini F. and Leister D. (2004). Mutants for photosystem I subunit D of *Arabidopsis thaliana*: effects on photosynthesis, photosystem I stability and expression of nuclear genes for chloroplast function. *The plant journal* **37**, 839-852

Ihnatowicz A., Pesaresi P., Lohrig K., Wolters D., Müller B. and Leister D. (2008). Impaired photosystem I oxidation induces STN7-dependent phosphorylation of the light-harvesting complex I protein Lhca4 in *Arabidopsis thaliana*. *Planta* **227**, 717–722

Ilik P., Schansker G., Kotabova E., Vaczi P., Strasser R.J. and Bartak M. (2006). A dip in the chlorophyll fluorescence induction at 0.2–2 s in *Trebouxia*-possesing lichens reflects a

fast reoxidation of photosystem I. A comparison with higher plants. *Biochim. Biophys. Acta* **1757**, 12–20

J

Jakob M., Kaiser S., Gutensohn M., Hanner P. and Klösgen R.B. (2009). Tat subunit stoichiometry in *Arabidopsis thaliana* challenges the proposed function of TatA as the translocation pore. *Biochimica et Biophysica Acta* **1793**, 388.394

Jaru-Ampornpan P., Chandrasekar S. and Shan S. (2007). Efficient interaction between two GTPases allows the chloroplast SRP pathway to bypass the requirement for an SRP RNA. *Mol. Biol. Cell* **18**, 2636–2645

Jarvis, P. and Soll, J. (2002). Toc, Tic, and chloroplast protein import. *Biochim. Biophys. Acta* **1590**, 177–189

Jelic M., Soll J. and Schleiff E. (2003). Two Toc34 homologues with different properties, *Biochemistry* **42**, 5906–5916.

K

Karimi M., Inze D. and Depicker A. (2002). GATEWAY vectors for *Agrobacterium*-mediated plant transformation. *Trends in Plant Science* **7**, 193–195

Karnauchov I., Cai D., Schmidt I., Herrmann R.G. and Klösgen R.B. (1994). The thylakoid translocation of subunit 3 of photosystem I, the *psaF* gene product, depends on a bipartite transit peptide and proceeds along an azide-sensitive pathway. *J Biol Chem* **269**, 32871–8

Karnauchov I., Herrmann R.G. and Klösgen R.B. (1997). Transmembrane topology of the Rieske Fe/S protein of the Cytochrome *b6/f* complex from spinach chloroplasts. *FEBS Lett.* **408**, 206–210

- Kessler F. and Blobel G.** (1996). Interaction of the protein import and folding machineries in the chloroplast. *Proc Natl Acad Sci USA* **93**, 7684–9
- Kessler F., Blobel G., Patel H.A. and Schnell D.J.** (1994). Identification of two GTP-binding proteins in the chloroplast protein import machinery. *Science* **266**, 1035–9
- Kim S.J., Robinson C. and Mant A.** (1998). Sec/SRP-independent insertion of two thylakoid membrane proteins bearing cleavable signal peptides. *FEBS Lett* **424**, 105–8
- Kirk J.T.O. & Tilney-Bassett R.A.E.** (1978). *The Plastids*. 2nd edn. Elsevier/North-Holland, Amsterdam, the Netherlands.
- Kleffmann T., Russenberger D., von Zychlinski A., Christopher W., Sjölander K., Gruissem W. and Baginsky S.** (2004). The *Arabidopsis thaliana* Chloroplast Proteome Reveals Pathway Abundance and Novel Protein Functions. *Current Biology* **14**, 354-362
- Klöggen R.B., Brock I.A., Herrmann R.G. and Robinson C.** (1992). Proton gradient-driven import of the 16 kDa oxygen-evolving complex protein as the full precursor protein by isolated thylakoids. *Plant Mol Biol* **18**, 1031–4
- Klughammer C. and Schreiber U.** (1994). An improved method, using saturating light pulses, for the determination of photosystem I quantum yield via P_{700}^+ absorbance changes at 830 nm. *Planta* **192**, 261-268
- König A.** (2005). Analyse einer Albino-Mutante mit einem Defekt in einem chloroplastidären Membranprotein in *Arabidopsis thaliana*. Diplomarbeit am Botanischen Institut der Universität zu Köln
- Komenda J., Reisinger V., Muller B.C., Dobakova M., Granvogl B. and Eichacker L.A.** (2004). Accumulation of the D2 protein is a key regulatory step for assembly of the photosystem II reaction center complex in *Synechocystis* PCC 6803. *Journal of Biological Chemistry* **279**, 48620–48629

- Komenda J., Nickelsen J., Tichy M., Prasil O., Eichacker L.A. and Nixon P.J.** (2008). The cyanobacterial homologue of HCF136/YCF48 is a component of an early photosystem II assembly complex and is important for both the efficient assembly and repair of photosystem II in *Synechocystis* sp PCC 6803. *Journal of Biological Chemistry* **283**, 22390–22399
- Kouranov A. and Schnell D.J.** (1997). Analysis of the interactions of preproteins with the import machinery over the course of protein import into chloroplasts. *J Cell Biol* **139**, 1677–85
- Kouranov A., Chen X., Fuks B. and Schnell D.J.** (1998). Tic20 and Tic22 are new components of the protein import apparatus at the chloroplast inner envelope membrane. *J Cell Biol* **143**, 991–1002
- Küchler M., Decker S., Hörmann F., Soll J. and Heins L.** (2002). Protein import into chloroplasts involves redox-regulated proteins. *EMBO J* **21**, 6136–45
- Kwon K.C. and Cho M.H.** (2008). Deletion of the chloroplast-localized *AtTerC* gene product in *Arabidopsis thaliana* leads to loss of the thylakoid membrane and to seedling lethality. *The Plant Journal* **55**, 428–442
- Kyhse-Anderson, J.** (1984). Electrophoretic transfer of multiple gels: A simple apparatus without buffer tank for rapid transfer of proteins from polyacrylamide gels to nitrocellulose membranes. *Biophys. Biochem. Methodol.* **10**, 203-209

L

- Laidler V., Chaddock A.M., Knott T.G., Walker D. and Robinson C.** (1995). A SecY homolog in *Arabidopsis thaliana*. *J Biol Chem* **270**, 17664–7
- Leister, D.** (2003). Chloroplast research in the genomic age. *Trends Genet.* **19**, 47–56
- Li X., Henry R., Yuan J., Cline K. and Hoffman N.E. (1995). A chloroplast homologue of the signal recognition particle subunit SRP54 is involved in the posttranslational integration of a protein into thylakoid membranes. *Proc Natl Acad Sci USA*;92, 3789–93

- Lima A., Lima S., Wong J.H., Phillips R.S., Buchanan B.B. and Luan S.** (2006). A redox-active FKBP-type immunophilin functions in accumulation of the photosystem II supercomplex in *Arabidopsis thaliana*. PNAS **103**, 12631-12636
- Lindahl M. and Kieselbach T.** (2009). Disulphide proteomes and interactions with thioredoxin on the track towards understanding redox regulation in chloroplasts and cyanobacteria. J. Proteomics **72**, 416-438
- Liu D., Gong Q., Ma Y., Li P., Li P., Yang S., Yuan L., Yu Y., Pan D., Xu F. and Wang N.N.** (2010). cpSecA, a thylakoid protein translocase subunit, is essential for photosynthetic development in *Arabidopsis*. Journal of Experimental Botany **61**, 1655-1669
- Lodish, H., Berk, A., Zipursky, S.L., Matsudaira, P., Baltimore, D., and Darnell, J.E.** (2000). Molecular cell biology, S. Tenney, ed New York: W.H. Freeman and Company
- Lorkovic Z.J., Schroder W.P., Pakrasi H.B., Irrgang K.D., Herrmann R.G. and Oelmüller R.** (1995). Molecular characterization of PsbW, a nuclear-encoded component of the photosystem II reaction center complex in spinach. Proc Natl Acad Sci USA **92**, 8930-4
- Lübeck J., Soll J., Akita M., Nielsen E. and Keegstra K.** (1996). Topology of IEP110, a component of the chloroplastic protein import machinery present in the inner envelope membrane. EMBO J **15**, 4230-8

M

- Ma J., Peng L., Guo J., Lu Q., Lu C. and Zhang L.** (2007). LPA2 Is Required for Efficient Assembly of Photosystem II in *Arabidopsis thaliana*. The Plant Cell **19**, 1980-1993
- Mallory A.C., Reinhart B.J., Jones-Rhoades M.W., Tang G., Zamore P.D., Barton M.K. and Bartell D.P.** (2004). MicroRNA control of PHABULOSA in leaf development: importance of pairing to the microRNA 5' region. The EMBO Journal **23**, 3356-3364
- Martin K., Hart C., Liu J., Leung W.Y. and Patton W.F.** (2003). Simultaneous trichromatic fluorescence detection of proteins on Western blots using an amine-reactive dye

in combination with alkaline phosphatase- and horseradish peroxidase-antibody conjugates. *Proteomics* **3**, 1215–1227

Marques J.P., Schattat M.H., Hause G., Dudeck I. and Klösgen R.B. (2004). In vivo transport of folded EGFP by the DpH/TAT-dependent pathway in chloroplasts of *Arabidopsis thaliana*. *J Exp Bot* **55**, 1697–706

Maxwell K. and Johnson G.N. (2000). Chlorophyll fluorescence-a practical guide. *J Exp Bot* **51**, 659-668

Meurer J., Plücker H., Kowallik K.V. and Westhoff P. (1998). A nuclear-encoded protein of prokaryotic origin is essential for the stability of photosystem II in *Arabidopsis thaliana*. *EMBO J.* **17**, 5286–5297

Meurer J., Grevelding C., Westhoff P. and Reiss B. (1998). The PAC protein affects the maturation of specific chloroplast mRNAs in *Arabidopsis thaliana*. *Molecular & General Genetics* **258**, 342–351

Michl D., Robinson C., Shackleton J.B., Herrmann R.G. and Klösgen R.B. (1994). Targeting of proteins to the thylakoids by bipartite presequences: CFoII is imported by a novel, third pathway. *EMBO J* **13**, 1310–7

Michl D., Karnauchov I., Berghöfer J., Herrmann R.G. and Klösgen R.B. (1999). Phylogenetic transfer of organelle genes to the nucleus can lead to new mechanisms of protein integration into membranes. *Plant J* **17**, 31–40

Molik S., Karnauchov I., Weidlich C., Herrmann R.G. and Klösgen R.B. (2001). The Rieske Fe/S protein of the Cytochrome *b₆/f* complex: missing link in the evolution of protein transport pathways in chloroplasts? *J Biol Chem* **276**, 42761–6

Moore R., Clark W.D., Vodopich D.S. (1998). *Botany*, 2nd edn. Boston, MA: WCB/McGraw-Hill

Mori H. and Cline K. (2002). A twin arginine signal peptide and the pH gradient trigger reversible assembly of the thylakoid DpH/Tat translocase. *J Cell Biol* **157**, 205–10

Motohashi R., Nagata N., Ito T., Takahashi S., Hobo T., Yoshida S. and Shinozaki K. (2001). An essential role of a TatC homologue of a Delta pH-dependent protein transporter in thylakoid membrane formation during chloroplast development in *Arabidopsis thaliana*. *Proc Natl Acad Sci USA* **98**, 10499–504

Mould R.M., Shackleton J.B. and Robinson C. (1991). Transport of proteins into chloroplasts. Requirements for the efficient import of two luminal oxygen-evolving complex proteins into isolated thylakoids. *J Biol Chem* **266**, 17286–9

Munekage Y., Hojo M., Meurer J., Endo T., Tasaka M. and Shikanai T. (2002). PGR5 is involved in cyclic electron flow around photosystem I and is essential for photoprotection in *Arabidopsis*. *Cell* **110**, 361-371

Murakami R., Ifuku K., Takabayashi A., Shikanai T., Endo T. and Sato F. (2005). Functional dissection of two *Arabidopsis* PsbO proteins: PsbO1 and PsbO2. *FEBS J.* **272**, 2165-75

N

Næsted H., Holm A., Jenkins T., Nielsen H.B., Harris C.A., Beale M.H., Andersen M., Mant A., Scheller H., Camara B., Mattsson O. and Mundy J. (2004). *Arabidopsis* VARIEGATED 3 encodes a chloroplasttargeted, zinc-finger protein required for chloroplast and palisade cell development. *Journal of Cell Science* **117**, 4807-4818

Nakagawa T., Kurose T., Hino T., Tanaka K., Kawamukai M., Niwa Y., Toyooka K., Matsuoka K., Jinbo T. and Kimura T. (2007). Development of Series of Gateway Binary Vectors, pGWBs, for Realizing Efficient Construction of Fusion Genes for Plant Transformation. *Journal of Bioscience and Bioengineering* **104**, 34–41

Nelson N. and Yocum C.F. (2006). Structure and function of photosystems I and II. *Annu. Rev. Plant Biol.* **57**, 521–565

O

Ossenbühl, F., Göhre, V., Meurer, J., Krieger-Liszkay, A., Rochaix, J.D. and Eichacker, L.A. (2004). Efficient Assembly of Photosystem II in *Chlamydomonas reinhardtii* Requires Alb3.1p, a Homolog of Arabidopsis ALBINO3. *Plant Cell* **16**, 1790-1800

Ouyang M., Li X., Ma J., Chi W., Xiao J., Zou M., Chen F., Lu C. and Zhang L. (2011). LTD is a protein required for sorting light-harvesting chlorophyll-binding proteins to the chloroplast SRP pathway. *Nature Communications* **2**, 277

P

Pasch J. C., Nickelsen J. and Schünemann D. (2005). The yeast split-ubiquitin system to study chloroplast membrane protein interactions. *Appl Microbiol Biot* **69**, 440-447

Peng L., Ma J., Chi W., Guo J., Zhu S., Lu Q., Lu C. and Zhang L. (2006). LOW PSII ACCUMULATION1 is involved in efficient assembly of photosystem II in *Arabidopsis thaliana*. *Plant Cell* **18**, 955–969

Pesaresi P., Hertle A., Pribil M., Kleine T., Wagner R., Strissel H., Ihnatowicz A., Bonardi V., Scharfenberg M., Schneider A., Pfannschmidt T. and Leister D. (2009). Balancing of excitation energy distribution between photosystems: functional relationship of state transitions to long-term photosynthetic acclimation. *Plant Cell* **21**, 2402-2423

Pfaffl M.W. (2001). A new mathematical model for relative quantification in real-time RT-PCR. *Nucleic Acids Research* **29**, e45

R

Richter S. and Lamppa G.K. (1998). A chloroplast processing enzyme functions as the general stromal processing peptidase. *Proc Natl Acad Sci USA* **95**, 7463–8

Robinson C., Cai D., Hulford A., Brock I.A., Michl D., Hazell L., et al. (1994). The presequence of a chimeric construct dictates which of two mechanisms are utilised for translocation across the thylakoid membrane: evidence for the existence of two distinct translocation systems. *EMBO J* **13**, 279–85

Röbbelen G. (1968). Genbedingte Rotlicht-Empfindlichkeit der Chloroplastendifferenzierung bei *Arabidopsis*. *Planta* **80**, 237–254

Rokka A., Suorsa m., Saleem A., Battchikova N. and Aro E.M. (2005). Synthesis and assembly of thylakoid protein complexes: multiple assembly steps of photosystem II. *Biochem. J.* **388**, 159–168

Rosenbaum-Hofmann N. and Theg S.M. (2005). Toc64 is not required for import of proteins into chloroplasts in the moss *Physcomitrella patens*. *Plant J* **43**, 675–87

S

Sambrook J., Fritsch E.F. and Maniatis T. (1989). *Molecular cloning*. New York: Cold Spring Harbor Laboratory Press

Schägger H. and von Jagow G. (1987). Tricine-sodium dodecyl sulfatepolyacrylamide gel electrophoresis for the separation of proteins in the range from 1 to 100 kDa. *Anal Biochem* **166**, 368-379

Schleiff E. and Klösgen R.B. (2001). Without a little help of “my” friends – direct insertion of proteins into chloroplast membranes? *Biochem Biophys Acta* **1541**, 22–33.

Schleiff E., Soll J., Sveshnikova N., Tien R., Wright S., Dabney-Smith C., et al. (2002). Structural and guanosine triphosphate/diphosphate requirements for transit peptide recognition by the cytosolic domain of the chloroplast outer envelope receptor, Toc34. *Biochemistry* **41**, 1934–46

- Schuenemann D., Amin P., Hartmann E. and Hoffman N.E. Chloroplast** (1999). SecY is complexed to SecE and involved in the translocation of the 33-kDa but not the 23-kDa subunit of the oxygen-evolving complex. *J Biol Chem* **274**, 12177–82
- Schünemann D.** (2007). Mechanisms of protein import into thylakoids of chloroplasts. *Biol. Chem.* **388**, 907-15
- Settles A.M., Yonetani A., Baron A., Bush D.R., Cline K. and Martienssen R.** (1997). Sec-independent protein translocation by the maize Hcf106 protein. *Science* **278**, 1467–70
- Shikanai T.** (2007). Cyclic electron transport around photosystem I: genetic approaches. *Annu Rev Plant Biol* **58**, 199-217
- Shoichi I.** (2010). Life Science web textbook, edited by CSLS/The University of Tokyo
- Sirpiö S., Khrouchtchova A., Allahverdiyeva Y., Hansson M., Fristedt R., Vener A.V., Scheller H.V., Jensen P.E., Haldrup A. and Aro E.M.** (2008). AtCYP38 ensures early biogenesis, correct assembly and sustenance of photosystem II. *Plant J.* **55**, 639-651
- Sohrt K. and Soll J.** (2000). Toc64, a new component of the protein translocon of chloroplasts. *J Cell Biol* **148**, 1213–21
- Stahl T., Glockmann C., Soll J. and Heins L.** (1999). Tic40, a new “old” subunit of the chloroplast protein import translocon. *J Biol Chem* **274**, 37467–72
- Stengel A., Benz P., Balsera M., Soll J. and Bölder B.** (2008). TIC62 redox-regulated translocon composition and dynamics. *J. Biol. Chem.* **283**, 6656–6667
- Strissel H.** (2007). Untersuchung einer Albino-Mutante von *Arabidopsis thaliana* mit einem „knock out“ eines chloroplastidären Proteins und Photosynthetische Messungen an der Mutante *psal* mittels Puls-Amplituden-Modulations (PAM)-Fluorometrie. Diplomarbeit am Botanischen Institut der Ludwig Maximilians Universität München
- Sveshnikova N., Grimm R., Soll J. and Schleiff E.** (2000). Topology studies of the chloroplast protein import channel Toc75. *Biol Chem* **381**, 687–93

Swiatek M., Kuras R., Sokolenko A., Higgs D., Olive J., Cinque G., Müller B., Eichacker L.A., Stern D.B. and Bassi R. et al. (2001). The chloroplast gene *ycf9* encodes a photosystem II (PSII) core subunit, PsbZ, that participates in PSII supramolecular architecture. *Plant Cell* **13**, 1347–1367

T

Thidholm E., Lindström V., Tissier C., Robinson C., Schröder W. P. and Funk C. (2002). Novel approach reveals localisation and assembly pathway of the PsbS and PsbW proteins into the photosystem II dimer. *FEBS Lett.* **513**, 217–222

Thompson S.J., Robinson C. and Mant A. (1999). Dual signal peptides mediate the signal recognition particle/Sec-independent insertion of a thylakoid membrane polyprotein, PsbY. *J Biol Chem* **274**, 4059–66.

Tsiotis G., Psylinakis M., Woplensinger B., Lustig A., Engel A. and Ghanotakis D. (1999). Investigation of the structure of spinach photosystem II reaction center complex. *Eur. J. Biochem.* **259**, 320–324

Tsien R.Y. (1998). The green fluorescent protein. *Annu. Rev. Biochem.* **67**, 509–44

V

van Dooren G.G., Tomova C., Agrawal S., Humbel B.M. and Striepen B. (2008). *Toxoplasma gondii* Tic20 is essential for apicoplast protein import. *Proc. Natl. Acad. Sci. U. S. A.* **105**, 13574–13579

Vojta L., Soll J. and Bölter B. (2007). Requirements for a conservative protein translocation pathway in chloroplasts. *FEBS Lett.* **581**, 2621–2624

W

Waegemann K. and Soll J. (1991). Characterization of the protein import apparatus in isolated outer envelopes of chloroplasts. *Plant J* **1**, 149–58

Walker M.B., Roy L.M., Coleman E., Voelker R. and Barkan A. (1999). The maize *tha4* gene functions in sec-independent protein transport in chloroplasts and is related to *hcf106*, *tatA*, and *tatB*. *J Cell Biol* **147**, 267–76

Wang Q., Sullivan R.W., Kight A., Henry R.L., Huang J., Jones A.M. and Korth K.L. (2004). Deletion of the chloroplast-localized *Thylakoid Formation1* gene product in *Arabidopsis* leads to deficient thylakoid formation and variegated leaves. *Plant Physiology* **136**, 3594–3604

Y

Yamamoto Y.Y., Puente P. and Deng X.-W. (2000). An *Arabidopsis* cotyledon-specific albino locus: a possible role in 16S rRNA maturation. *Plant & Cell Physiology* **41**, 68–76

Yu F., Fu A., Aluru M., Park S., Xu Y., Liu H., Liu X., Foudree A., Nambogga M. and Rodermel S. (2007). Variegation mutants and mechanisms of chloroplast biogenesis. *Plant, Cell and Environment* **30**, 350–365

Yuan J. and Cline K. (1994). Plastocyanin and the 33-kDa subunit of the oxygen-evolving complex are transported into thylakoids with similar requirements as predicted from pathway specificity. *J Biol Chem* **269**, 18463–7

Yuan J., Henry R., McCaffery M. and Cline K. (1994). SecA homolog in protein transport within chloroplasts: evidence for endosymbiont-derived sorting. *Science* **266**, 796–8

Z

Zaltsman A., Feder A. and Adam Z. (2005). Developmental and light effects on the accumulation of FtsH protease in *Arabidopsis* chloroplasts – implications for thylakoid formation and photosystem II maintenance. *Plant Journal* **42**, 609–617

Zhang L., Paakkarinen V., Suorsa M. and Aro E.M. (2001). A SecY Homologue Is Involved in Chloroplast-encoded D1 Protein Biogenesis. *THE JOURNAL OF BIOLOGICAL CHEMISTRY* **276**, 37809–37814

Zybailov B., Rutschow H., Friso G., Rudella A., Emanuelsson O., Sun Q. and van Wijk K.J. (2008). Sorting signals, N-terminal modifications and abundance of the chloroplast proteome. *PLoS ONE* **3**, e1994

Acknowledgements

I am deeply grateful to Prof. Dr. Dario Leister for the critical discussions about my thesis and the funding of my work.

I want to thank Prof. Dr. Peter Geigenberger for being second reviewer of my thesis.

I am very thankful to my supervisor Dr. Anja Schneider who always came out with new ideas and taught me to work independently.

A special thank to the group of Prof. Dr. Ingo Flügge for providing me with lots of vectors during my thesis, Prof. Dr. Danja Schünemann for the Split Ubiquitin analyses and PD Stefan Geimer for the TEM pictures.

For their help and the nice time in the lab I want to thank Ashraf, Gabi and Sabine.

Thanks to all gardeners for taking so much care of my plants.

I am most thankful to the whole AG Leister and all other colleagues who made the time period of my thesis such an interesting, informative and most of all funny time. Although I can not mention every single one of you, you all can be sure that you enriched my life and supported me a lot to stand the sometimes difficult time. Especially all former and present office members (Rhea, Jessy, Mathias, Yafei and Wenteng) helped me a lot with the supply of coffee, the interesting discussions and the nice chats during which we all forgot our problems.

Many, many thanks to Elena, Michael, Jessy and Mathias for the nice time we spent together inside and outside of the institute. I hope we will stay in contact wherever life will let us happen to be.

I would like to thank my handball team mates for the extraordinary season we played last year, the fun we have together and for the possibility to let off steam during training and games.

I would have never come so far without my family. Thus, I am so thankful to my brother Thorsten and my sister Christine who helped me so much during my time at the LMU and also now with my thesis. But my parents contributed most to my work. They supported me with everything I needed from my early years on. I wish my mother could join us and celebrate together with us!

Finally, I have to thank the most important person in my life, Jacqueline. Although it was not always easy to stand my bad mood and sometimes even depression, she gave me all the time and support I needed to finish my PhD. Thanks!

Curriculum vitae

Personal Profile

Henning Volker Strissel

Born 4th of February 1982 in Kempten (Germany)

Citizenship: German

Research Experience

- | | |
|-------------------|--|
| 11/2007 – 07/2011 | Ludwig-Maximilians-Universität München (Germany)
Department Biology I, Botany
-PhD Supervisor Prof. Dr. Dario Leister |
| 01/2007 – 09/2007 | Ludwig-Maximilians-Universität München (Germany)
Department Biology I, Botany
-Diploma thesis Supervisor Prof. Dr. Dario Leister |
-

Education

- | | |
|-------------------|--|
| 11/2007 – 07/2011 | PhD at the Ludwig-Maximilians-University München (Germany)
Topic of the thesis:
„ TerC – an essential protein for the integration of Cp43 into the thylakoid membrane and its assembly into photosystem II “ |
| 10/2002 – 09/2007 | Studies of Biology at the Ludwig-Maximilians-University München (Germany)
Diploma Degree (grade 1,0) |
| 09/1992 – 07/2001 | Hildegardis grammar school in Kempten (Germany),
A-levels (grade 2.1); majors (biology and mathematics) |
-

Publications

Strissel, H., Schünemann, D., Flügge, U.-I., Leister, D. and Schneider, A. (2011). TerC is interacting with photosystem II core protein CP43 and is essential for its integration into thylakoid membrane and its assembly into PSII. (in preparation)

Pesaresi, P., Hertle, A., Pribil, M., Kleine, T., Wagner, R., Strissel, H., Ichnatowicz, A., Bonardi, V., Scharfenberg, M., Schneider, A., Pfannschmidt, T., and Leister, D. (2009). Arabidopsis STN7 Kinase Provides a Link between Short- and Long-Term Photosynthetic Acclimation. *Plant Cell* 21:2402-2423

Language Skills

German: native
English: fluent
French: school level

Declaration / Ehrenwörtliche Versicherung

Hiermit versichere ich, dass ich die vorliegende Arbeit selbständig und nur unter Verwendung der angegebenen Hilfsmittel und Quellen angefertigt habe. Der Autor hat zuvor nicht versucht, anderweitig eine Dissertation einzureichen oder sich einer Doktorprüfung zu unterziehen. Die Dissertation wurde keiner weiteren Prüfungskommission weder in Teilen noch als Ganzes vorgelegt.

München, 29. Juni 2011

.....

Henning Strissel